IMM-Roma

The Microwave WEB

High Frequency Micro- and Nano-Systems: Technology and Reliability for Ground and Space Applications

Romolo MARCELLI
CNR-IMM Roma

Romolo.Marcelli@imm.cnr.it
http://www.artov.imm.cnr.it
http://m2t.psm.rm.cnr.it

IMM-Roma

IMM-Roma

Research Line on High Frequency Micro- and Nano-Systems: Technologies and Reliability for Ground and Space Applications

Staff

Surname	Name	Position	Role / Skill
Bartolucci	Giancarlo	Associate Professor - University of Roma "Tor Vergata"	Microwave and mm wave Design and Modelling
Beccherelli	Romeo	Senior Researcher - CNR	Photonic Devices
D'Alessandro	Antonio	Associate Professor - University of Roma "La Sapienza" (from September 2008)	Design and Technologies on Photonic Devices
De Angelis	Giorgio	PhD Student - CNR	Microwave and mm wave Design and Test
De Rosa	Rita	Secretary - CNR	IMM-Roma Secretary
Gilardi	Giovanni	PhD Student - CNR	Design and Technologies on Photonic Devices
Lampasona	Antonio	Technician - CNR	Clean Room Thin Film Technologies
Lucibello	Andrea	PhD Student - CNR	Clean Room Processes
Maiani	Marco	Technician - CNR	Clean Room Thin Film Technologies
Maita	Luigi	Administration - CNR	Administrative Secretary of IMM
Marcelli	Romolo	Senior Researcher - CNR	Group Leader
Proietti	Emanuela	Technologist - CNR	Clean Room Processes
Risi	Claudio	Technician - CNR	Clean Room Thin Film Technologies
Totale			**13**

Collaborations
(industrial and academic)

- European Space Agency – Technology Centre (ESA-ESTEC), Noordwijk, The Netherlands
- THALES ALENIA SPACE Italy (TAS-I), Roma and L'Aquila
- THALES ALENIA SPACE France (TAS-F), Toulouse, France
- Italian National Agency for New Technologies, Energy and the Environment (ENEA), Frascati Research Centre
- Finmeccanica, mainly through SELEX-SI, Roma
- ST Microelectronics, Agrate Brianza
- Fondazione Bruno Kessler (ex-ITC)-irst, Trento
- University of Roma 2 "Tor Vergata", Electronics Engineering Department
- Nat. Institute for Research and Development in Microtechnologies (IMT), Bucharest, Romania
- EU Network of Excellence AMICOM (FP7 follow-up)
- The George Washington University, Washington, DC, USA
- Institute of Radio-Engineering and Electronics, Moscow, Russia
- University of Perugia, Electronics Engineering Department
- Technische Universität München, Germany
- Technical Research Centre of Finland (VTT), Helsinki and Oulu, Finland
- Southwest Institute of Applied Magnetics, P.R. China
- University of Roma 1, "La Sapienza"
- University of Roma Tre, Engineering Department
- Università della Calabria
- Ministero degli Affari Esteri (Foreign Ministery)
- Aristotle University of Thessaloniki (Greece)
- University of Padova, Electronics Engineering Department
- University of Athens, Greece
- Comicion Nacional de Energia Atomica (CONEA), Buenos Aires, Argentina

Motivations

- The development of Micro- and Nano-Systems for high frequency components and sub-systems determined a growing requirement on the feasibility of the involved technologies, especially when functionalities quite different between them *(electrical or electromagnetic, electro-mechanical, and chemical-physical)* have to be integrated in the same configuration.
- The feasibility of Micro- and Nano-Systems especially minded for high frequency applications is also a hot topic.
- Special care is devoted to:

i. Optimization of bulk and surface micromachining techniques for different substrates which can host configurations for guided and free space propagation as well as resonating structures and nano-devices (wafers of Si and GaAs, alumina, substrates of LTCC and LTCF, magnetic materials, photo-sensitive polymers, based also on liquid crystals;

ii. Design and realization of innovative components, for which no commercial software solution exists for the full design, especially when different and/or combined solicitations are involved;

iii. Reliability of micro- and nano-systems as a function of their applications, for ground as well as for space applications for on-wafer and packaged devices.

→ SMART SYSTEMS, *high number of components and functions, network-embedded*

→ INTERNET OF THINGS

IMM-Roma

Technology focus

Products

BAW resonators

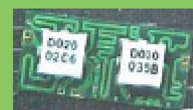

Cavity resonators

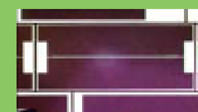

Tunable capacitors

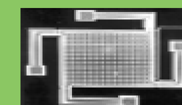

MEMS switches

Micromechanical resonators

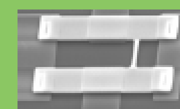

MEMS inductors

Technologies

Silicon MEMS

Non MEMS: PIN diodes, GaAs, SoS, GaN…

Breakthrough: Carbon Nanotubes, Polymer electronics…

Roadmap example for mobile handsets

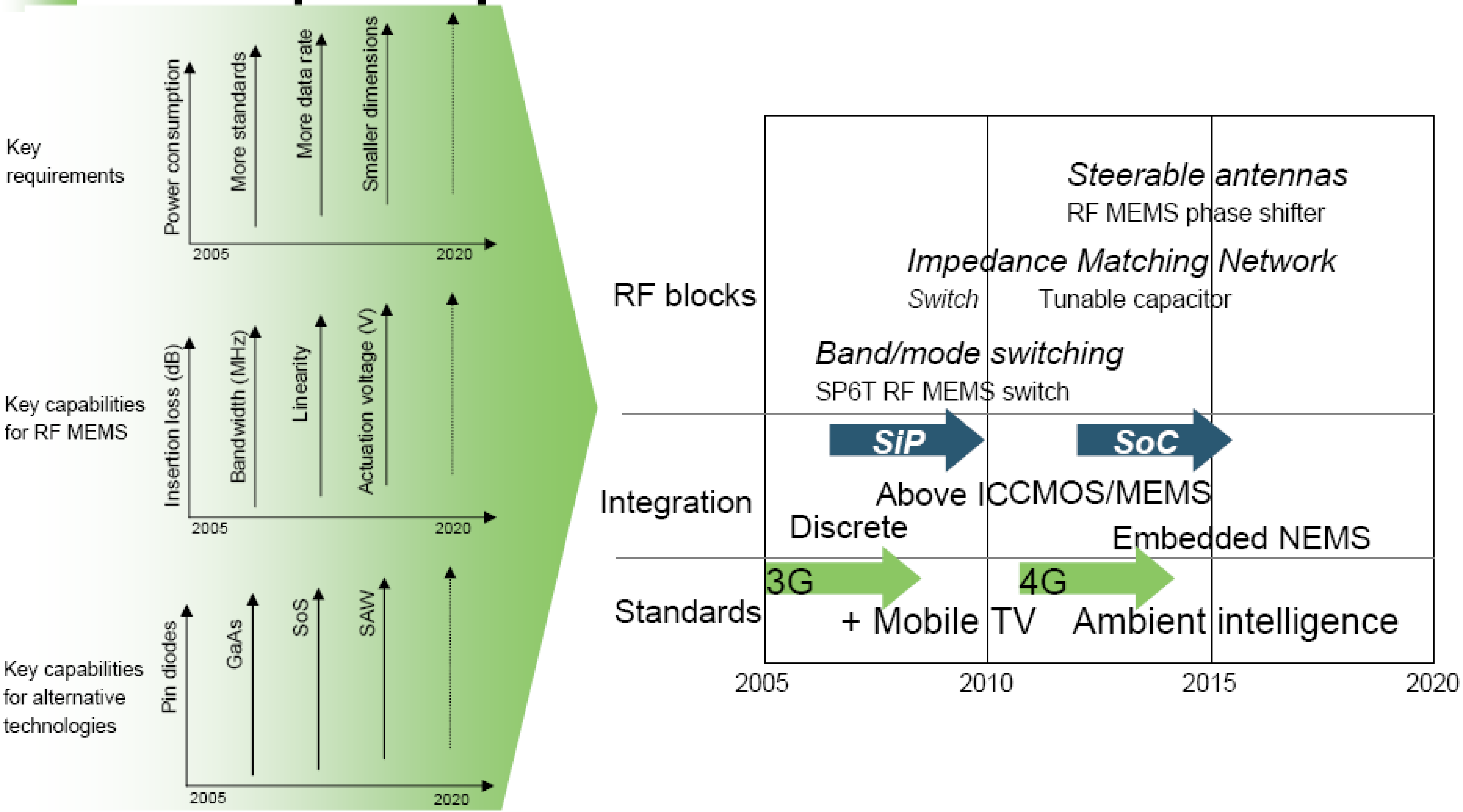

Top 30 worldwide MEMS companies ranking
2009 revenues
(US $M)

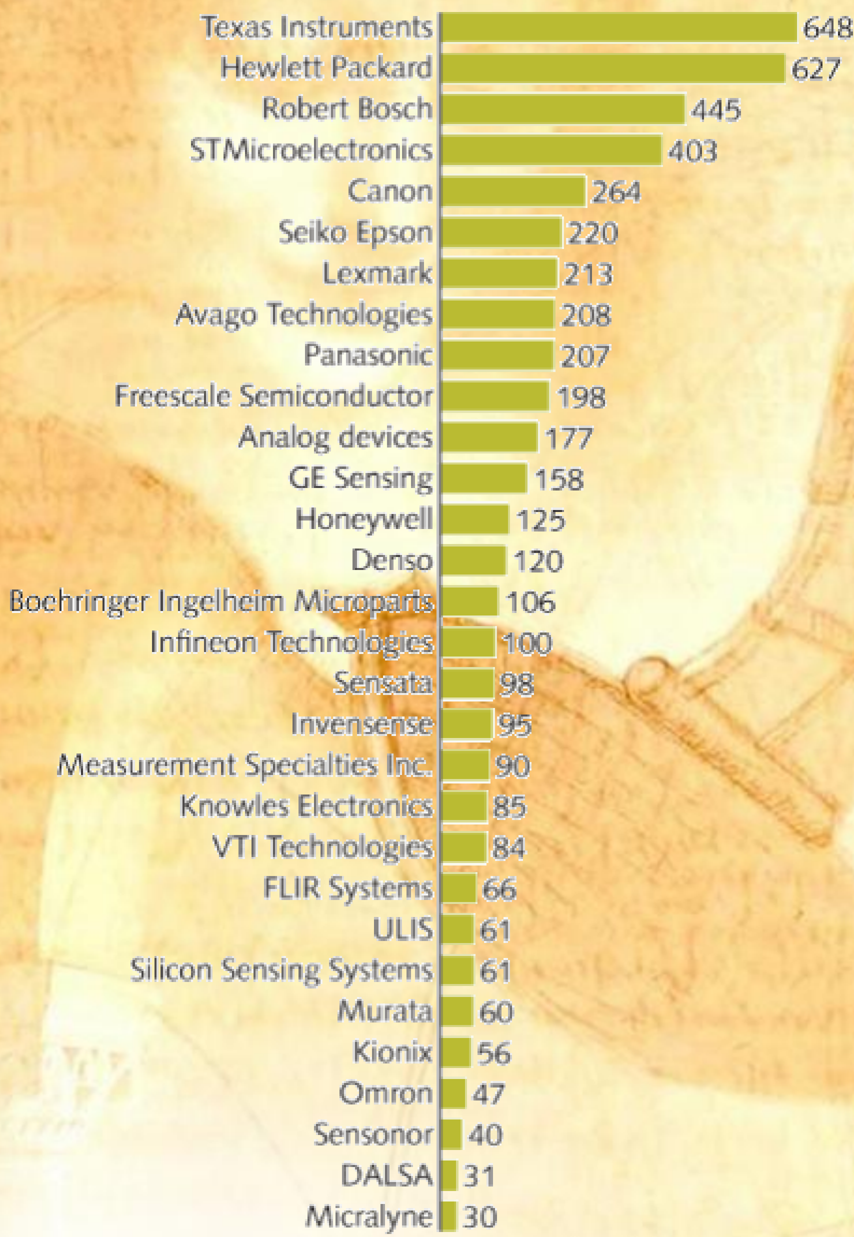

WaferNews source: Yole Développement estimates, February 2010

Annual growth rate
2008/2009
(%)

WaferNews source: Yole Développement estimates, February 2010

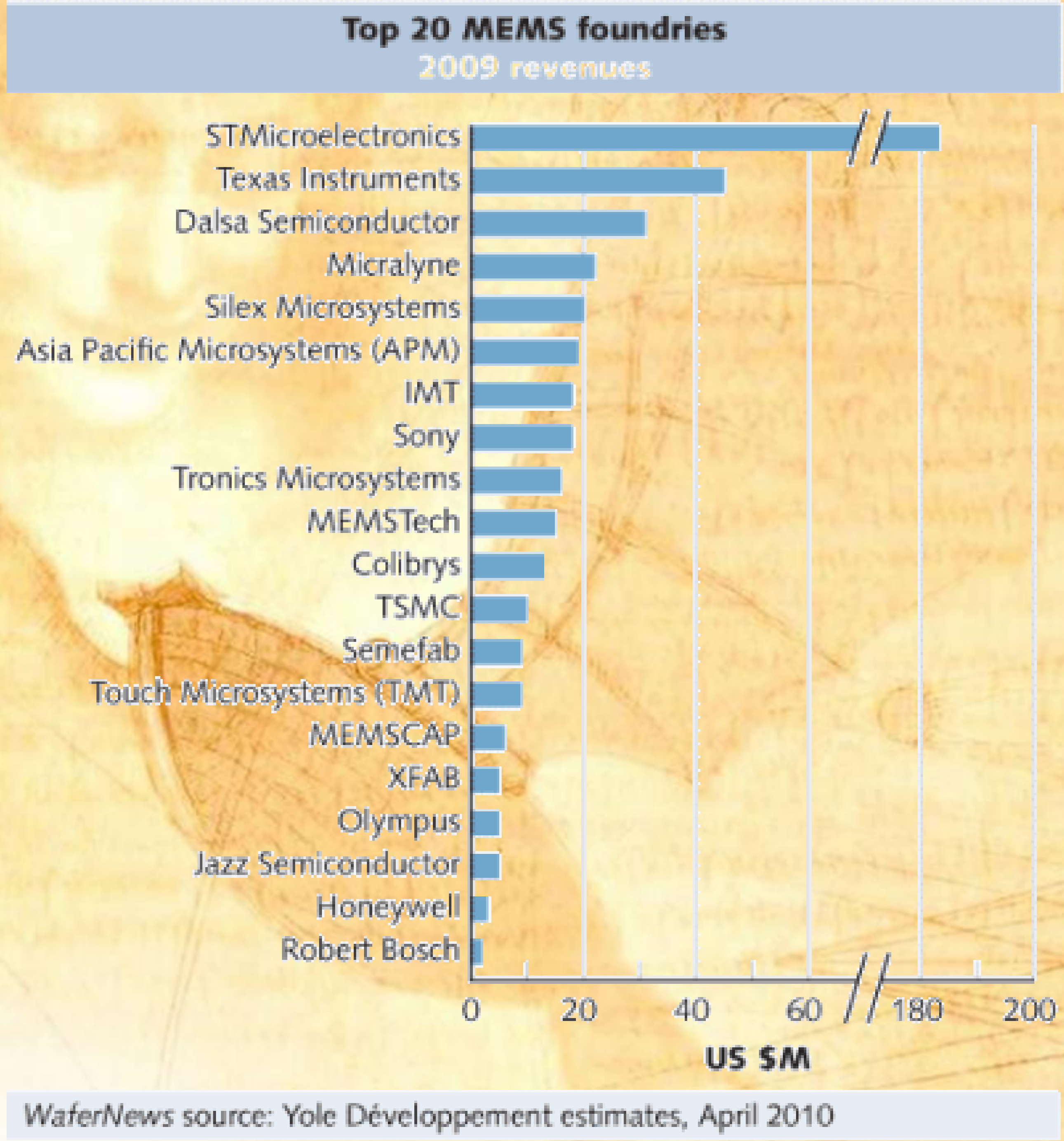

Top 20 MEMS foundries
2009 revenues
STMicroelectronics
Texas Instruments
Dalsa Semiconductor
Micralyne
Silex Microsystems
Asia Pacific Microsystems (APM)
IMT
Sony
Tronics Microsystems
MEMSTech
Colibrys
TSMC
Semefab
Touch Microsystems (TMT)
MEMSCAP
XFAB
Olympus
Jazz Semiconductor
Honeywell
Robert Bosch
0
20
40
60
180
200
US $M
WaferNews source: Yole Développement estimates, April 2010

IMM-Roma

The Microwave WEB

RF MEMS Roadmap and Market Forecast - 1

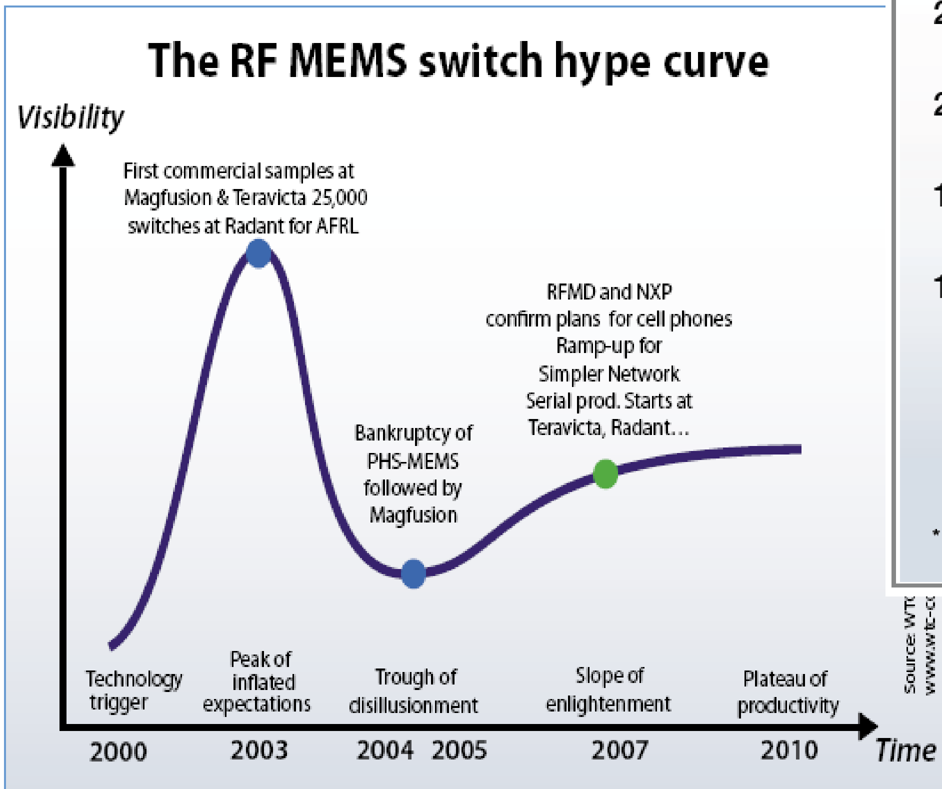

Industry Quote: Dr Georg Fischer, Alcatel-Lucent

"I think we are 2 to 3 years away from this event." — on the prospects for market insertion of RF MEMS in base stations.

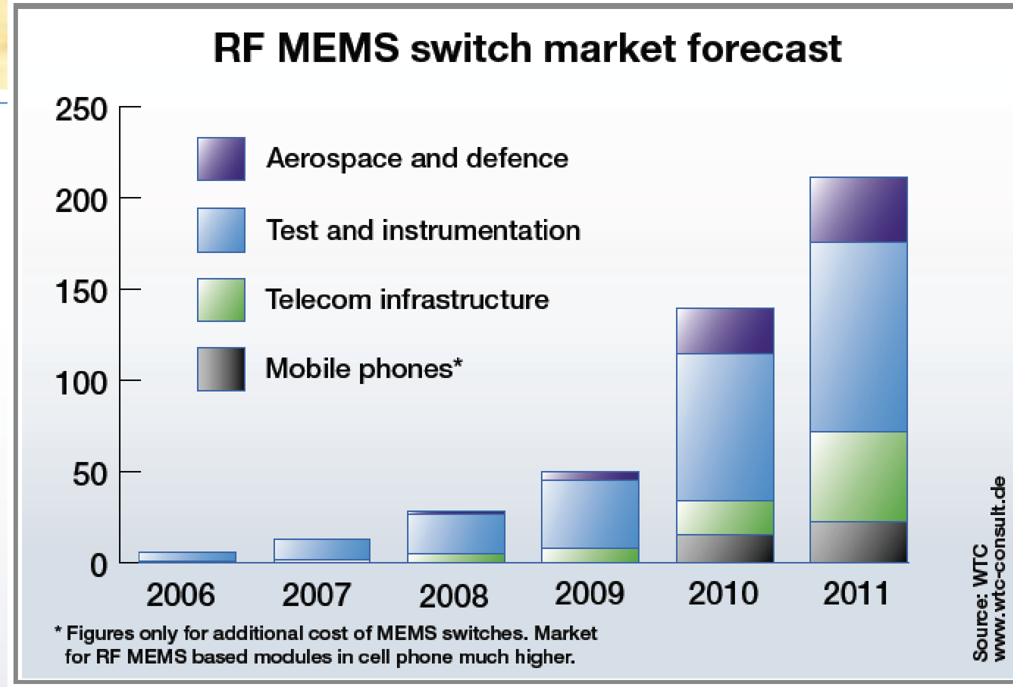

IMM-Roma

The Microwave WEB

RF MEMS Roadmap and Market Forecast - 2

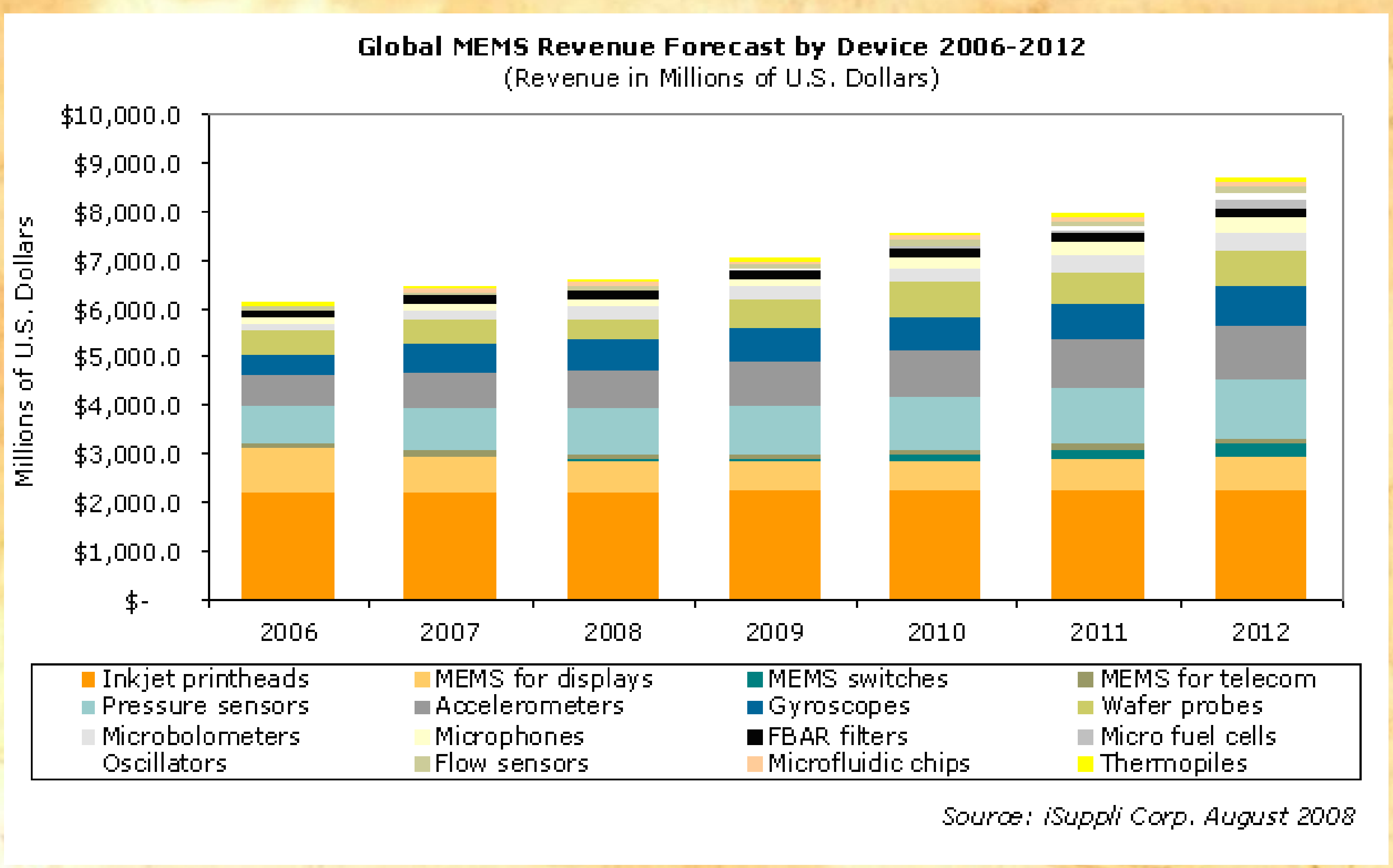

Source: Small Times, September, 2008

Issues in Design, Technologies and Test for RF MEMS @ IMM

Owing to the complexity of RF MEMS switches a multidisciplinary approach is needed

Software:

- Commercial 2D and 3D RF Design Techniques, supported by circuital modelling for complicated configurations (matrices, phase shifters, delay lines, …)
- Multiphysics simulations, involving commercial and purposely developed software codes for non-RF and RF properties or harsh environment evaluations (Temperature, RF Power, DC Actuation, Mechanical Response, Charging…)

Technologies:

- Thin Film Deposition and Processing (evaporation, DC and RF sputtering, PECVD, …. For metal and dielectric layers), followed by sacrifical layers removal (the critical point).

Characterization:

- Morphological and Mechanical
- DC and RF Electrical Measurements for on-wafer and packaged devices
- Development of specific Calibration Techniques for on-wafer measurements when low-loss RF transmission line devices are considered

Device Feasibility in Terms of Short- and Medium-Term evaluation involving:

- Physical and Circuital Modelling of structures under combined solicitations (like power and temperature, or number of actuations, technology yield, …)
- Specific reliability tests for ground and space applications, charging, failure mechanisms and aging
- Need for a “Figure of Merit”, not yet defined for RF MEMS

Ferromagnetic Resonance and Magnetostatic Waves

The magnetic response is due to the presence of the Fe3+ ions – ferrimagnetic material

Two Sub-lattices

$3Fe^{3+}$ ***$2Fe^{3+}$***

↑ ↑ ↑ ↓ ↓

Site d ***Site a***

precession motion of $\overrightarrow{M}_0$

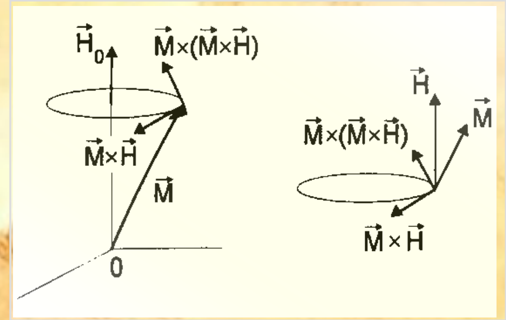

$$f_0 \propto H_0$$

$$\gamma = 2.802\ MHz\ / Oe$$

Propagation of magnetostatic waves, slower than the electromagnetic ones, is excited through the spin system

IMM-Roma

The Microwave WEB

Magnetic Film Frequency Tunable Resonators, F≤40 GHz

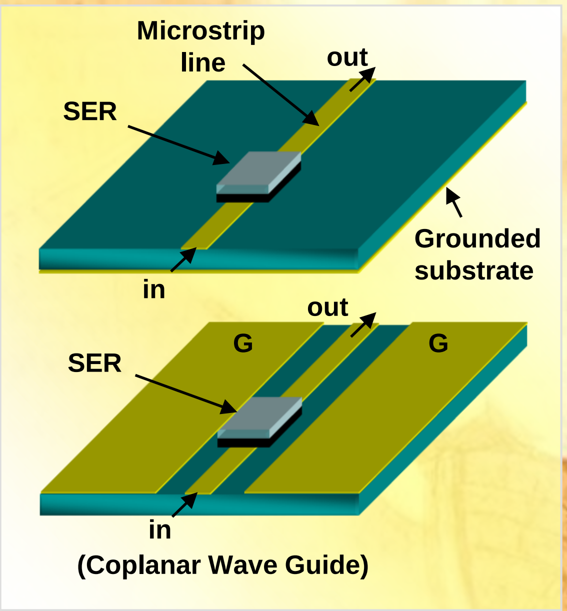

Microstrip

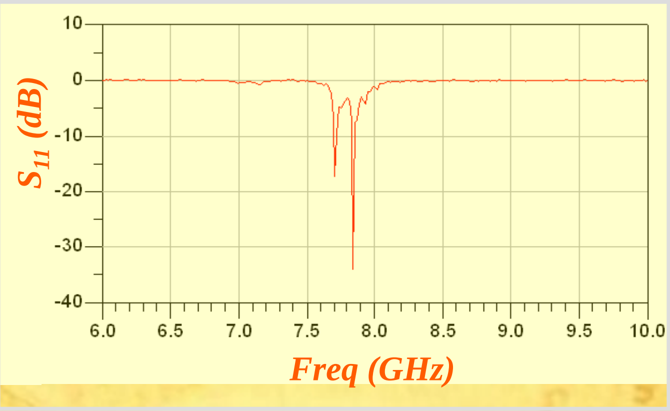

Coplanar waveguide

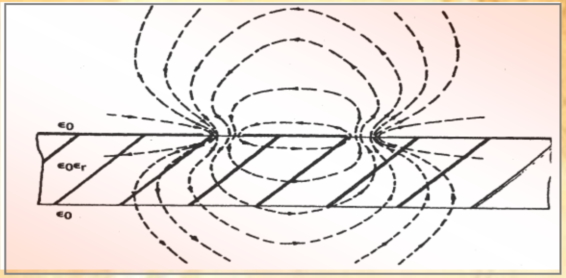

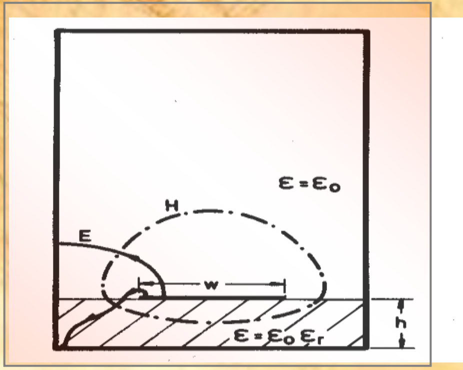

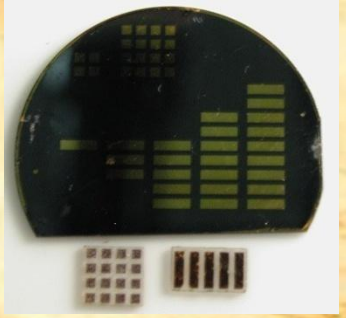

Micromachining by hot H_3PO_4 of magnetic garnet films for integrated coupled resonator structures

In cooperation with IMT, Bucuresti, T. Koike ex-Univ. of Tamagawa, University of Roma “Tor Vergata”

IMM-Roma

Magnetic Film Frequency Tunable Oscillators , F≤40 GHz

In cooperation with University of Roma “Tor Vergata”, SELEX-SI

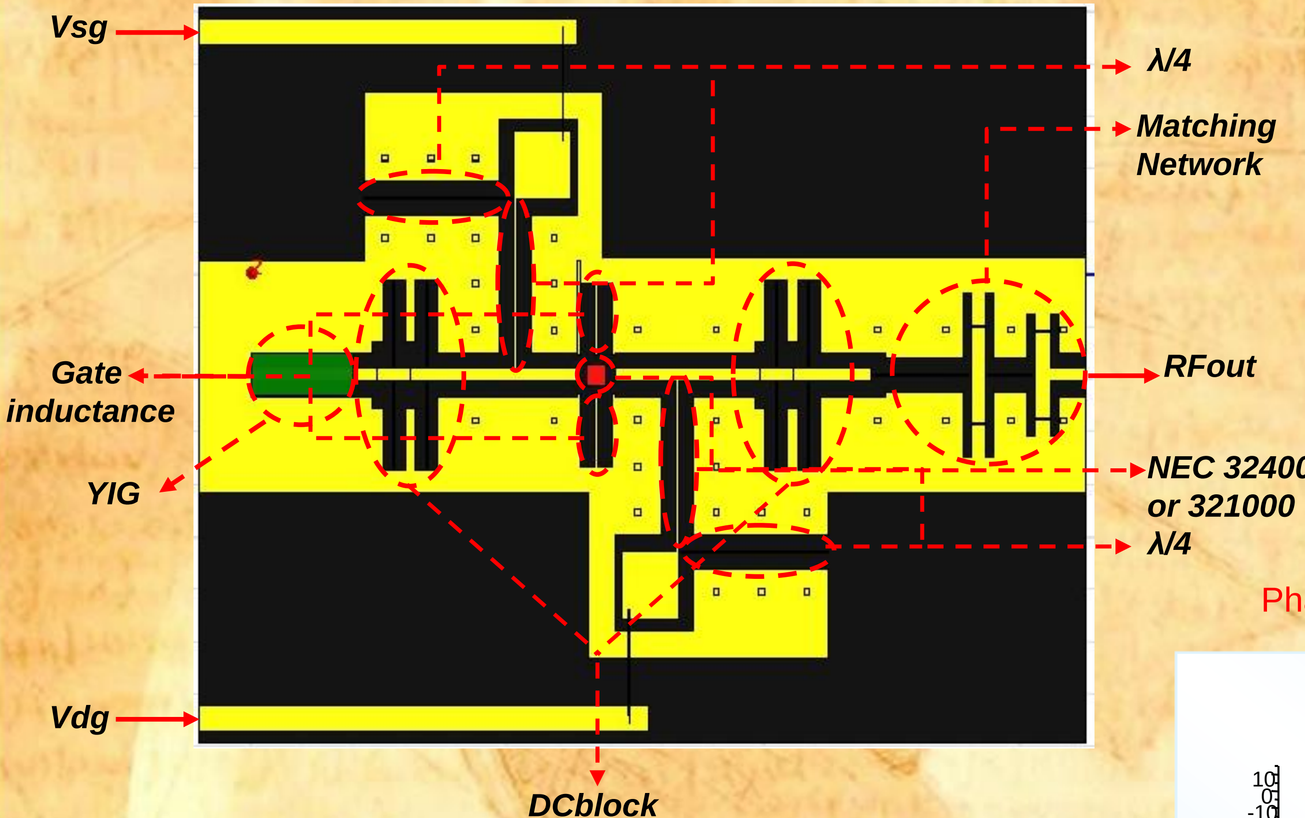

Distance between the via holes must be **≤λ/20** and the distance from the external edge of the lateral ground plane must greater than the side of the Via Holes

-

Phase Noise = 100 dBC @ 100kHz

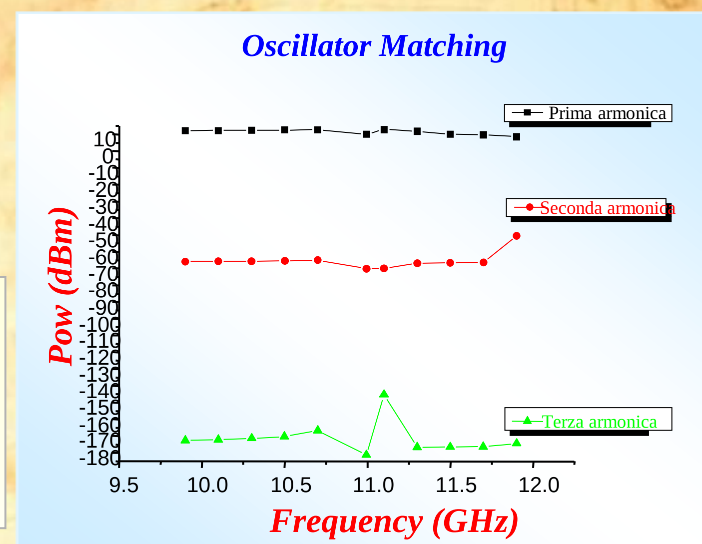

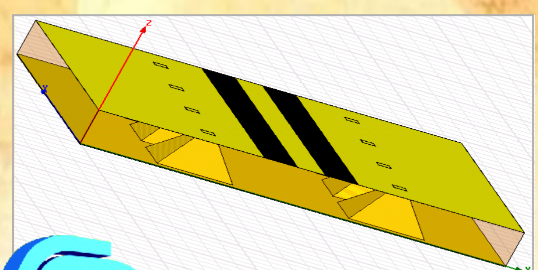

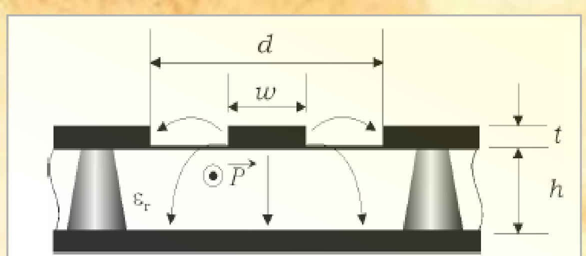

IMM-Roma

Membrane Supported Filters and Antennas TEM – modes, no substrate contribution 30 GHz ≤ F ≤ 800 (?) GHz

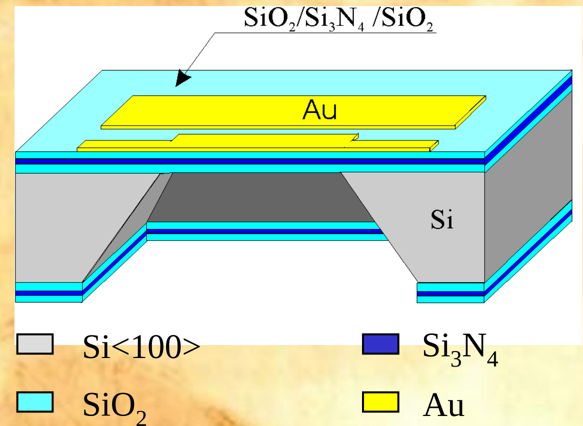

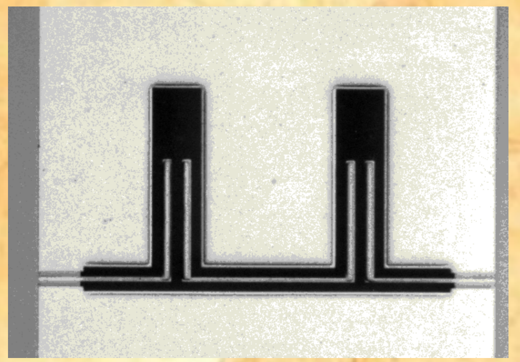

$SiO_2/Si_3N_4/SiO_2$ membrane supported coupled line filter for 38 and 77 GHz

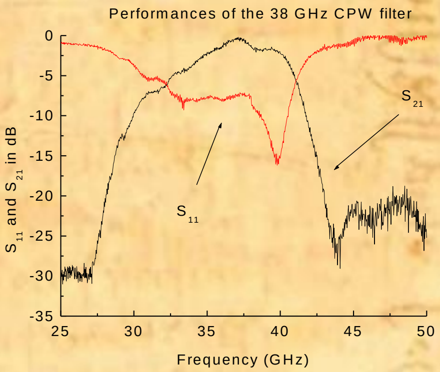

Anisotropic etching by TMAH or KOH in water

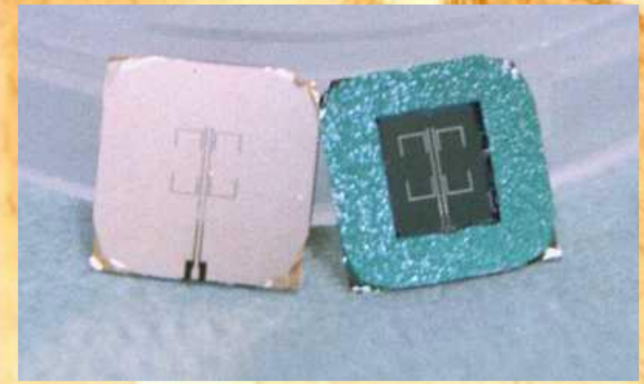

Double arm, double folded cpw antenna on $SiO_2/Si_3N_4/SiO_2$ membrane for 38 GHz

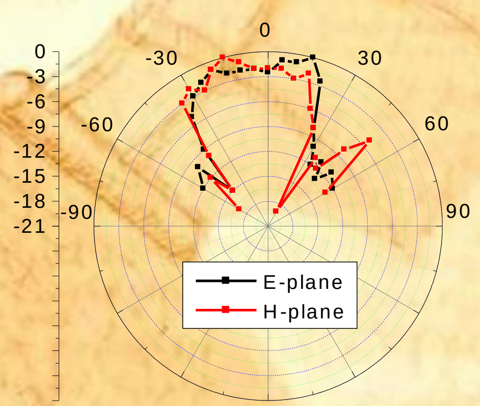

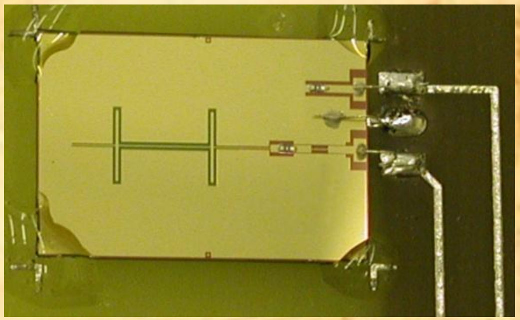

38 GHz hybrid receiver structure with Schottky diode mounted on Si bulk and antenna on membrane

In cooperation with FBK-irst, Trento, University of Roma "Tor Vergata" and IMT, Bucuresti + ex-Consortium MEMSWAVE

IMM-Roma

SU-8 based Micro-Systems, F≥30 GHz
Implementation for End-Fire Antennas, F>200 GHz

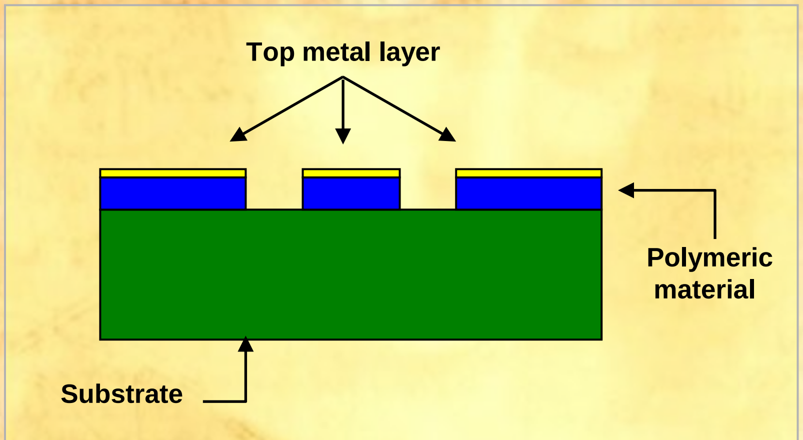

The elevation of the CPW structure with respect to the silicon substrate allows for an almost *on-the-air* propagation (quasi TEM with no dielectric losses nor dispersion) analogously to the membrane supported passive filters, but with less critical and cheaper technology

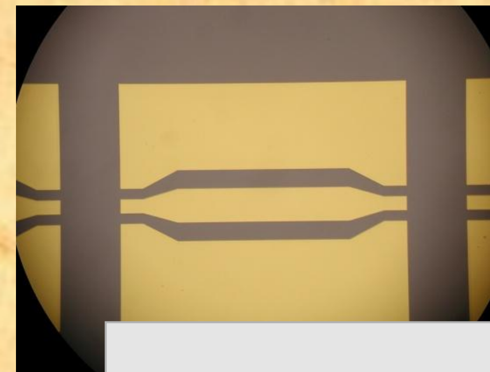

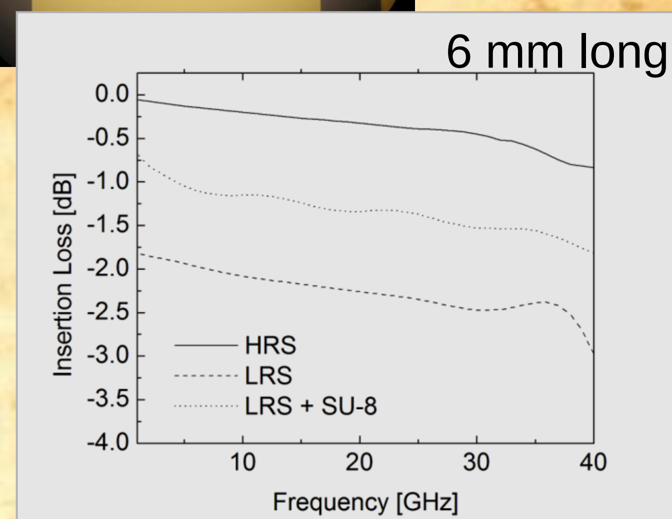

Quantity	Value	Description
Dielectric loss tangent: tan δ	0.08	At 100GHz, post baked at 100°C(+8 hours at 65°KOH)
Relative dielectric constant: εr	4.2-4.5	Up to 20 GHz
Breakdown voltage	1.1x10^5 V/m	Electrical breakdown 1.2 V for an 11μm thick SU8(10) film

SU-8 negative resist general properties

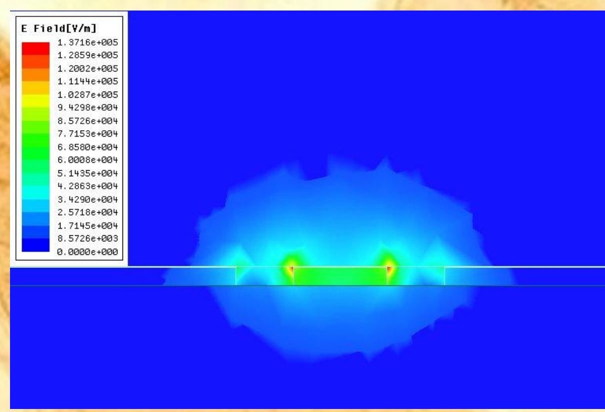

Simulated E-Fields intensity at the I/O ports of a CPW

Two effects:

Quasi TEM on-the-air propagation

Possible LRS utilization

IMM-Roma

RF - MEMS Switches

IMM-Roma

(presently in cooperation also with IMM Lecce)

RF MEMS Switches are devices processing RF signals via a TX line. By means of an electrostatic actuation due to a voltage applied between membrane and electrode , they pass from a state UP to a state DOWN (o.c / s.c on TX line)

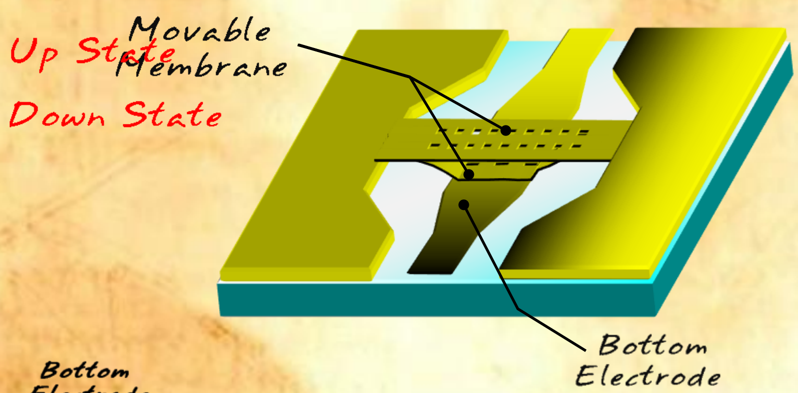

The three main elements for the classification are:

1) Contact Metal- metal / Capacitive
2) Mechanical structure Bridge / Cantilever
3) Configuration Series / Shunt

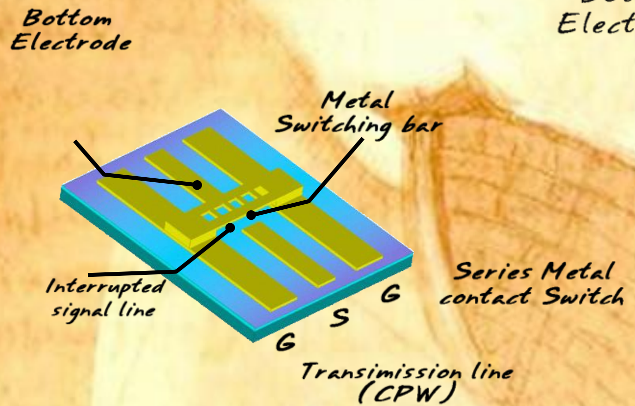

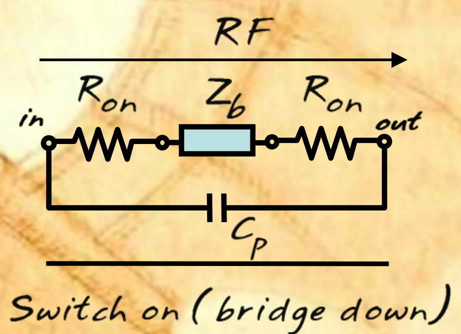

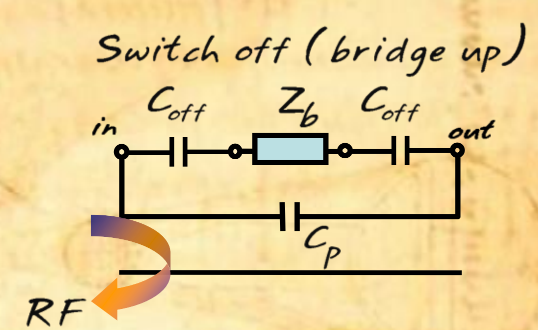

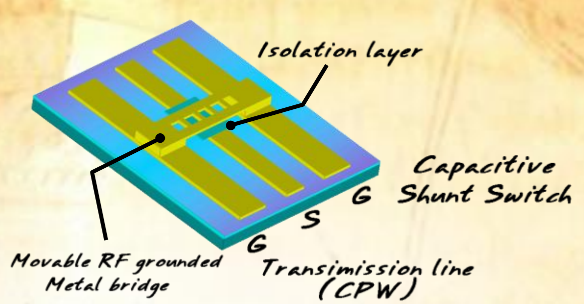

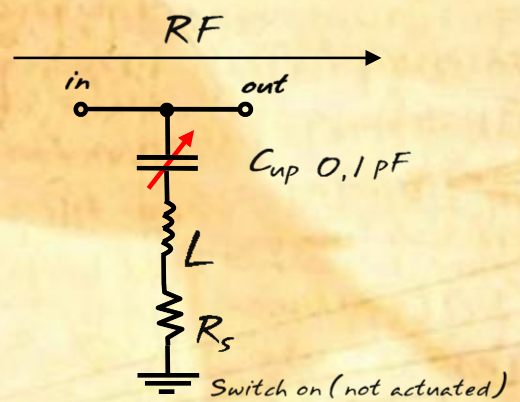

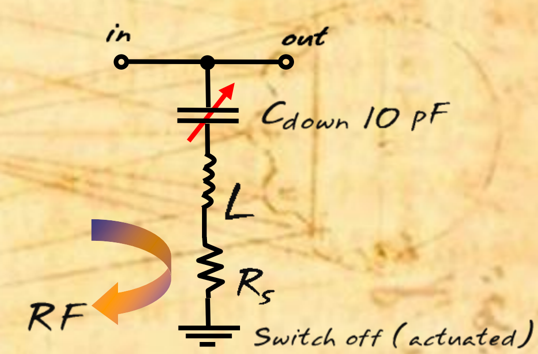

FBK-irst Technology - Silicon

- Status base line process
  - 8 mask layer
  - ~ 200 unit process steps
  - 10 - 20 4” wafer batch’s
  - ~15 week cycle time
  - 18 run completed
  - 4 run under way
- Updates & Improvements
  - Flow optimization
  - Planned measure steps
  - Standard data output
- N.B. In blue solved problems
- In red open issues

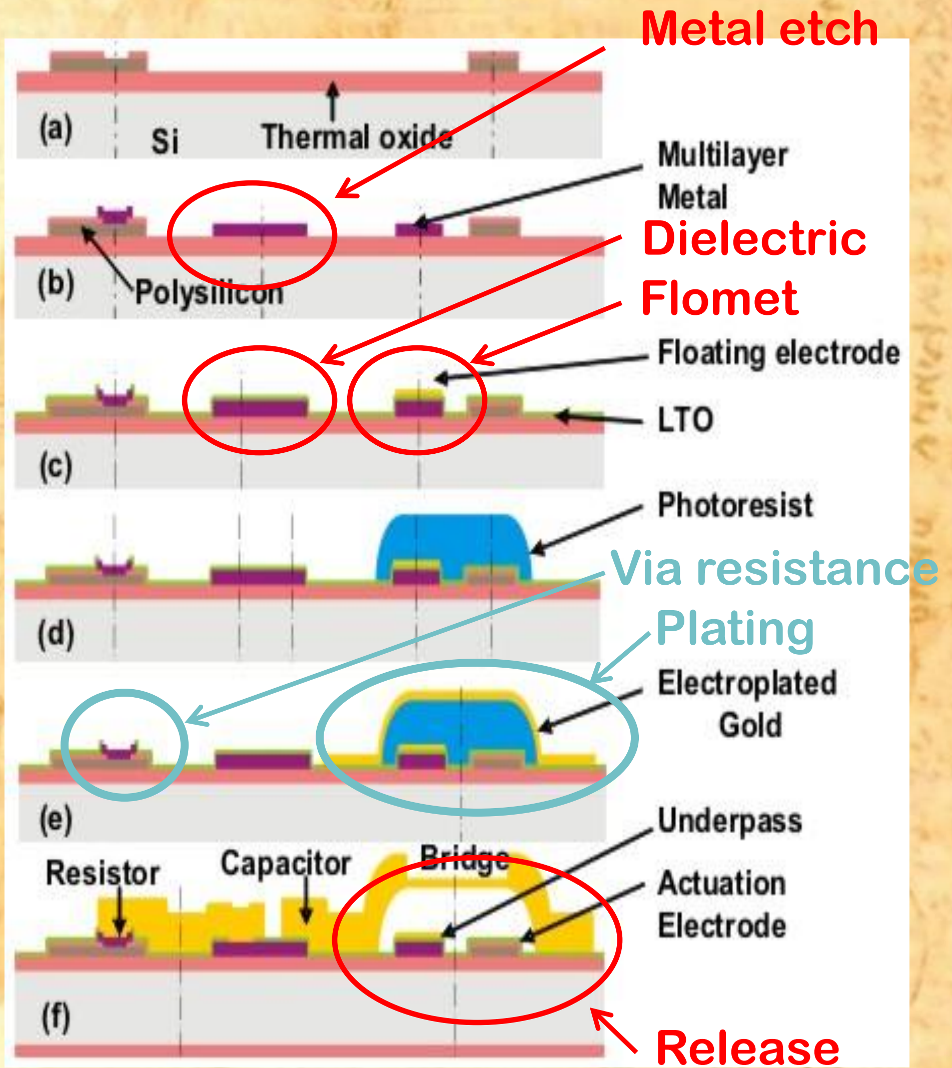

DC electrical parametric tests

the measured Con/Coff is **only used to evaluate the process stability/repeatability**.

Value	Unit	Mean Values
Poly-silicon sheet resistance 630 nm	Ω/□	1764 ± 62
Multimetal sheet resistance	Ω/□	0.0685 ± 0.0006
Au BRIDGE sheet resistance	Ω/□	0.0098 ± 0.0004
Poly-Si/multimetal. DC contact resistance	Ω	163 ± 7
Multimetal/Au DC contact resistance	Ω	0.29 ± 11
Poly-Si/multimetal DC contact chain resistance	Ω	9375 ± 902
Multimetal./Au DC contact chain resistance	Ω	1963 ± 3424
Poly-Si/Au capacitance	pF	14.5 ± 2.2
Poly-Si/multilayer capacitance	pF	6.17 ± 0.75
Multilayer/Au capacitance	pF	20.0±0.5
LTO thick. (Multilayer/Au capacitance)	nm	68.5 ± 1.6
TEOS thick. (Poly-Si/TiN capacitance)	nm	219 ± 7
TEOS+LTO thick. (Poly-Si/Au capac.)	nm	98 ± 30
% of measurable test patterns*		100%

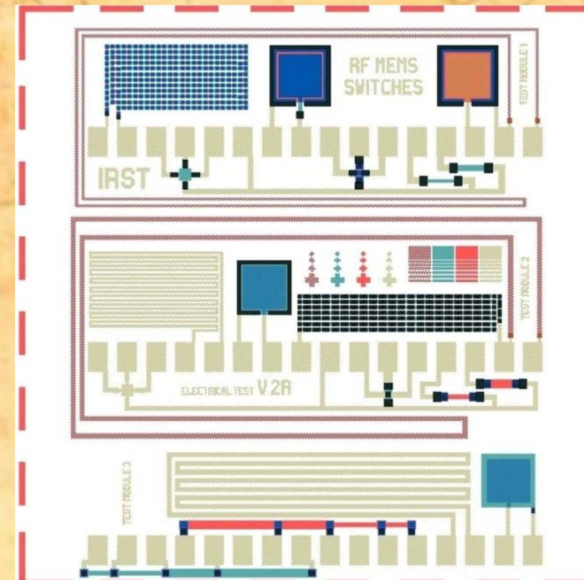

WAFER : 19	Substrate Si standard	Spacer 3 μm	Poly 630 nm					
	FIRST MEASUREMENT				SECOND MEASUREMENT			
1-A	Vact1(V)	Coff1(pF)	Con1(pF)	% of working devices	Vact2(V)	Coff2(pF)	Con2(pF)	% of working devices
mean	40.3	0.084	0.476		51.2	0.086	0.511	
σ	2.6	0.006	0.026	93%	1.9	5.3	3.3	93%
σ(%)	6%	7%	6%		4%	6%	6%	
2-C (1-A with flomet)	Vact1(V)	Coff1(pF)	Con1(pF)	% of working devices	Vact2(V)	Coff2(pF)	Con2(pF)	% of working devices
mean	41.7	0.133	6.002		49.88	0.132	6.016	
σ	2.7	0.029	0.159	93%	2.48	0.028	0.144	93%
σ(%)	6%	22%	3%		5%	21%	2%	
1-B	Vact1(V)	Coff1(pF)	Con1(pF)	% of working devices	Vact2(V)	Coff2(pF)	Con2(pF)	% of working devices
mean	59.0	0.103	0.596		67.3	0.108	0.657	
σ	3.0	0.082	0.083	100%	2.6	0.017	0.111	100%
σ(%)	5%	8%	14%		4%	15%	17%	
2-D (1-B with flomet)	Vact1(V)	Coff1(pF)	Con1(pF)	% of working devices	Vact2(V)	Coff2(pF)	Con2(pF)	% of working devices
mean	57.1	0.106	6.192		63.0	0.108	6.198	
σ	2.4	0.026	0.144	93%	1.6	0.024	0.155	93%
σ(%)	4%	24%	2%		3%	23%	2%	

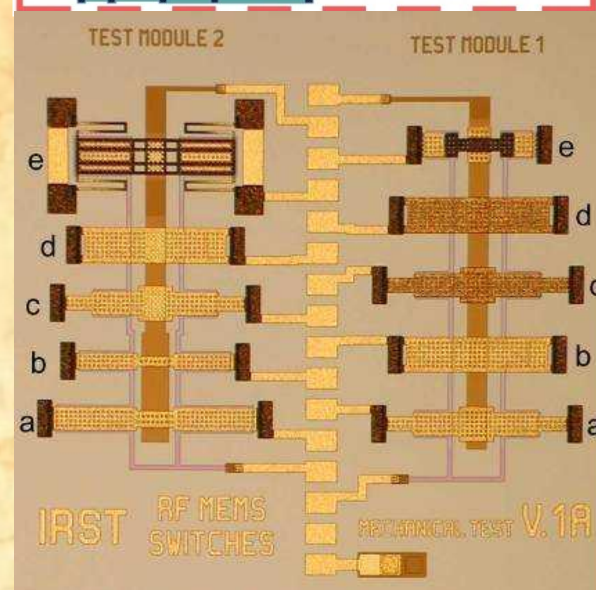

Electromechanical test structure.

Reliability of Micro-Switches

- ✓ Micro-electromechanical switches are minded as low-loss building blocks, for distortion free configurations in signal routing, redundancy logic, matrices, phase shifters, …

- ✓ Switch Test, including SPDT and Matrices has to fulfil: technology yield (statistics on the same wafer), number of actuations, lifetime (dynamics, total actuation time, charging processes, …)

SPST Series and Shunt RF MEMS -1

S1

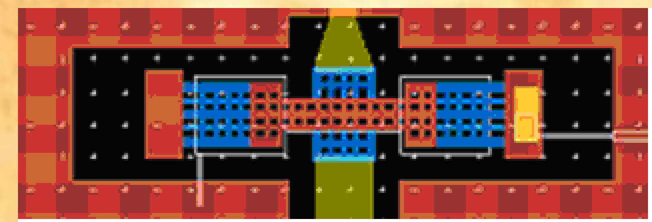

S8

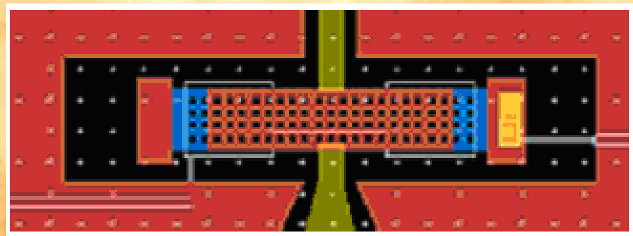

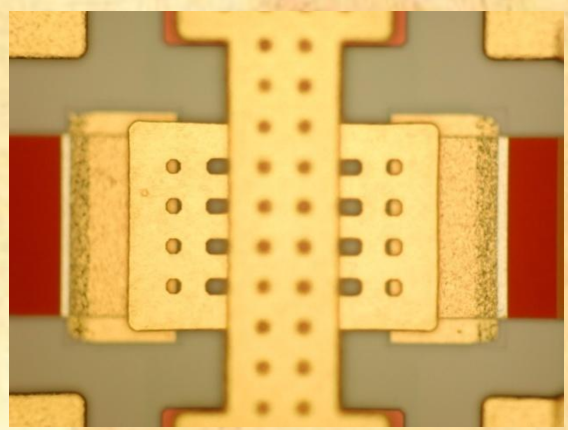

RF MEMS SERIES SWITCHES

- S1: “standard” series switch
- S2: S1 with the anchor directly connected to ground
- S3: S1 with modified bias lines
- S4: S1 with a single long line instead of 5 separated dimples
- S5: S1 with 2 dimples instead of 5
- S6: S1 without wings on the bridge
- S7: S1 with the bridge completely in “BRIDGE” layer
- S8: narrow CPW line, bridge without wings
- S9: S1 without dimples

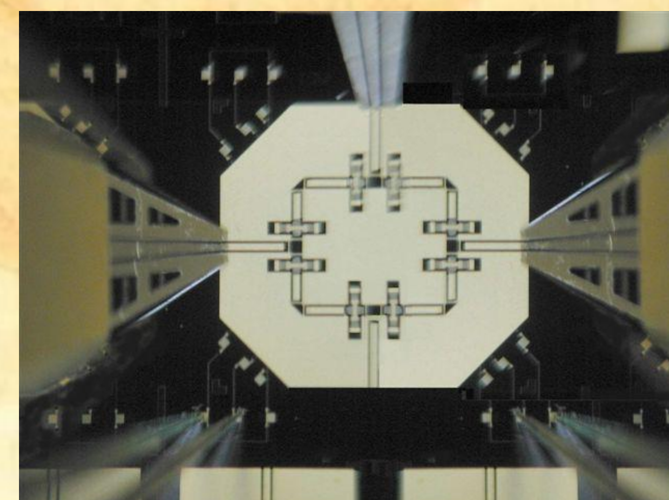

In cooperation with: Thales Alenia Space-Italia, FBK-irst, UNI PG, TUM München

IMM-Roma

SPST Series and Shunt RF MEMS - 2

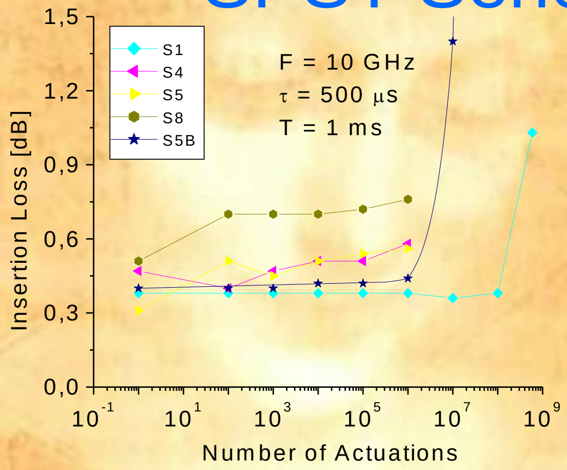

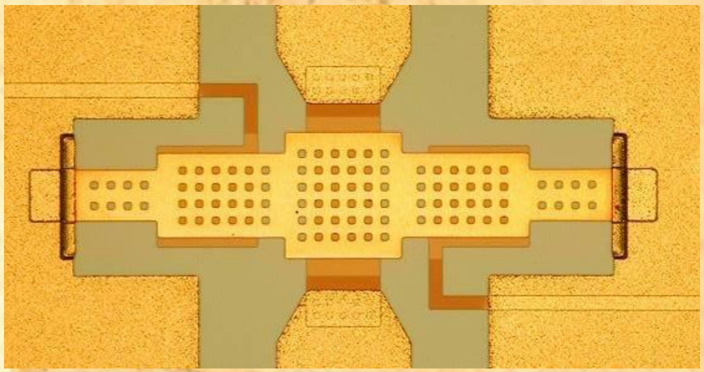

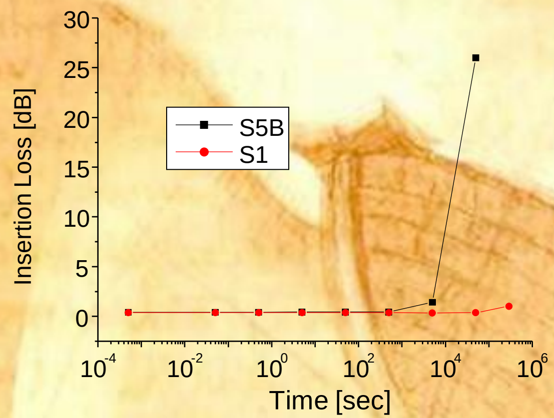

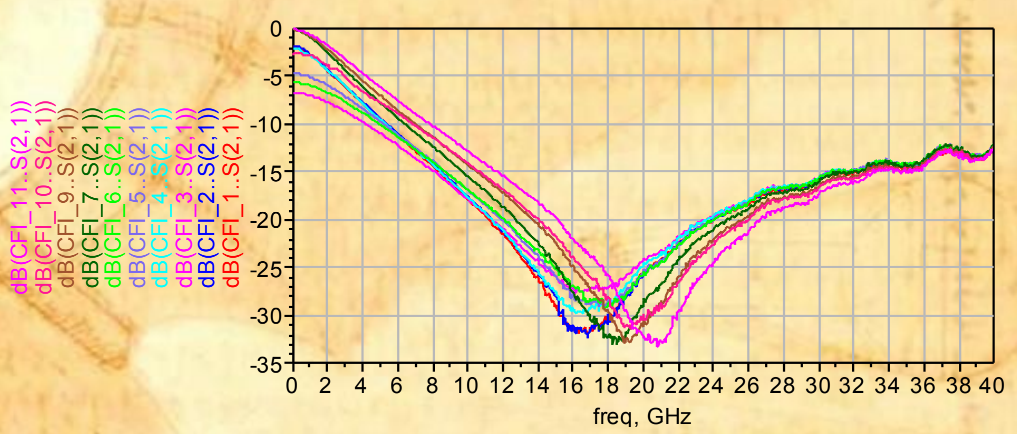

A: Failure analysis for RF MEMS Series Switches up to 5.9×10^8 actuations. S1 seems to be non-sensitive with respect to the others, thus confirming that the robust solution (thick Au) with 5 dimples is the winning choice for the series switch.

B: Isolation at resonance for a Shunt SPST. The frequency of resonance has a small spread, due to a different thickness in the LTO deposition and etching. Negligible is the change in its dielectric properties.

In cooperation with: Thales Alenia Space-Italia, FBK-irst, UNI PG, TUM München

IMM-Roma

Charging Effects in RF MEMS - TEOS

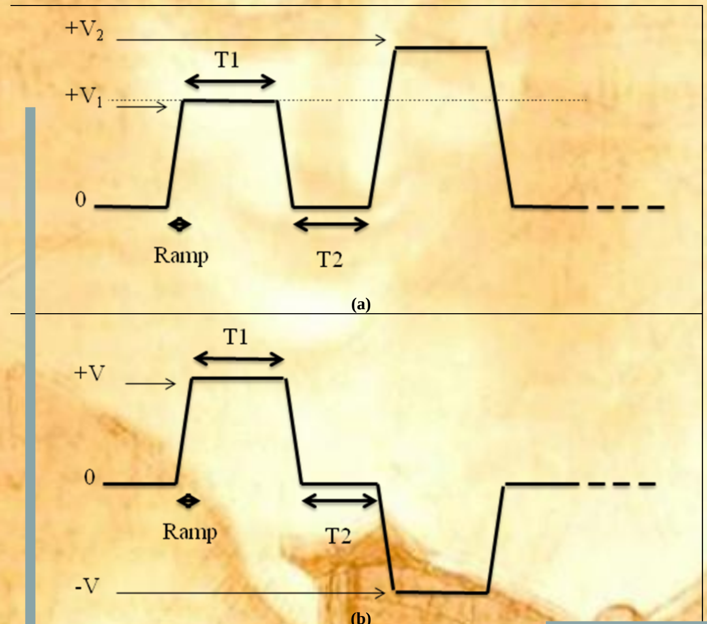

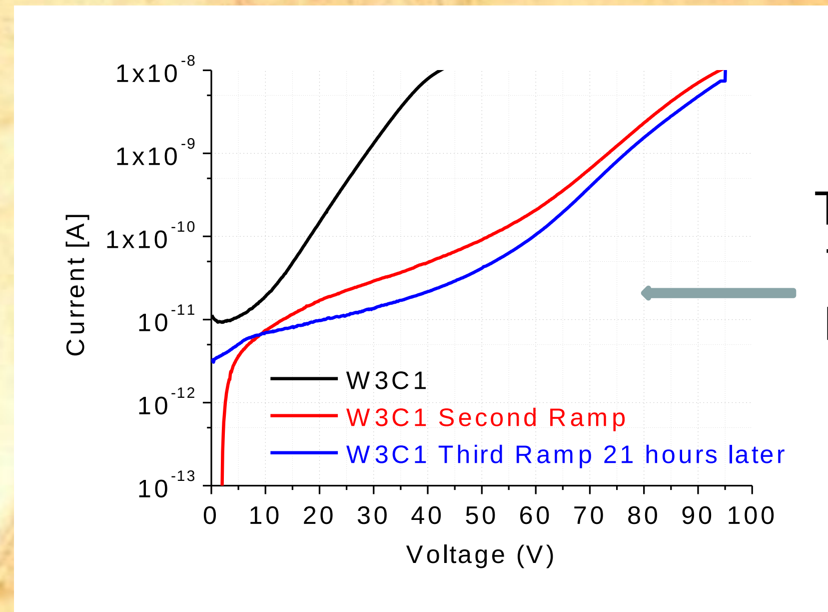

Test on TEOS Based MIM

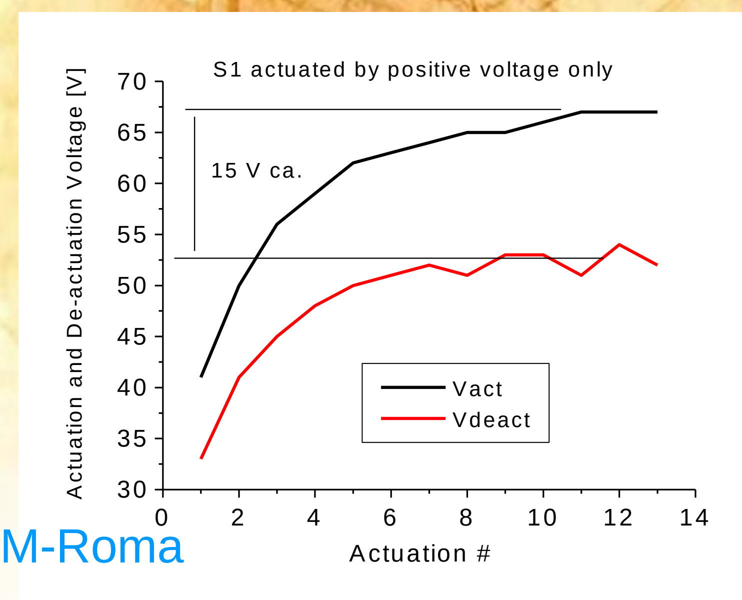

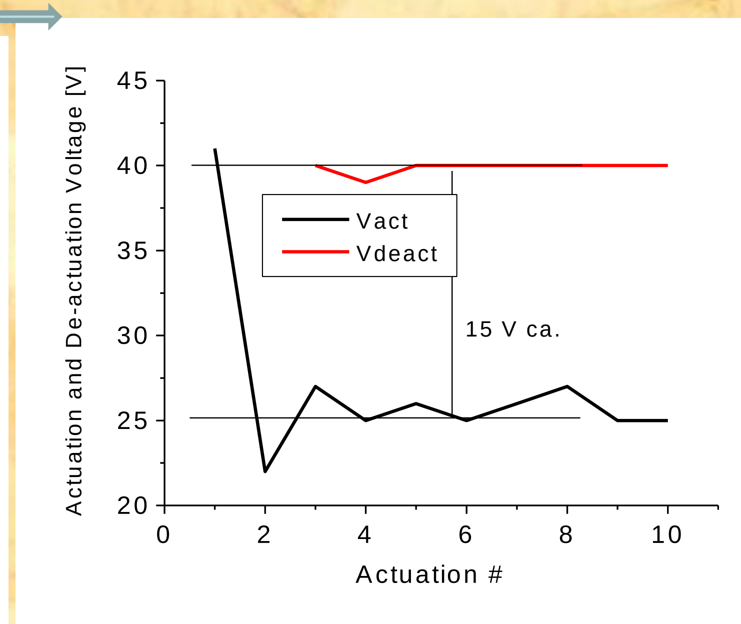

IMM-Roma

Charging saturation in uni-polar regime

$$\Delta V_{th}(t) = d\,|\vec{E}_{ch}(t)| = d\,|\vec{E}_{ch,0}|\exp\left(-\frac{t}{\tau_{ch}}\right)$$

Threshold increase by charge accumulation

$$\Delta V_{th}^{(1)} = d\,|\vec{E}_{ch,0}^{(1)}|\exp\left(-\frac{(T-\tau)}{\tau_{ch}}\right)$$

$$\Delta V_{th}^{(2)} = d\left[|\vec{E}_{ch,0}^{(1)}|\exp\left(-2\frac{(T-\tau)}{\tau_{ch}}\right)+|\vec{E}_{ch,0}^{(2)}|\exp\left(-\frac{(T-\tau)}{\tau_{ch}}\right)\right]$$

$$\Delta V_{th}^{(3)} = d\left[|\vec{E}_{ch,0}^{(1)}|\exp\left(-3\frac{(T-\tau)}{\tau_{ch}}\right)+|\vec{E}_{ch,0}^{(2)}|\exp\left(-2\frac{(T-\tau)}{\tau_{ch}}\right)+|\vec{E}_{ch,0}^{(3)}|\exp\left(-\frac{(T-\tau)}{\tau_{ch}}\right)\right]$$

....

$$\Delta V_{th}^{(n)} = d\,|\vec{E}_{ch,0}|\exp\left(-n\frac{(T-\tau)}{\tau_{ch}}\right) \quad \textit{and}$$

$$\Delta V_{th} = d\,|\vec{E}_{ch,0}|\sum_n \exp\left(-n\frac{(T-\tau)}{\tau_{ch}}\right) = d\,|\vec{E}_{ch,0}|\sum_n x^n = d\,|\vec{E}_{ch,0}|\frac{1}{1-x} = \frac{d\,|\vec{E}_{ch,0}|}{1-\exp\left(-\frac{T-\tau}{\tau_{ch}}\right)}$$

$$\textit{where} \quad x = \exp\left(-\frac{T-\tau}{\tau_{ch}}\right) < 1$$

Main Results on RF MEMS on Si (FBK Foundry)

- Low insertion loss for series (down) and shunt (up) switches ($\cong$-0.2 dB @ 20 GHz)
- High technological and electrical reliability and performances (more than 10^8 cycles for series, reliability over long actuation times for series and shunt, R=0.25 ohm or less for the contact resistance by using dimples)
- Exact frequency of operation for shunt switch by using the floating metal solution
- Circuital modelling of series and shunt
- IL < 1 dB for SPDT and IL < 2 dB for Matrices @ 20 GHz (CPW lines and bendings included)
- Isolation and Return Loss enhancement by using shunt SPST as additional components in SPDT and Matrices
- *Individuation and Theory of the charging effects in the realized devices, to mantain the pull-down voltages in the order of 40-50 volt and to prevent failure due to charging in dielectric materials (Schottky, Poole-Frenkel, Breakdown Voltages)*
- *Power handling up to 5 watt for actuation times in the order of 5 min with unchanged S-parameters after the power treatment*
- All of the above SPST configurations are currently studied for SPMT and Matrices

Charging Prevention

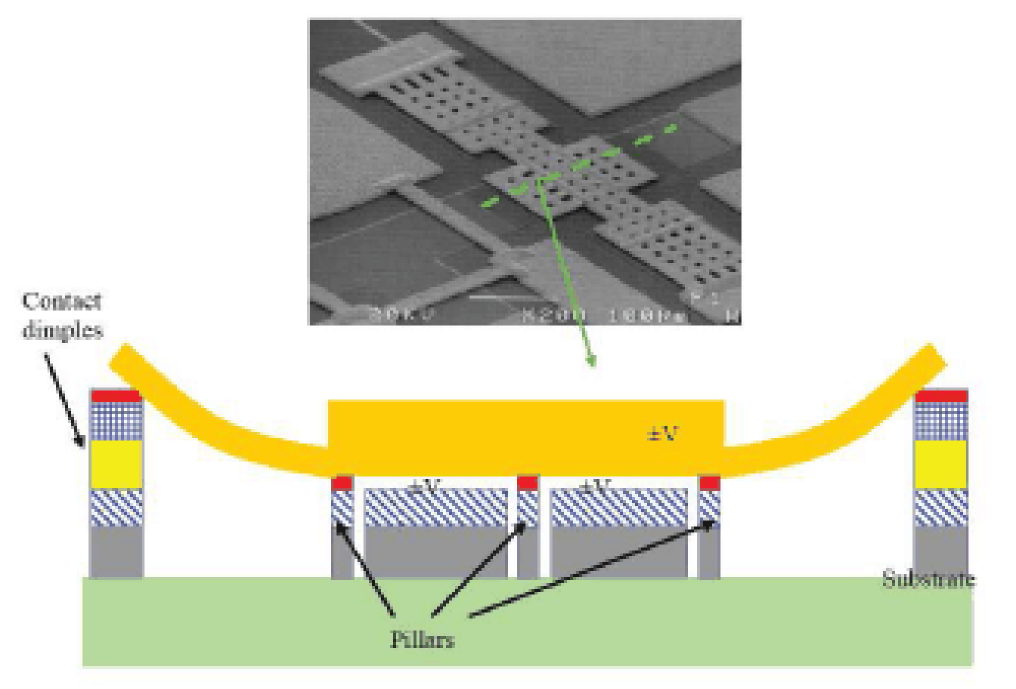

- Cross section of the double clamped series ohmic switch. Two lateral wings are used for improving the electrical contact at the I/O ports. The same no-contact actuation solution is used for the cantilever
- *Since no contact is imposed for the actuation pads charging prevention is obtained*.
- Vact= 40 to 50 volt ca. also after 10^5 cycles, and with unchanged RF performances up to 10^4.
- Problem to be solved: increase in the IL due to pillars damage after several actuations for the double clamped one.

Design and Technology for Pillars

Solution

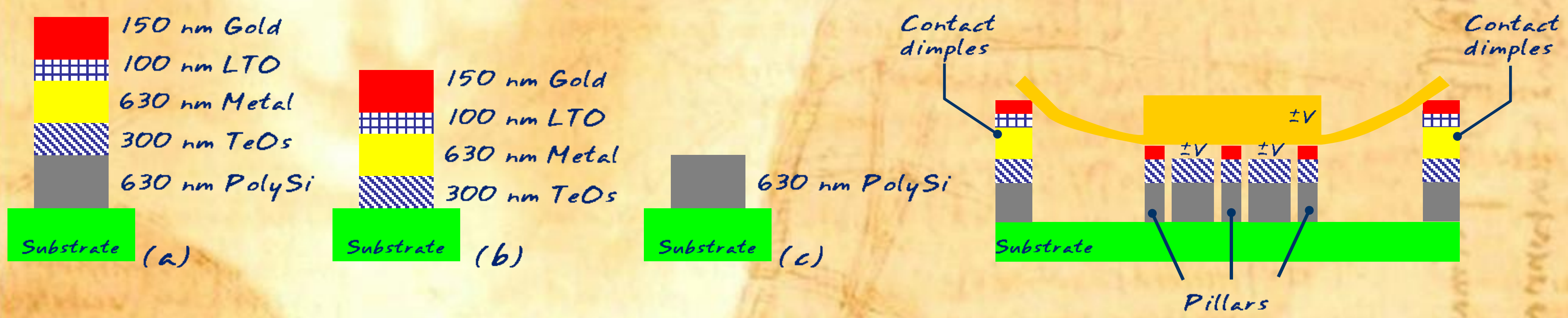

All SPST switches are monolithically manufactured on p-type, 200 μm thick, highly resistive silicon wafers by using the eight mask MEMS process developed at FBK-irst .

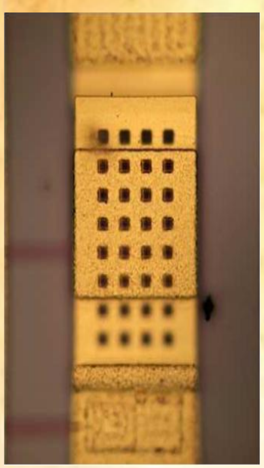

Name	Description
S_W	Stopping Pillars, no dielectric above the polysilicon pad, 5 circular bumps
S_W2	Stopping Strips instead of Pillars, no dielectric above the polysilicon pad, 5 circular bumps
S_W3	Like SW, 3 square bumps , longer and shaped wings, larger pad, no dielectric above the polysilicon pad, minimum overlap area
S_W4	Like SW, no dielectric above the polysilicon pad,11 rectangular bumps
S_Wdiel	Like SW but no stopping pillars, TEOS and LTO above the pad, 5 circular bumps

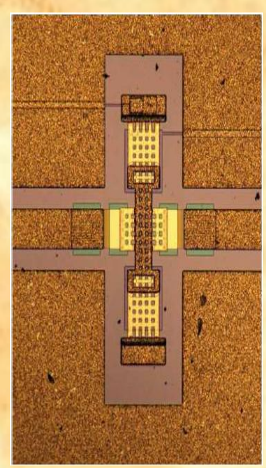

Name	Description
C_W	Stopping Pillars, No dielectric above the polysilicon pad, 7 circular bumps, dimensions 110x170 μm^2
C_W2	Stopping Pillars, No dielectric above the polysilicon pad, 7 circular bumps, dimensions 110x145 μm^2
C_W3	Stopping Pillars, No dielectric above the polysilicon pad,3 circular bumps, shaped cantilever tip
C_W4	Stopping Pillars, No dielectric above the polysilicon pad, 13 rectangular bumps, dimensions 110x170 μm^2
C_W5	Like CW, thicker Cantilever, No dielectric above the polysilicon pad, larger pads, no wing mechanism, 2 circular bumps
C_Wdiel	Like CW no pillars, TEOS and LTO above the polysilicon pad

IMM-Roma

Goals

Single Pole Single Throw (SPST) Ohmic series switches to be implemented in different topologies of Single Pole 4 Throw (SP4T), Double Pole Double Throw (DPDT) and then integrated in LTCC technology for the realization of Large Order Clos 3D networks.

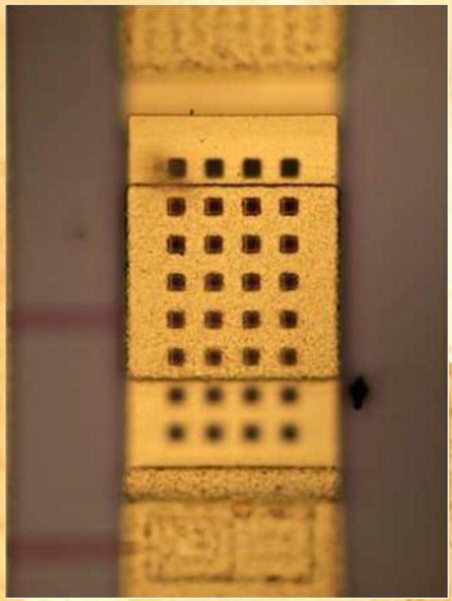

Top view of the cantilever MEMS switch

Top view of Series ohmic winged switch

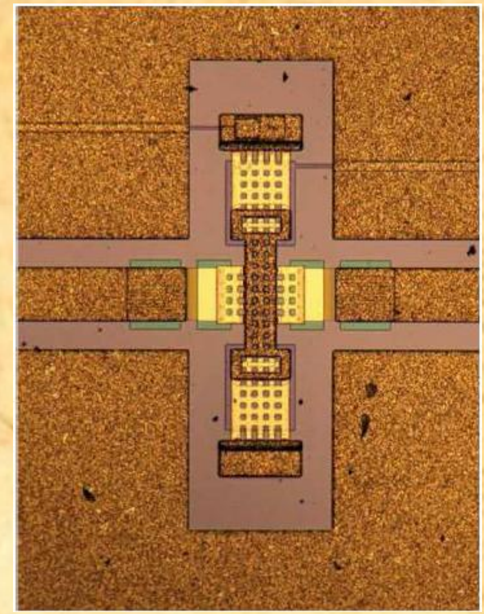

❖Recorded data vital for simulations on a 16x16 matrix, to decide the matrix topology and the expected fulfillment of the electrical performances for the overall system.

❖From preliminary simulations, based on single switch experimental data, Large Order Clos 3D networks embedded in a LTCC structure would be the best candidates for the final matrix.

Large Order Clos 3D networks, SP4T and DPDT technical specifications

Parameter	16x16 Switch Matrix Specifications	DPDT, SP4T Switching Unit Requirements
Frequency band	L, S, C, Ku or Ka-band	0-6 GHz
Bandwidth	Covering whole frequency band	0-6 GHz
Input match (50 Ohms)	15 dB max	22 dB max
Output match (50 Ohms)	15 dB max	22 dB max
Insertion losses	10 dB max	1 dB max
Gain variation	+/- 1dB	+/- 0 dB
Isolation between channels	50 dB min	40 dB min
Maximum input power	0 dBm	0 dBm

No failure is allowed for Matrix Applications !!!

SW RF Test

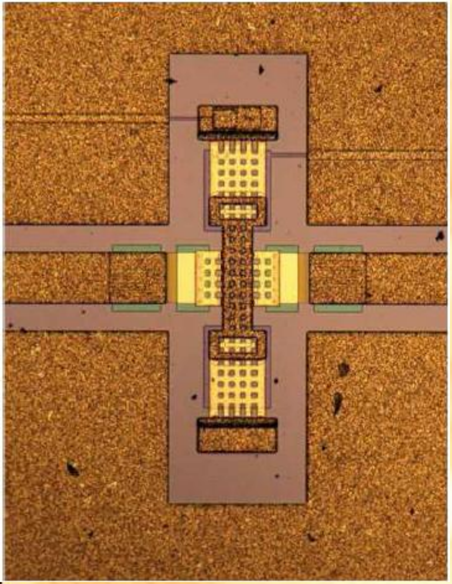

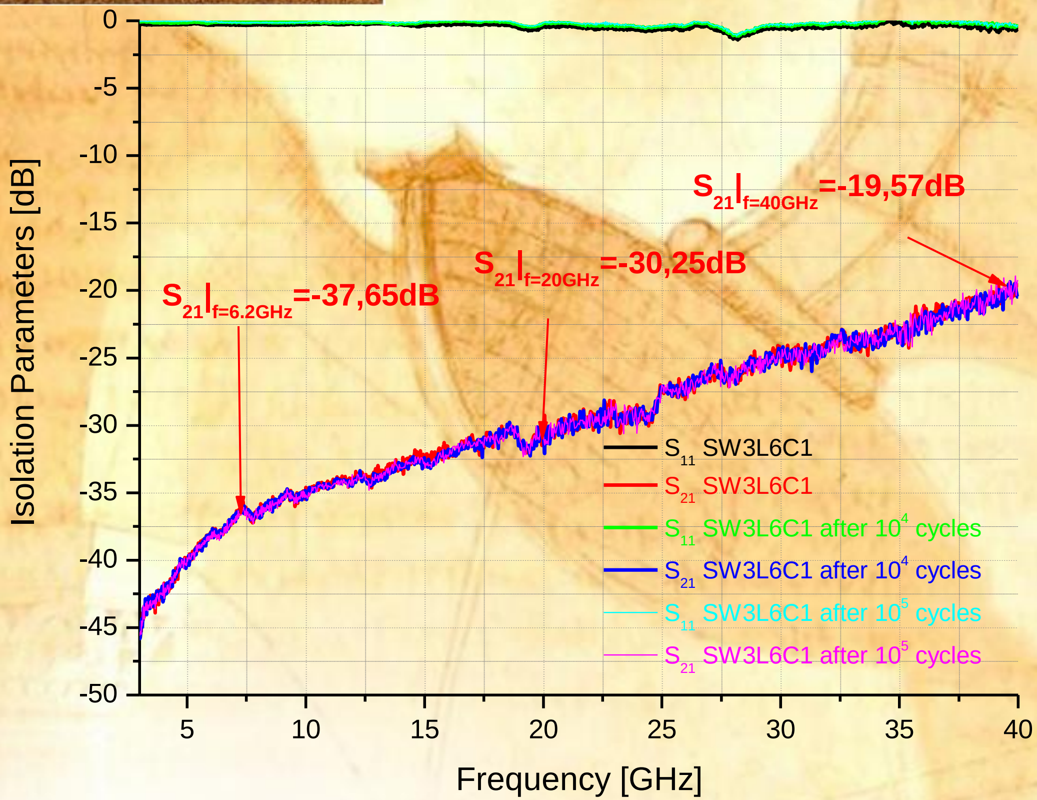

Isolation Parameters [dB]
Frequency [GHz]
$S_{21}|_{f=6.2GHz}$=-37,65dB
$S_{21}|_{f=20GHz}$=-30,25dB
$S_{21}|_{f=40GHz}$=-19,57dB
S_{11} SW3L6C1
S_{21} SW3L6C1
S_{11} SW3L6C1 after 10^4 cycles
S_{21} SW3L6C1 after 10^4 cycles
S_{11} SW3L6C1 after 10^5 cycles
S_{21} SW3L6C1 after 10^5 cycles

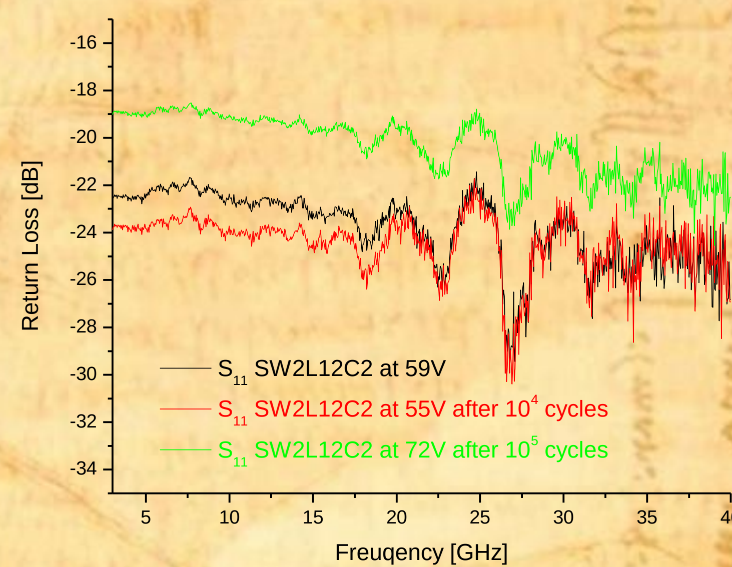

Return Loss [dB]
Freuqency [GHz]
S_{11} SW2L12C2 at 59V
S_{11} SW2L12C2 at 55V after 10^4 cycles
S_{11} SW2L12C2 at 72V after 10^5 cycles

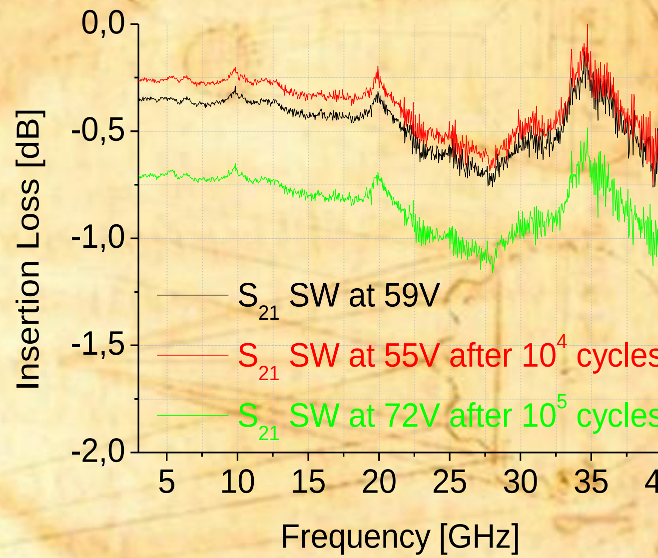

Insertion Loss [dB]
Frequency [GHz]
S_{21} SW at 59V
S_{21} SW at 55V after 10^4 cycles
S_{21} SW at 72V after 10^5 cycles

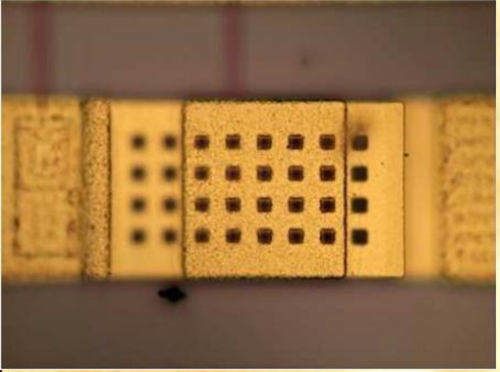

CW RF Test

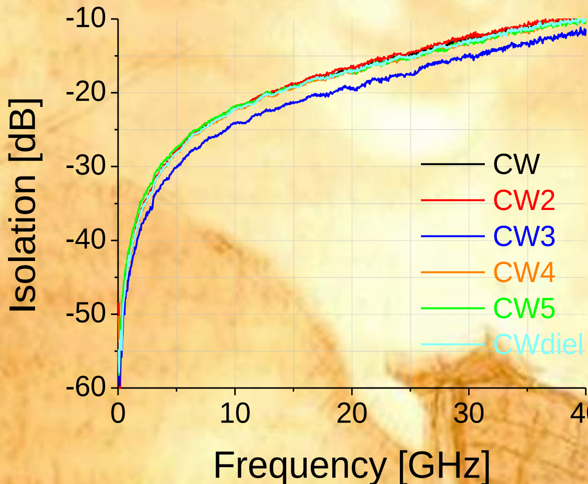

Isolation [dB]
Frequency [GHz]
CW
CW2
CW3
CW4
CW5
CWdiel

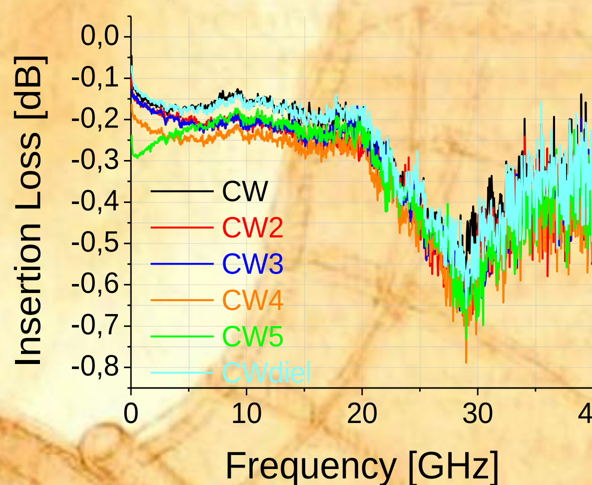

Insertion Loss [dB]
Frequency [GHz]
CW
CW2
CW3
CW4
CW5
CWdiel

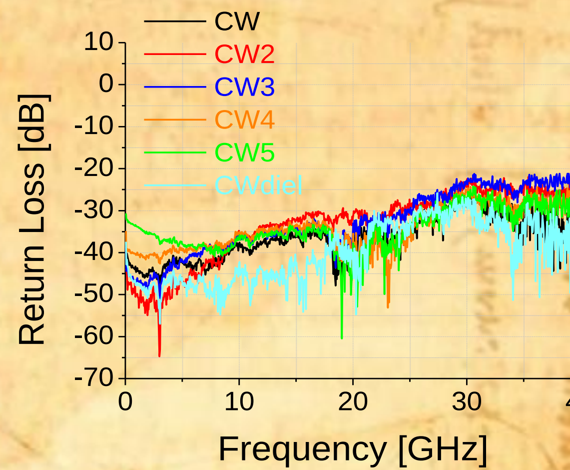

Return Loss [dB]
Frequency [GHz]
CW
CW2
CW3
CW4
CW5
CWdiel

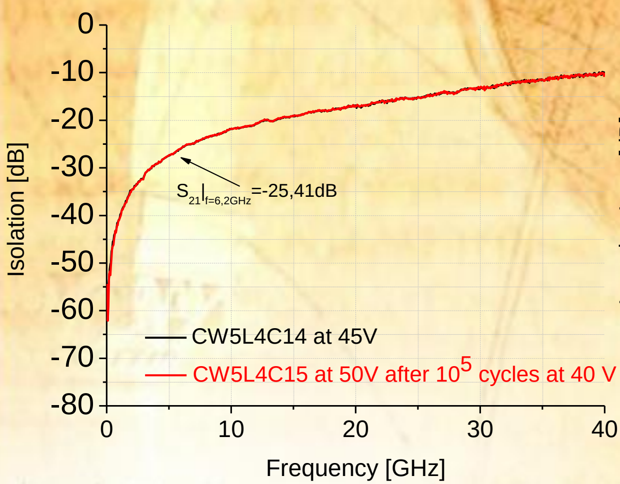

Isolation [dB]
Frequency [GHz]
S21|f=6,2GHz=-25,41dB
CW5L4C14 at 45V
CW5L4C15 at 50V after 10^5 cycles at 40 V

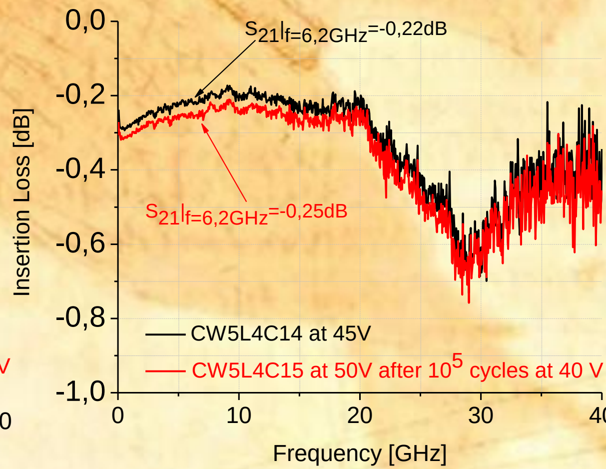

Insertion Loss [dB]
Frequency [GHz]
S21|f=6,2GHz=-0,22dB
S21|f=6,2GHz=-0,25dB
CW5L4C14 at 45V
CW5L4C15 at 50V after 10^5 cycles at 40 V

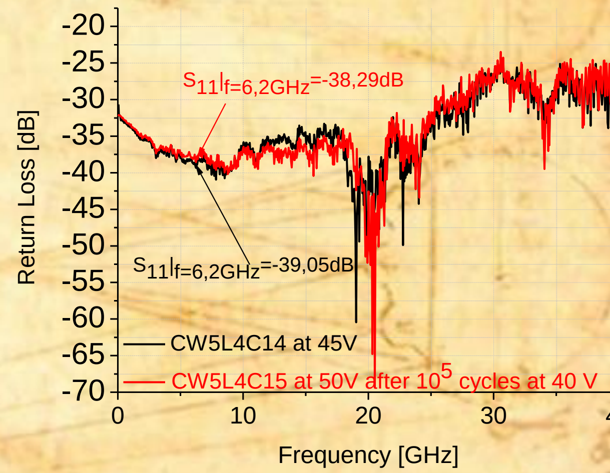

Return Loss [dB]
Frequency [GHz]
S11|f=6,2GHz=-38,29dB
S11|f=6,2GHz=-39,05dB
CW5L4C14 at 45V
CW5L4C15 at 50V after 10^5 cycles at 40 V

CNR-IMM Lecce Technology - GaAs

- RF MEMS shunt capacitive switches based on alternative materials like:
  - TaN films for the actuation pads (highly resistive)
  - Ta_2O_5 films for high ε dielectric layers to enhance the ON/OFF capacitance ratio
- Geometrical implementation of the switch (dimples on the bridge) and GaAs technology compatibility (III-V)

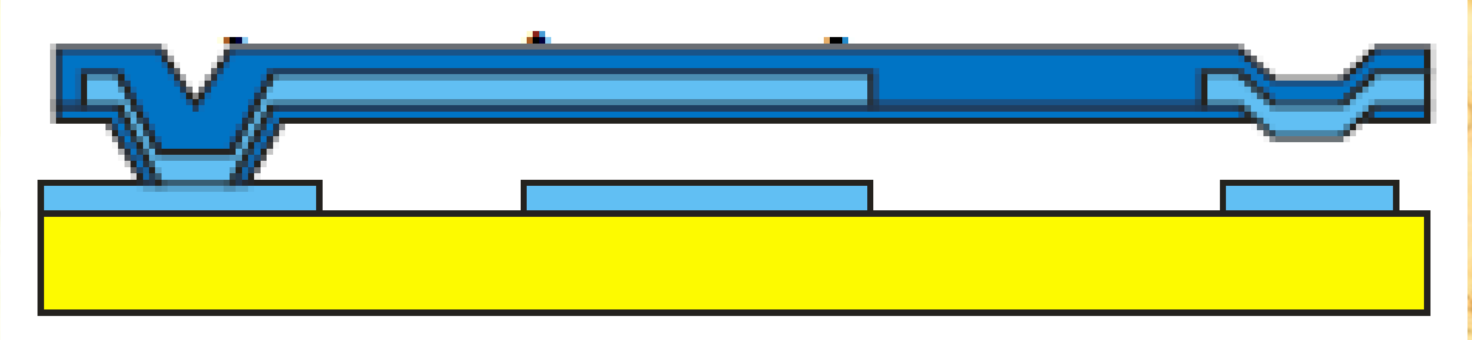

Actuation Electrodes

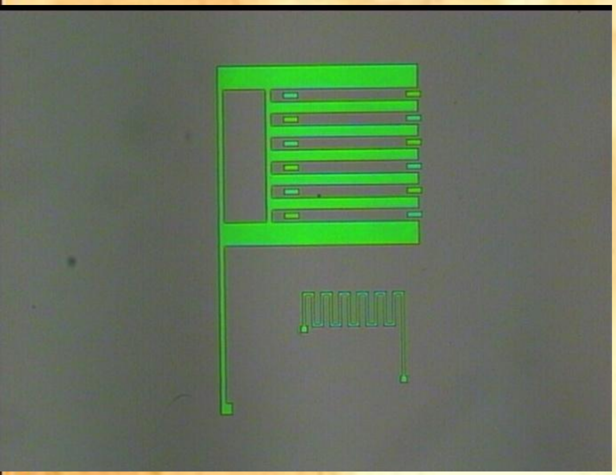

- TaN
  - Resistivity can change by six ordes of magnitude depending on the partial pressure during deposition
  - Thickness control by design requirements:
  - Manufacturing by Lift-off or by F dry-etching
- NiCr (?)
  - Evaluation in progress

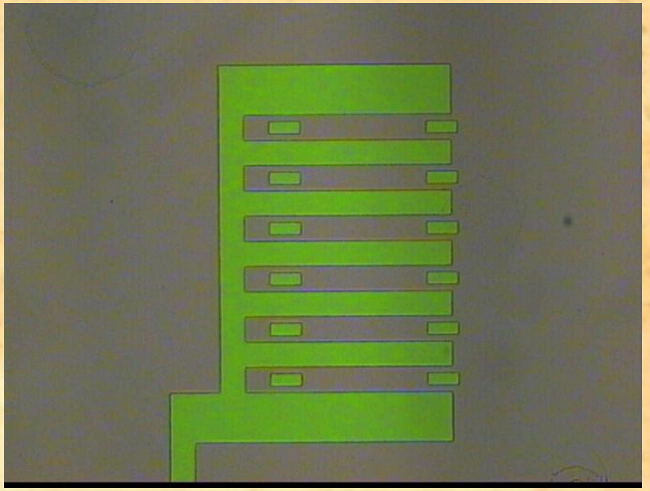

Tantalum Oxides

- Reactive DC magnetron sputtering, with Ta target
- Various mixtures for plasma feeding, with O2/(Ar+O2) = 30 – 50 – 66 – 100 %
- Various deposition temperatures, with T = 25 – 300 °C

Capacitance Measurements

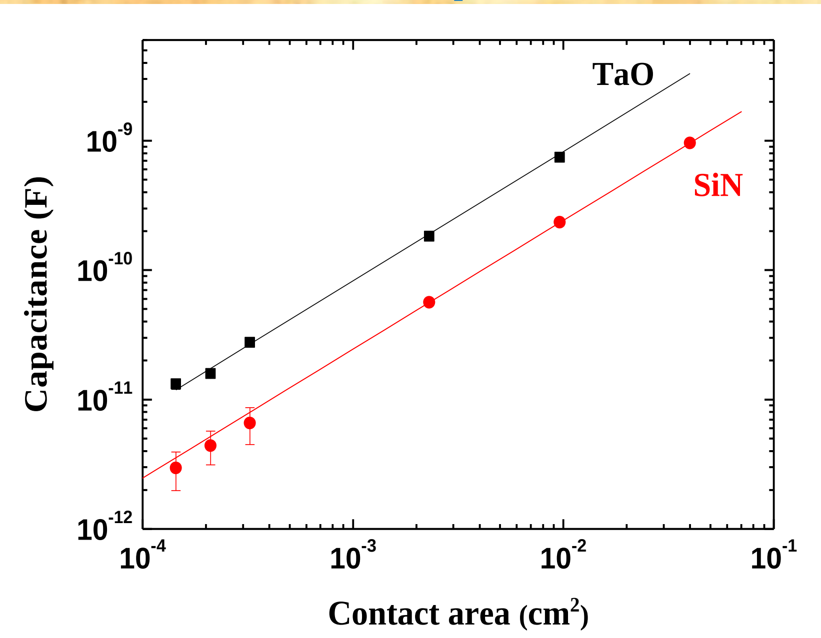

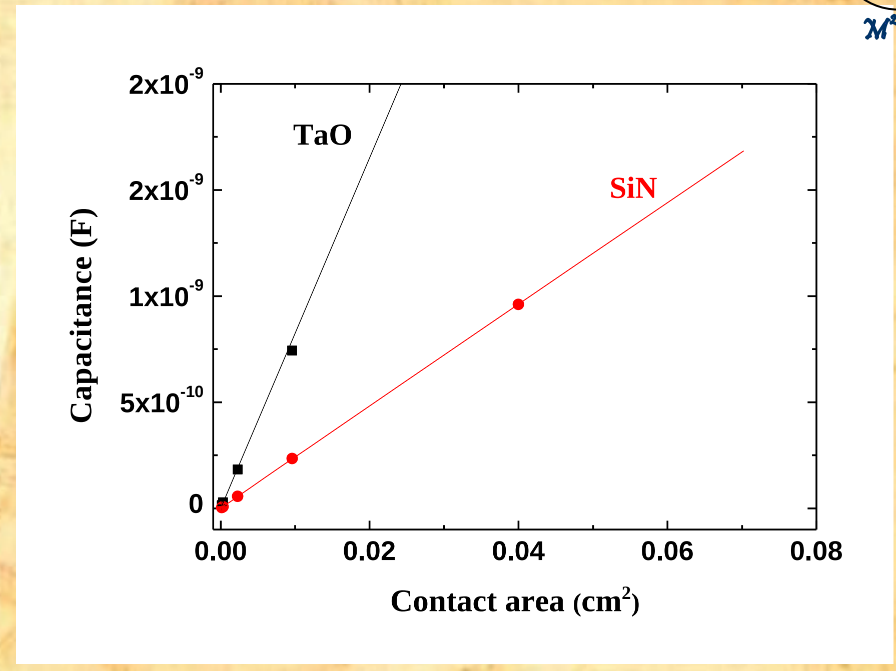

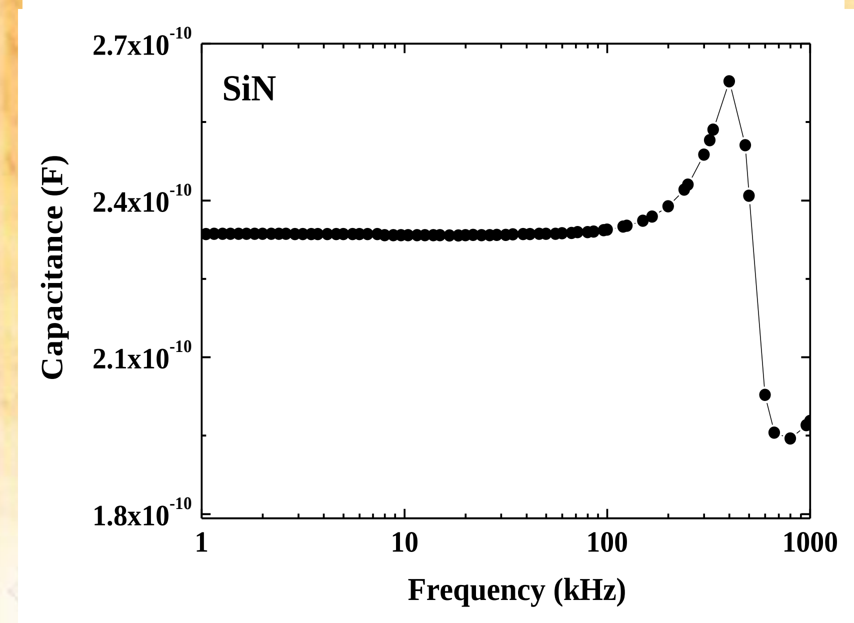

- Linear Capacitance Vs MIM Area
- Dielectric Constant (as in literature):
  - TaO ~ 28
  - SiN ~ 6.4
- Stable response Vs frequency in the range 1kHz-1MHz, exception done for a resonance effect around 500 kHz

I-V Characteristics (Charging)

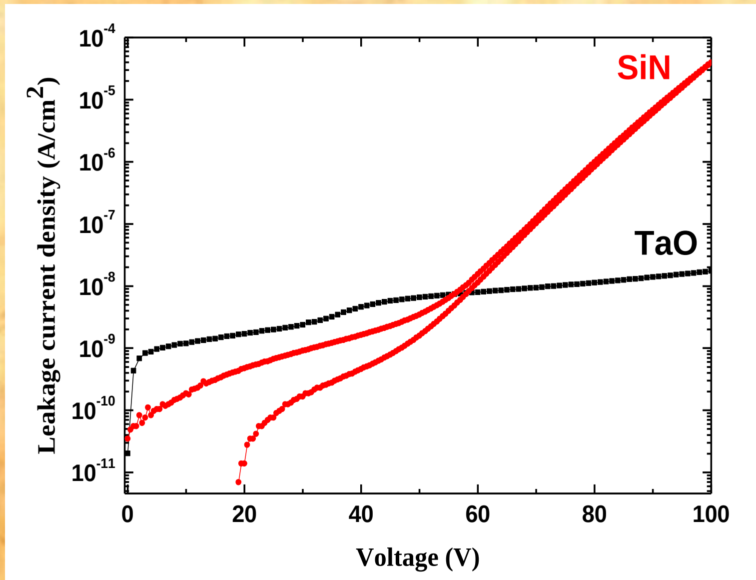

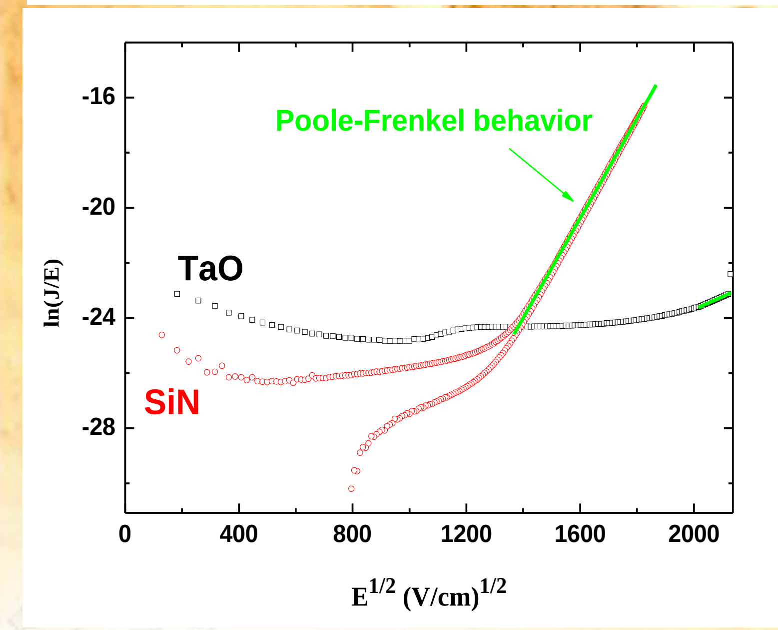

- Poole-Frenkel Effect
  - SiN when V > 50 V. Slope close to that expected for εr = 6.4 (0.018 Vs 0.012
  - TaO when V~breakdown
- Current densities:
  - Lower for TaO with respect to SiN when V > 50 V
  - Higher stability for SiN by increasing the MIM area,
  - SiN more homogeneous than TaO
- The same breakdown for both of them (~140 V)

RF characteristics of shunt switches with Ta_2O_5 and TaN

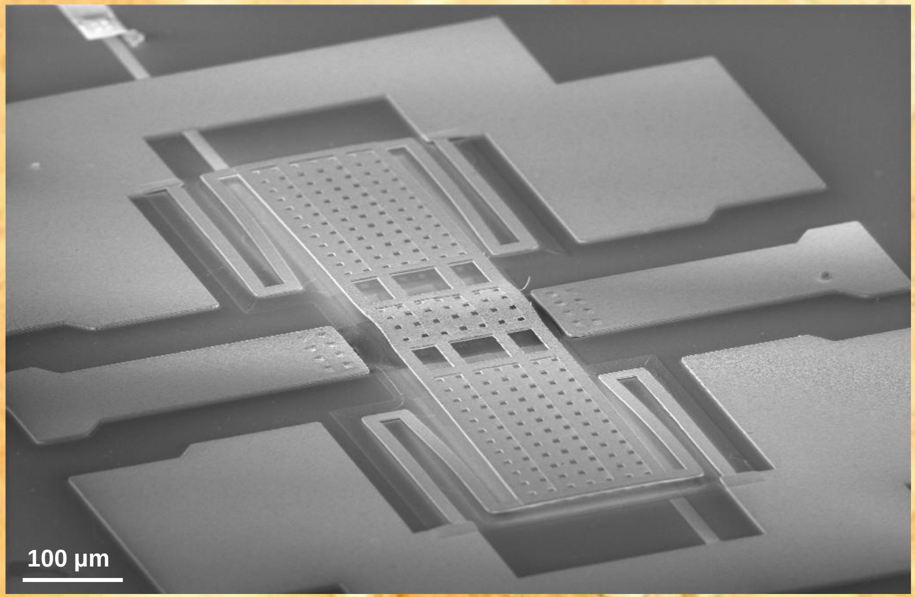

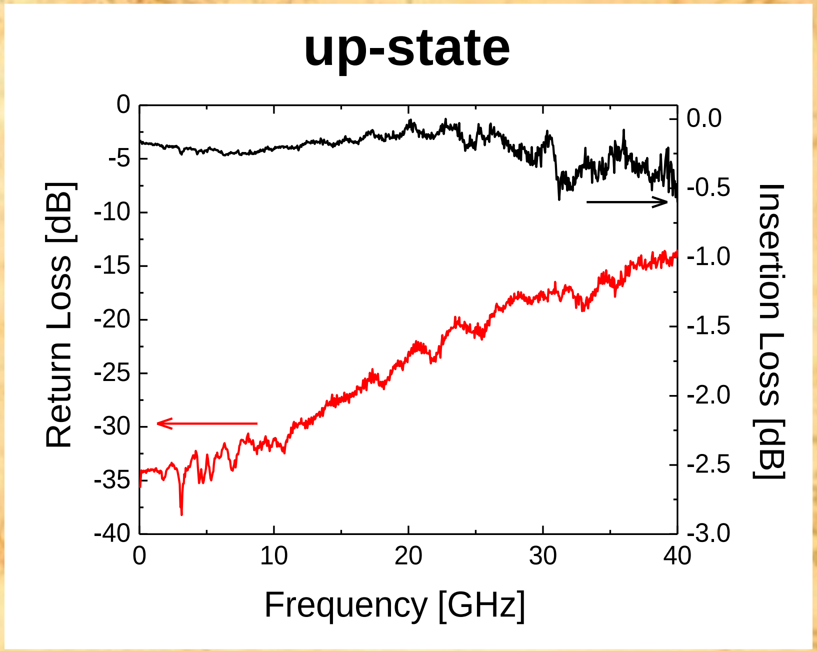

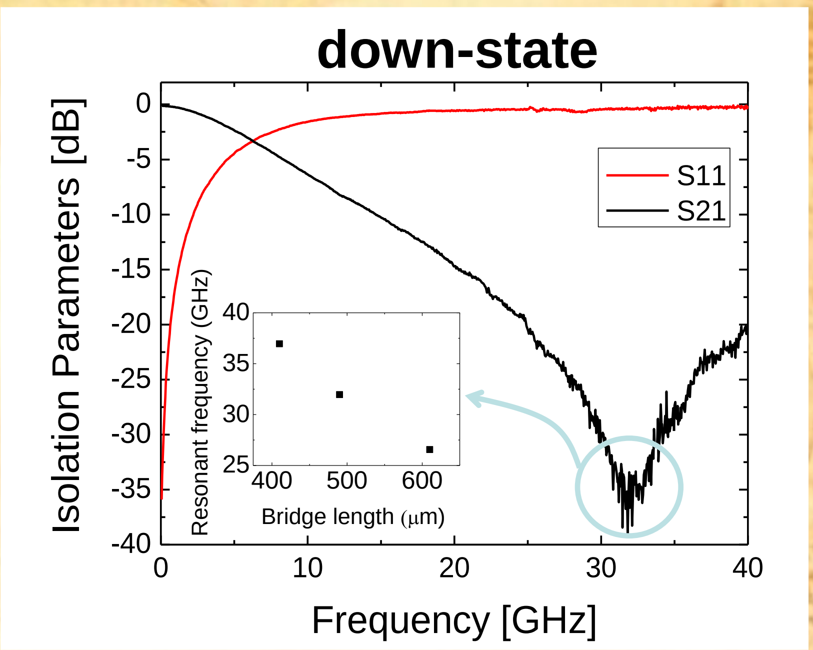

Up-state

- Insertion Loss ≦ 0.2 dB up to 28 GHz
- Return Loss < - 20 dB up to 26 GHz

Actuation voltage = 10-15 V ca.

Down-state

- Resonant frequency = 20-40 GHz (isolation≈-40dB)

IMM Roma
SU-8 based Micro-Systems, DC≤F ≤100 (?) GHz

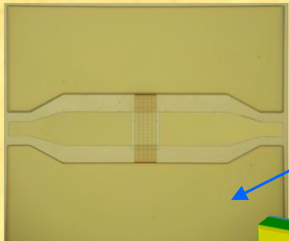

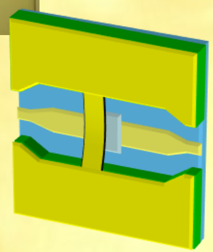

Micro-mechanical switches for low-loss, all-passive redundancy circuits and phase shifters

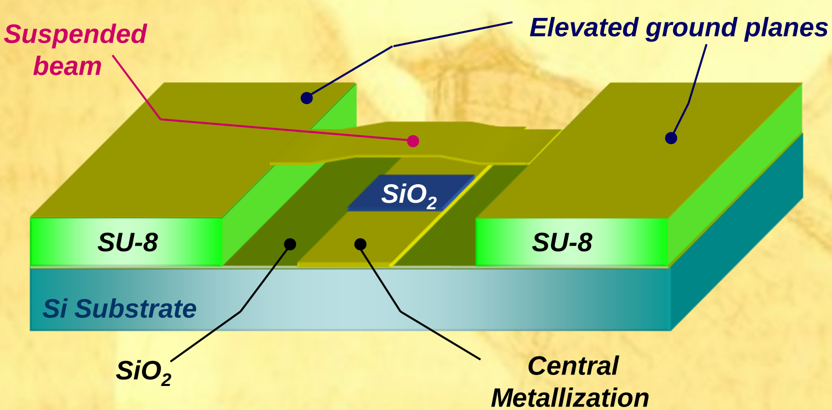

Release of the sacrificial layer

Plasma O_2 (*)

Wet etching

Work in Progress

(*) with SELEX-SI
Currently at IMM Roma in cooperation with IMM Lecce

1. The f_0 peak decreases, as expected, when the bridge width increases
2. The amplitude of S_{21} allows an isolation of 30 dB or better as expected from simulations.

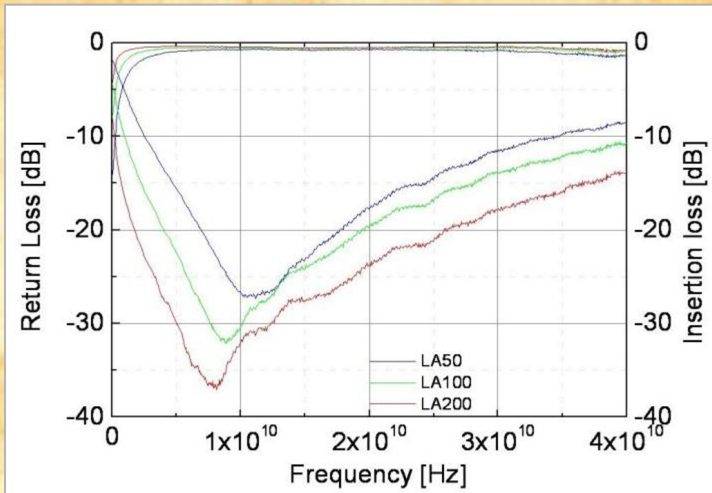

IMM-Roma

IMM-Roma

IMM Roma Switch

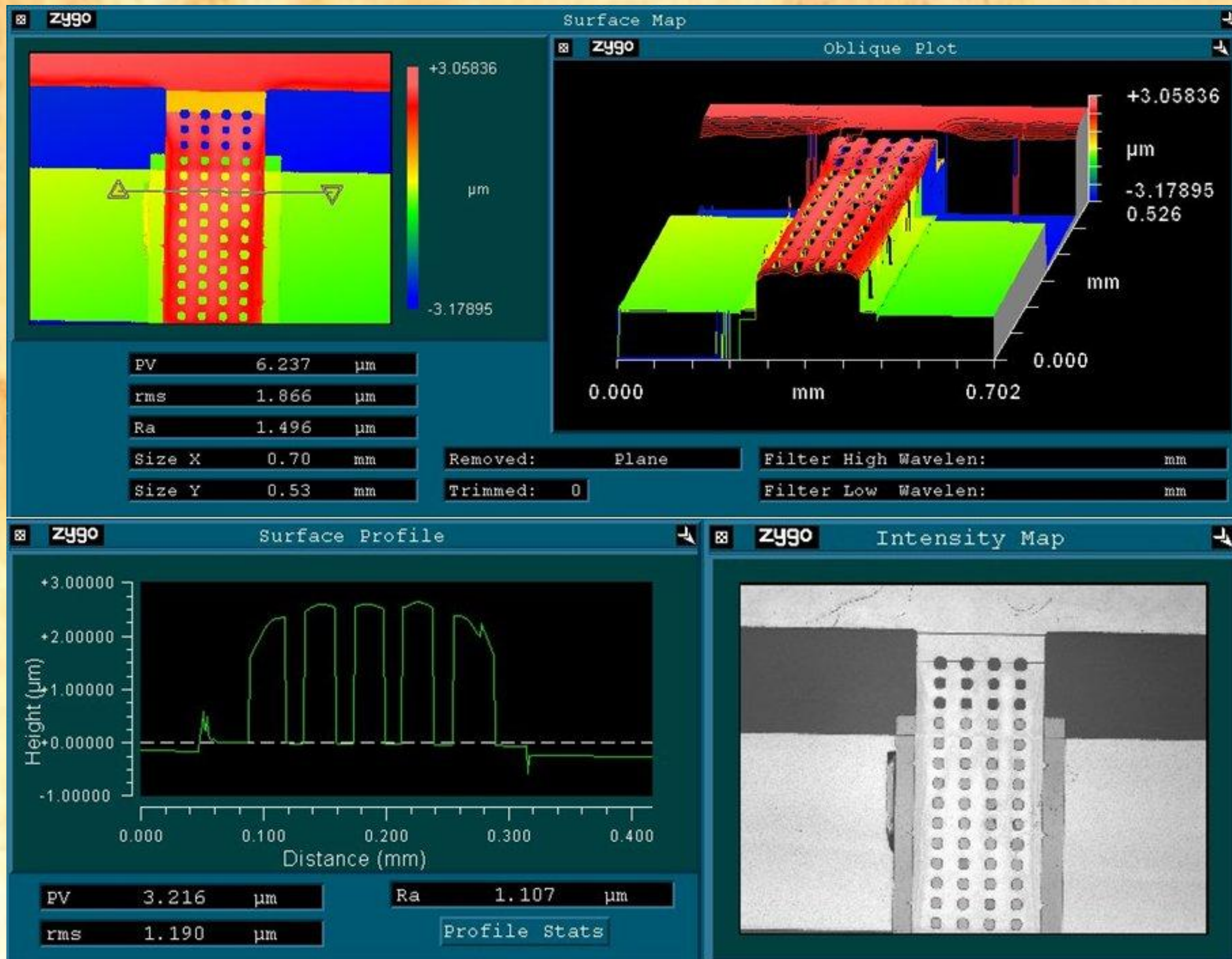

Optical microscopy characterization of the RF MEMS switch realized by means of SU-8 photo-lithography with evidence for the optimized profile of the beam after the removal of the sacrificial layer.

Mechanical Simulations (analytical and FEM)

$$m\ddot{z} = F_e + F_s + F_p + F_d + F_c$$

$$v_{act}(d) = \sqrt{\frac{(C_{OFF} - C_{ON})V^2 - kg^2 - \frac{1}{2}k_s g^4}{m + 2\frac{\alpha}{\omega}}} \rightarrow \left(\sqrt{\frac{(C_{OFF} - C_{ON})V^2 - kg^2 - \frac{1}{2}k_s g^4}{m}}\right)_{\alpha \to 0}$$

$$v_{act}(z) = \sqrt{\frac{[C(z) - C_{ON}]V^2 - k[z - (d+g)]^2 - \frac{1}{2}k_s[z - (d+g)]^4}{m + 2\frac{\alpha}{\omega}}}$$

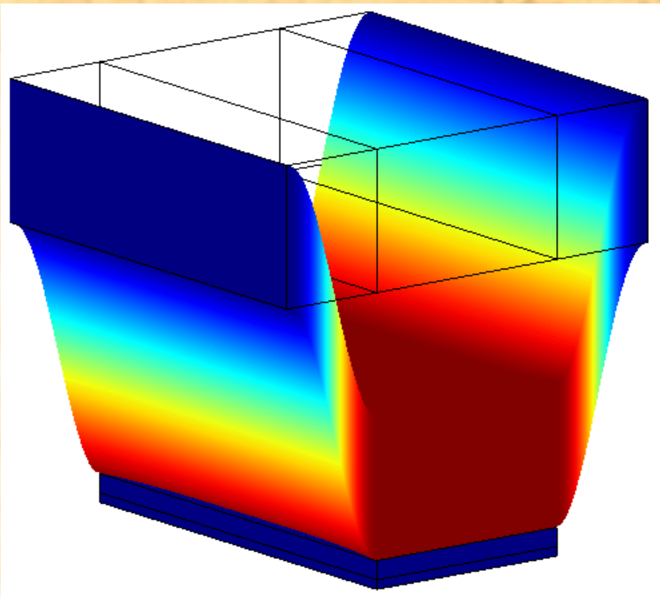

$$\tau_{act} = \int_0^{\tau_{act}} dt = \int_{v_{in}}^{v_{act}} \frac{dz}{v(z)}$$

3D COMSOL simulation of the RF MEMS shunt capacitive switch in the OFF state (bridge in the down position), centrally actuated. The result is coherent with the prediction performed by using the analytical approach and the 2D actuation. V=20 volt ca. is expected and V=24 volt experimentally obtained. Actuation times around 50 µs are estimated.

IMM-Roma

Nonlinear response of a double clamped beam (instability)

$$P_{RF} = \frac{1}{2} V_{RF} I_{RF} = \frac{1}{2} \frac{V_{RF}^2}{Z_0} = P_{in}$$

$$P_{out} = P_{in} - \left[P_M + P_r \right]$$

$$V_{RF} = \sqrt{2 Z_0 P_{in}} < V_{threshold} = \sqrt{\frac{8}{27} \frac{k}{\varepsilon A} g^3}$$

$$k = k_E + k_\sigma = K_1 \left(32\, E w r^3 \right) + \\ + K_2 \left[8 \sigma (1 - \nu) w r \right]$$

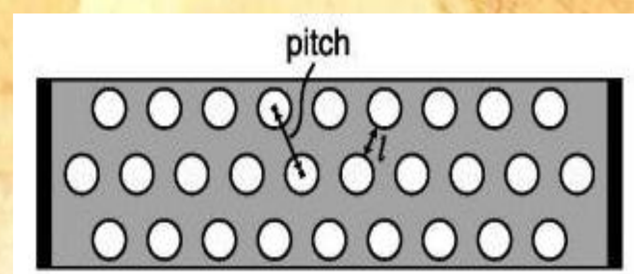

Transversal excitation

$$E_M = \frac{1}{2} C V_{RF}^2 \qquad \omega_M = \sqrt{\frac{k}{m}} = 2\pi f_M \quad ; \quad f_M = \frac{1}{2\pi} \sqrt{\frac{k}{m}}$$

$$P_M = \omega_M E_M = \frac{1}{2} \omega_M C V_{RF}^2$$

Longitudinal excitation

$$P_{long} = \frac{1}{2} \omega_{long} C V_{RF}^2$$

$$f_{long} = \frac{v_{long}}{\lambda_{long}} = \frac{1}{2L} \sqrt{\frac{T}{\mu_{eff}}} = \\ = \frac{1}{2L} \sqrt{\frac{T}{m_{eff} L}} = \frac{1}{2L} \sqrt{\frac{k_\sigma}{m_{eff}}}$$

Spectrum

$$I_{out}(\omega_{RF}) = 1 - \frac{2\left(P_M + P_{long} \right)}{P_{in}} = 1 - 2 Z_0 \left(\omega_M + \omega_{long} \right) C$$

$$I_{out}(\omega_{RF} \pm \omega_M) = \frac{P_M}{P_{in}} = Z_0 \omega_M C$$

$$I_{out}(\omega_{RF} \pm \omega_{long}) = \frac{P_{long}}{P_{in}} = Z_0 \omega_{long} C$$

200 µm wide bridge RF response
24 volt actuation voltage

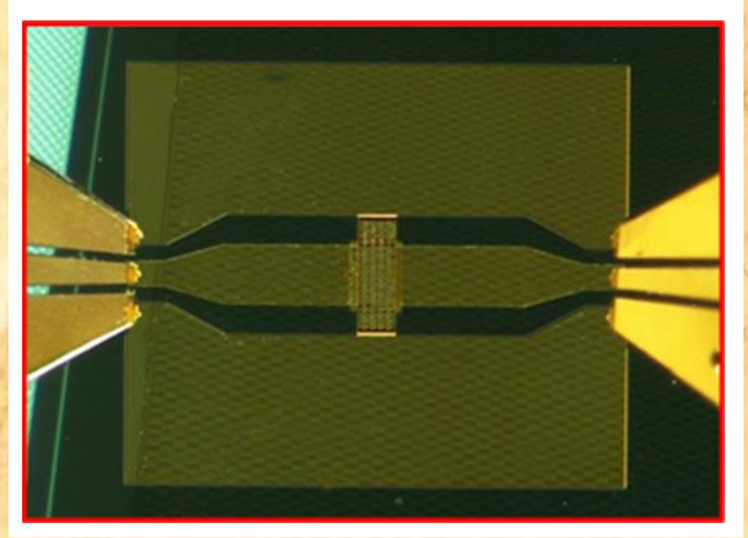

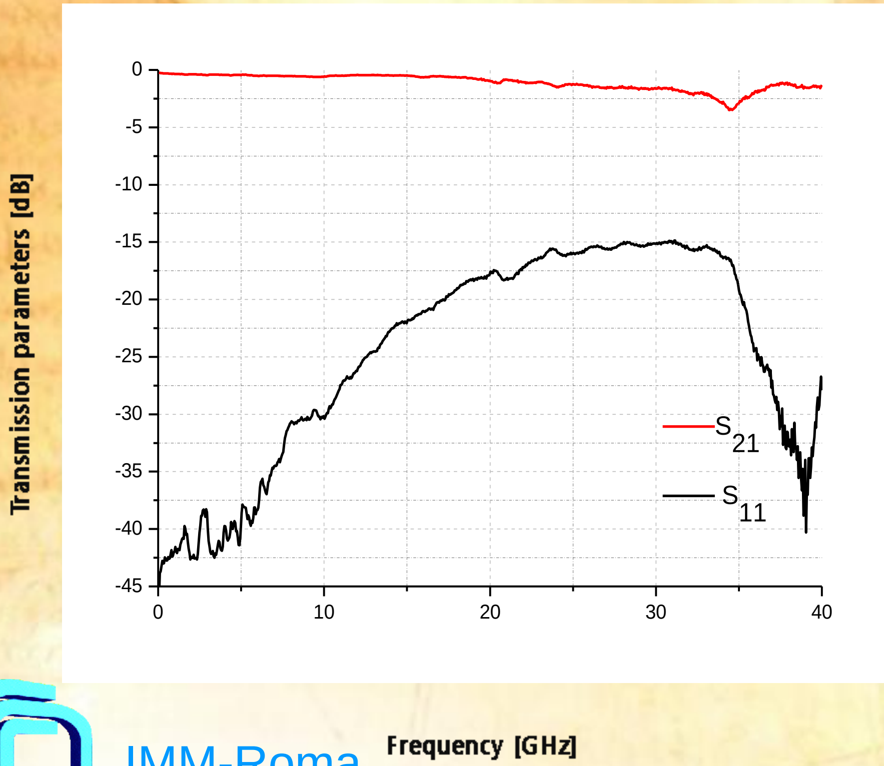

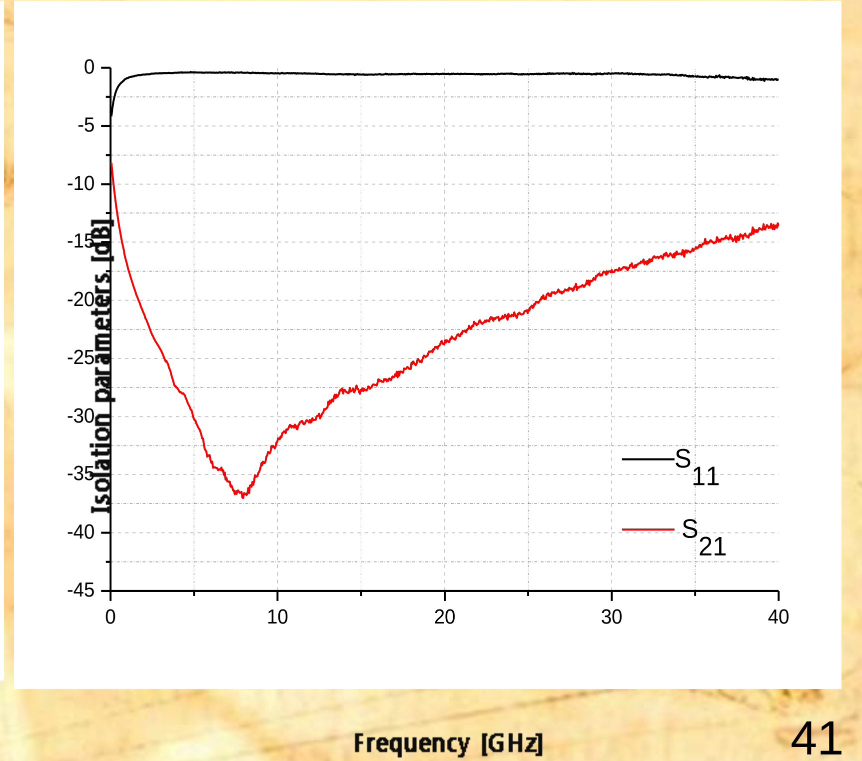

LTCC based Micro-Systems (F≤50 (?) GHz)

Phase
0 Substrate preparation
1 Conductive Pattern
2 DC Actuation Lines
3 High R Lines
4 Passivation film
5 Anchors windows
6 Dimples
7 Bridge Membrane
8 Sacrificial layer release

In cooperation with SELEX-SI and VTT-Oulu, Finland

Low-Temperature Co-fired Ceramics, LTCC, is a low cost ceramic material suitable of high level packaging and good electrical performances, presently studied for ground and space subsystems, like micro-switches and true-time-delay-lines, TTDL

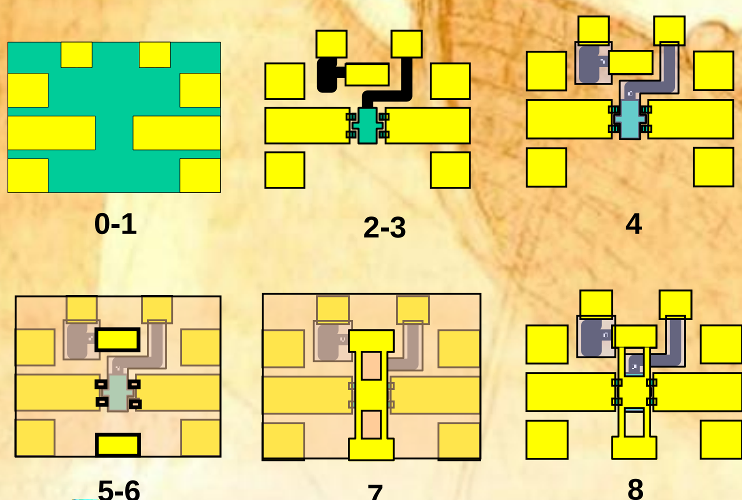

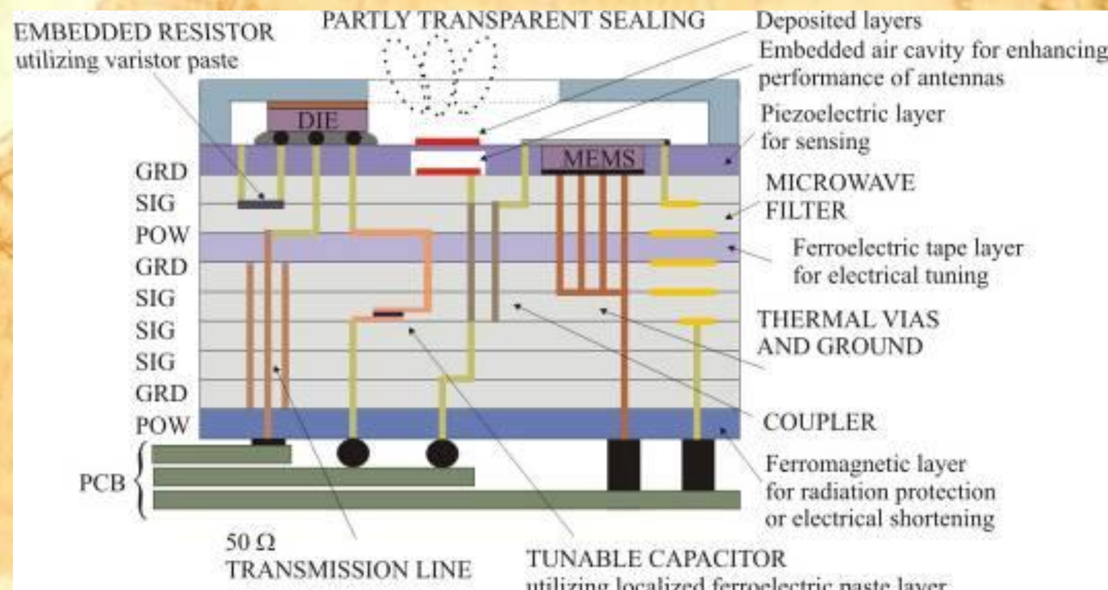

IMM-Roma

True Time Delay Line (TTDL) Generalities

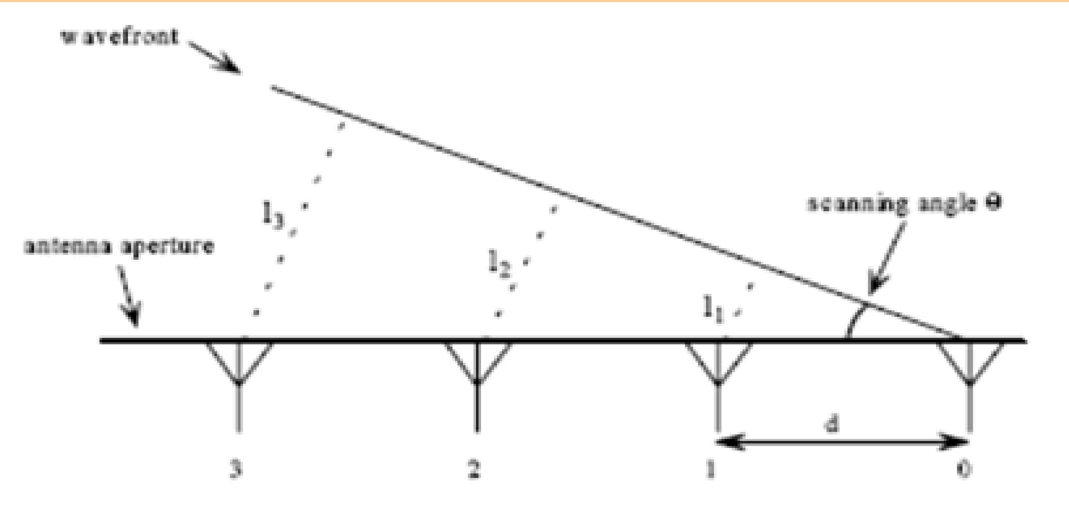

To synchronize the different arrival times of the wave-front with respect to the antenna radiating elements, the incident signal at the radiating element with the number ‘0’ has to be delayed by a time τ_{max} with a TTDL.

$$\tau_{MAX} = \frac{(n-1)\cdot d \cdot \sin(\vartheta)}{c}$$

n =number of radiating element

c =velocity of the light respect to the vacuum

d =distance between antenna radiating elements

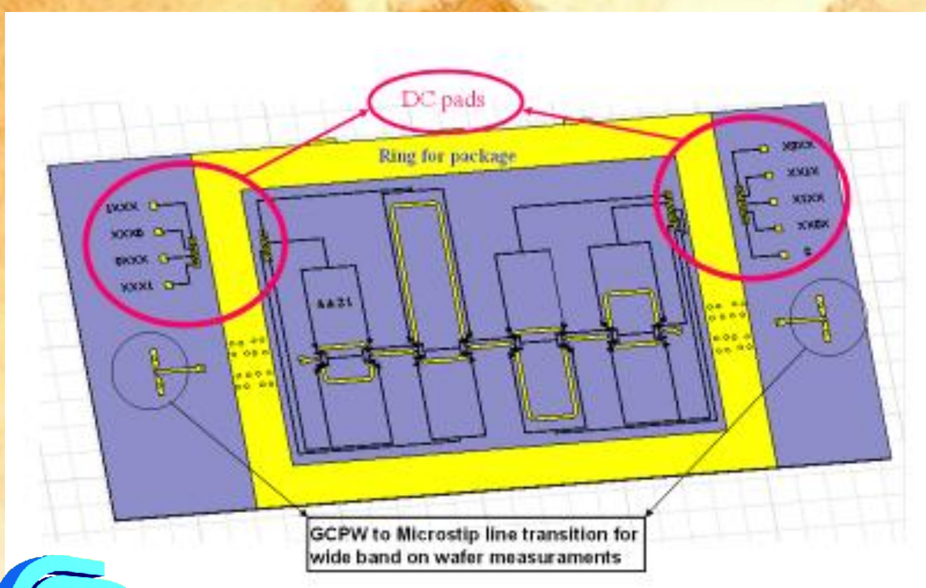

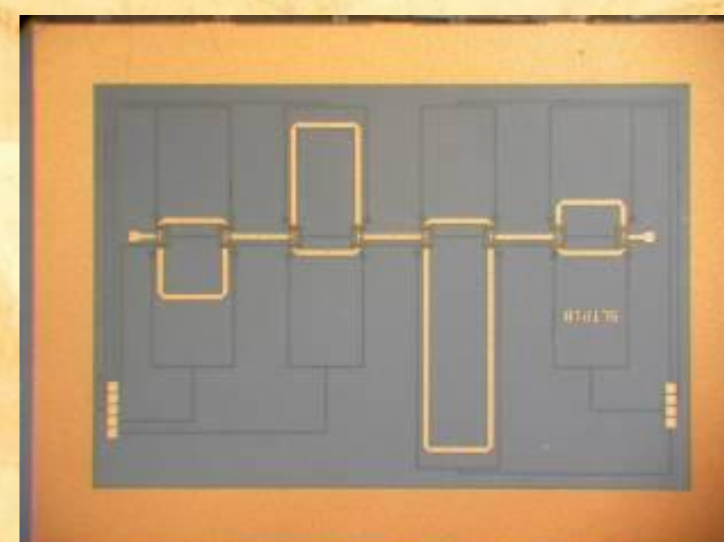

IMM-Roma

IMM-Roma

LTCC TTDL RF Performances

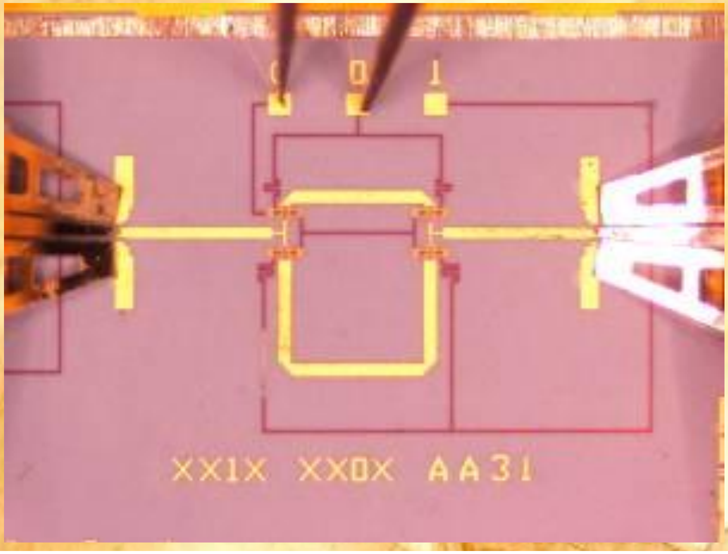

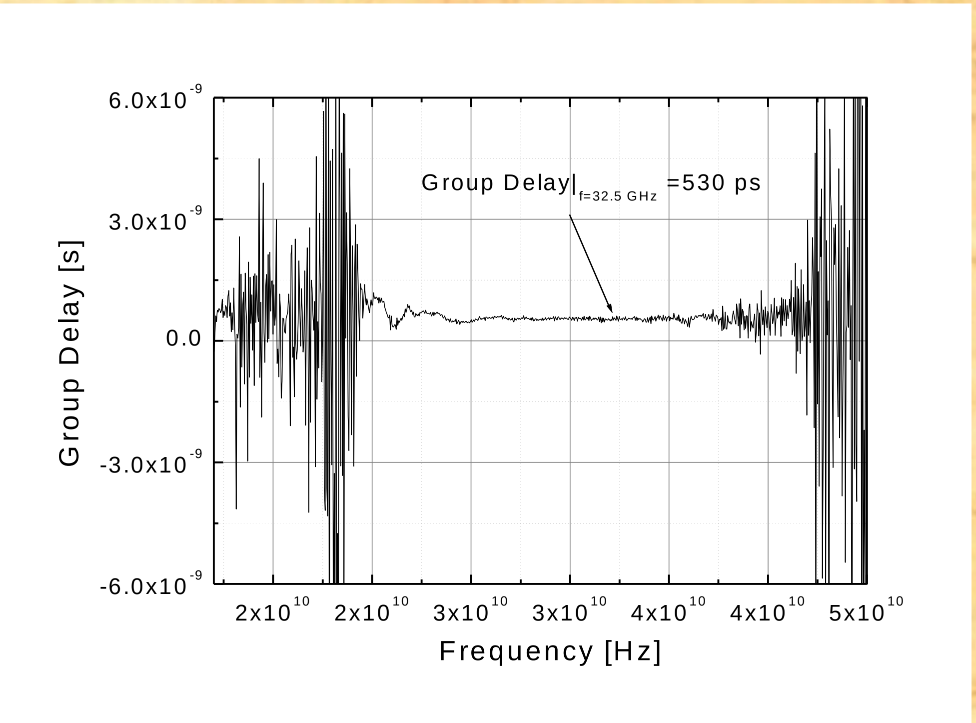

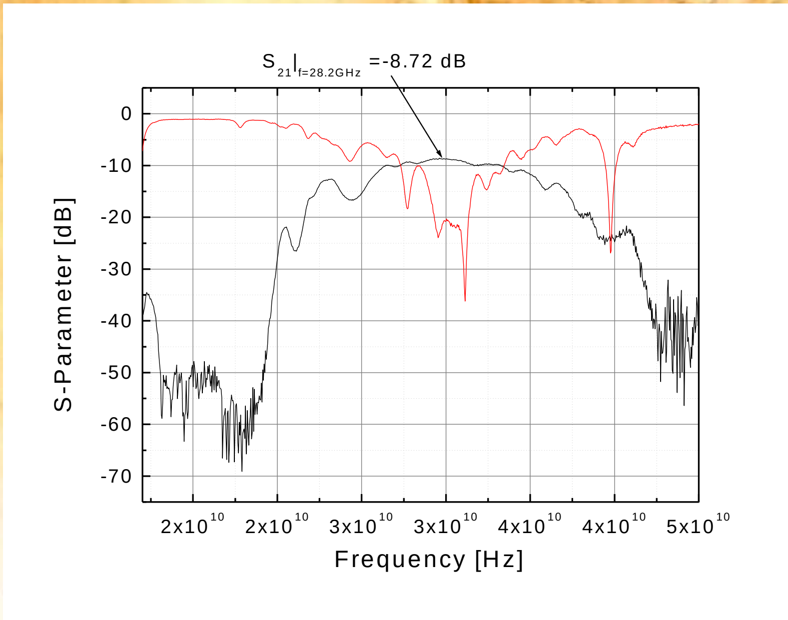

RF response and Delay Time of the TTDL

IMM-Roma

Hybrid Solutions for TTDL: Si RF MEMS with alumina packaging

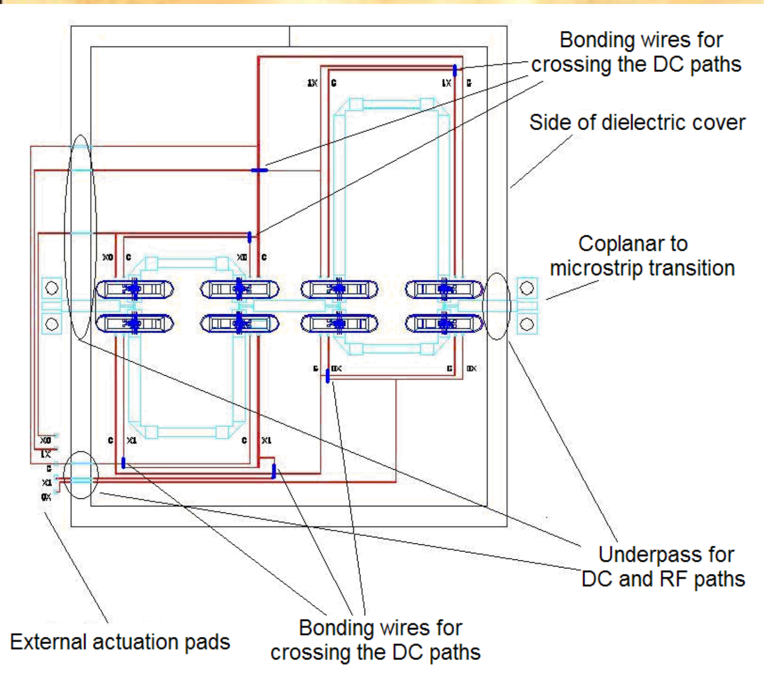

With SELEX-SI, FBK-irst and STM

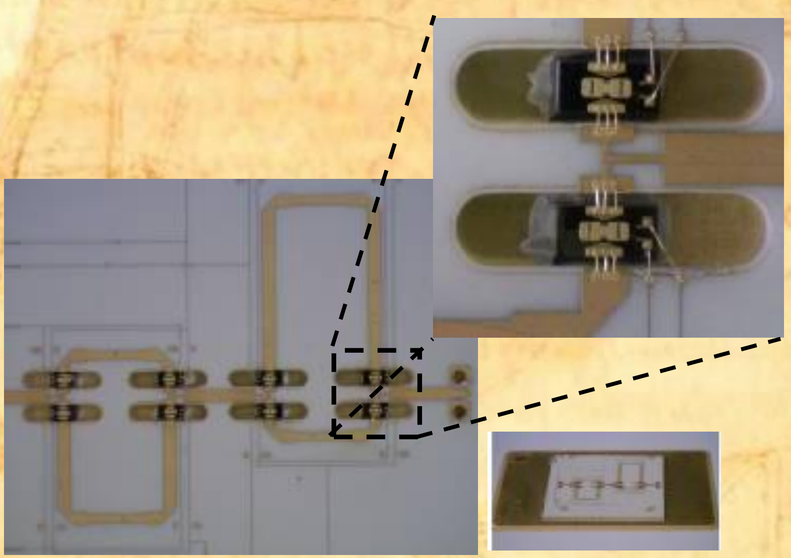

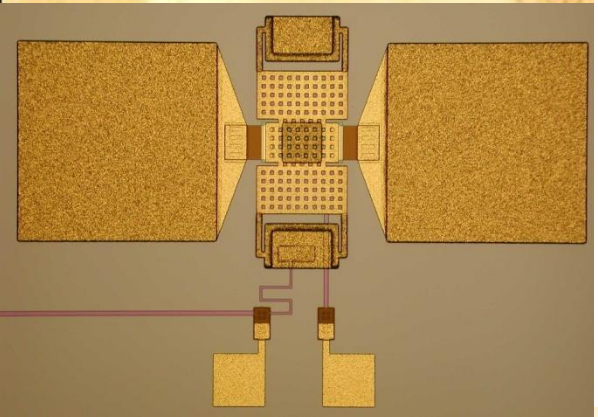

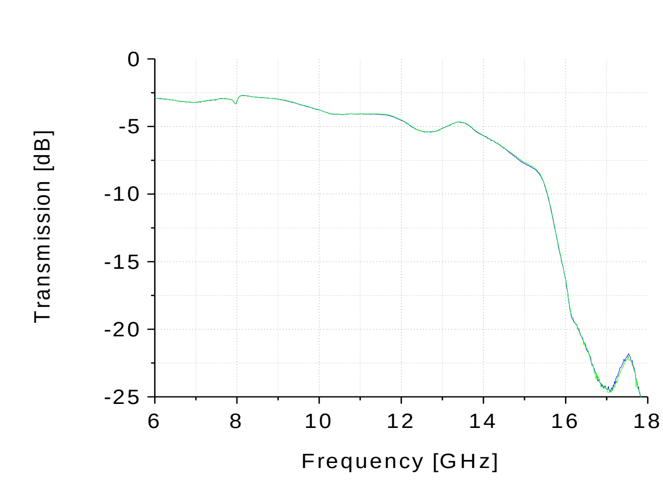

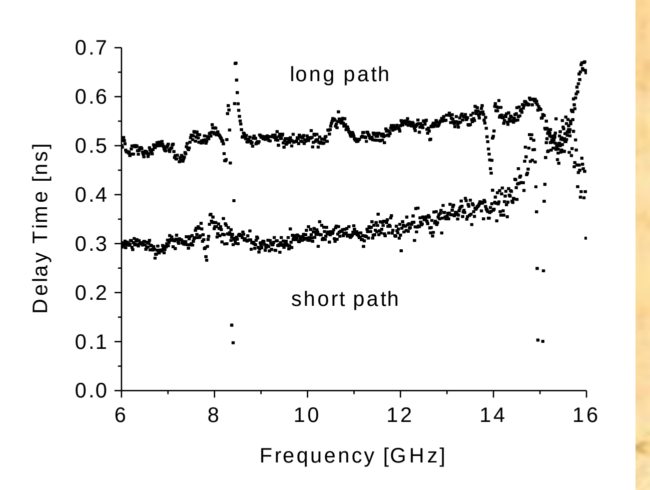

Implementation of RF MEMS in Phase Shifter Configurations

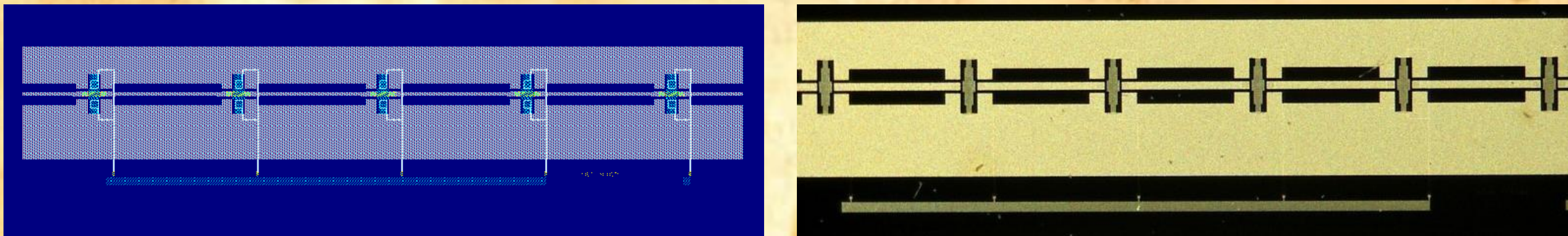

GDS Layout and photo of a 5 cells, Loaded Line Phase Shifter

In cooperation with FBK-irst, Povo (TN) and University of Roma "Tor Vergata", CONAE Argentina

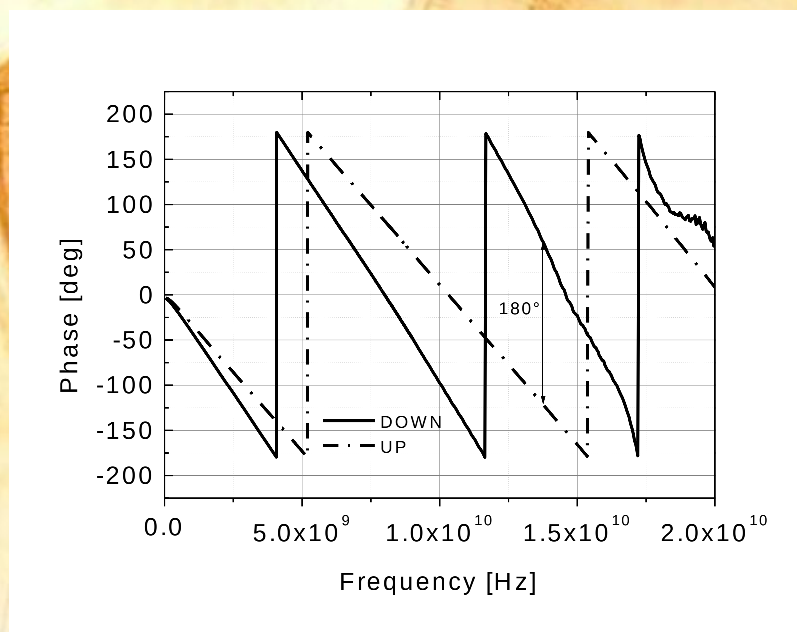

IL=-1.5 dB
RL=-20 dB

IMM-Roma

Backed (Grounded) Coplanar Waveguides - 1

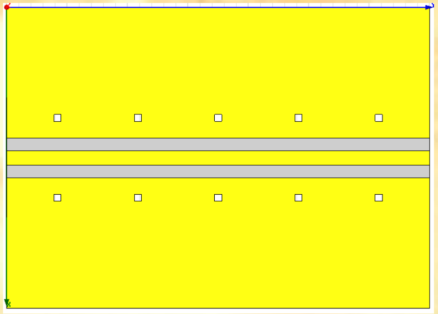

(a)

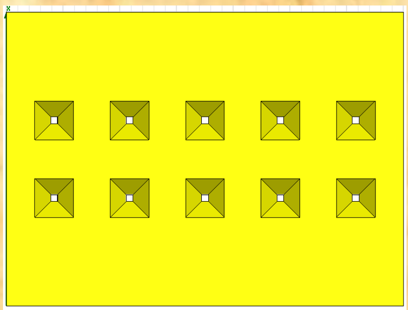

(b)

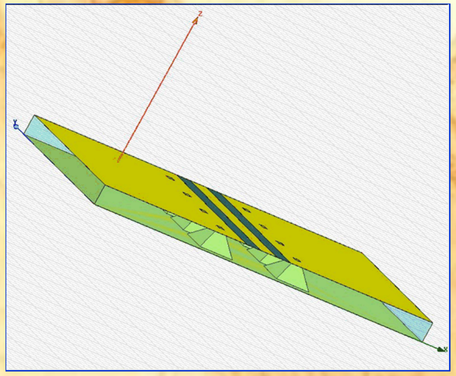

(c)

Example of the studied CPWG: (a) top view, (b) bottom view, and (c) tilted view with evidence for the 3D structure.

IMM-Roma

Backed (Grounded) Coplanar Waveguides - 2

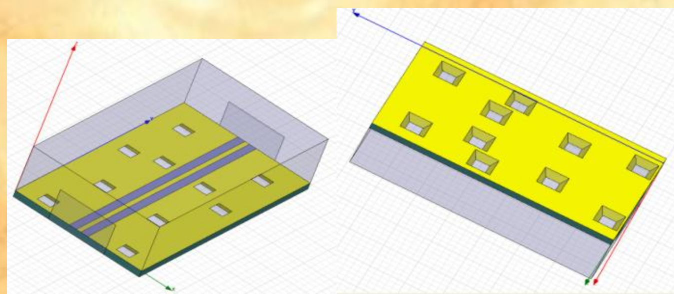

(a)

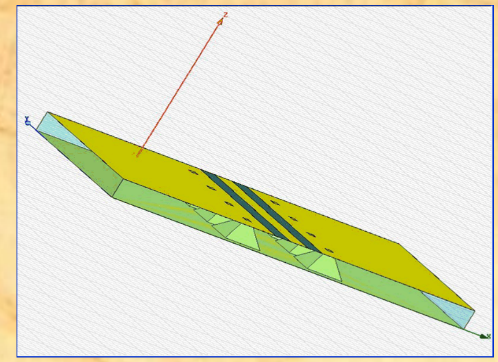

(b)

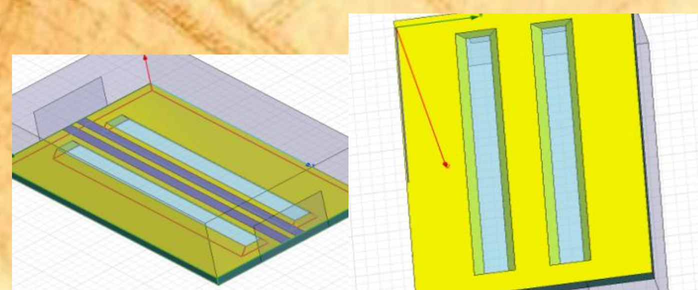

(c)

Studied CPWG structures: (a) random position of the via holes, (b) in line position of the via holes and (c) long vias.

IMM-Roma

The Microwave WEB

Backed (Grounded) Coplanar Waveguides - 3

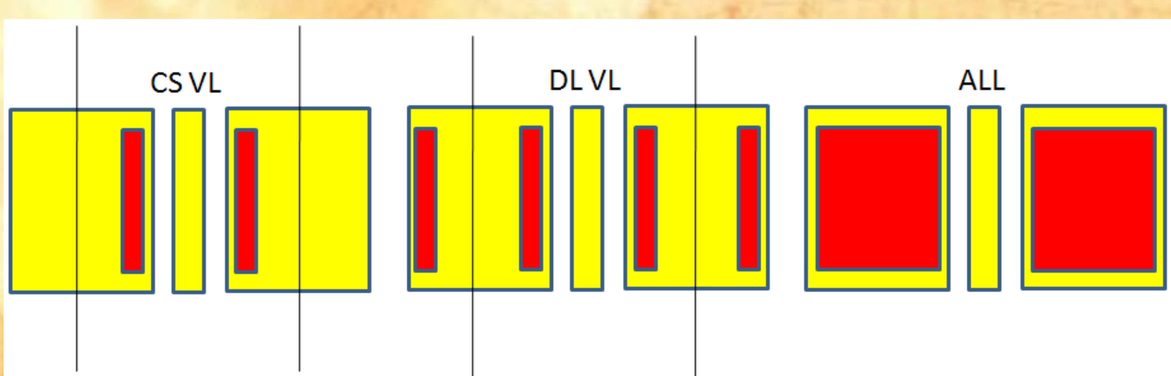

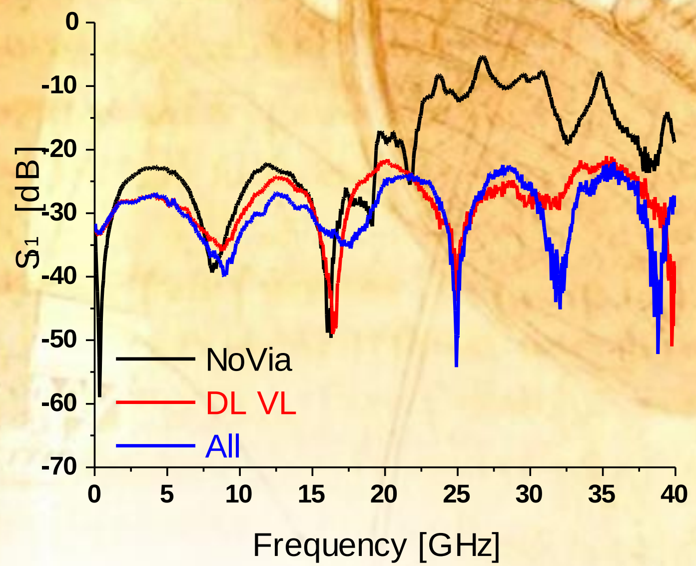

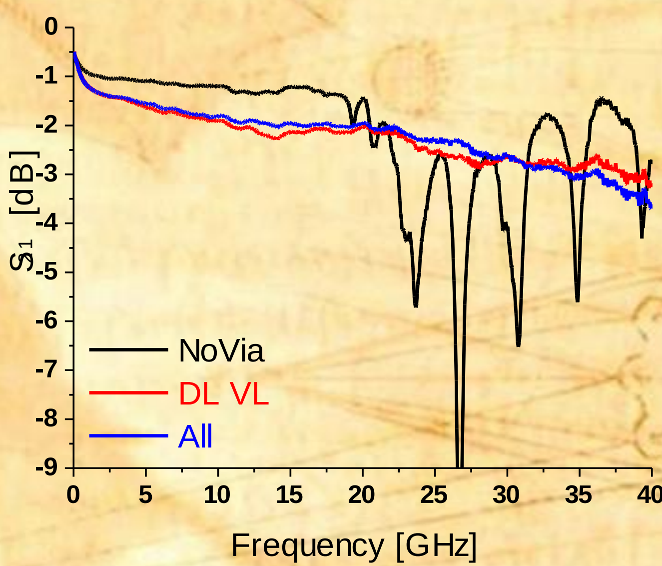

Current and Future Perspectives

- Phase Shifters and TTDL implementation by using micro-switches and frequency tunability solutions (LC and magnetic materials, like LTCF or permalloy)
- Meta-materials and Meta-circuits (antennas, transmission lines, resonators). Implementation in filters and phase shifters
- Electro-Magnetic and Photonic Band-Gap (EMBG and PBG) configurations (possibly THz Devices)
- High Frequency Properties (Modelling and Test) of nano-structured devices and related Measurement Techniques (HF-AFM)

Liquid crystals photonics - Theory

- Refractive indices:
  - Excellent transparency in NIR
  - Ordinary index typically 1.45 - 1.6
  - Birefringence 0.15 - 0.4

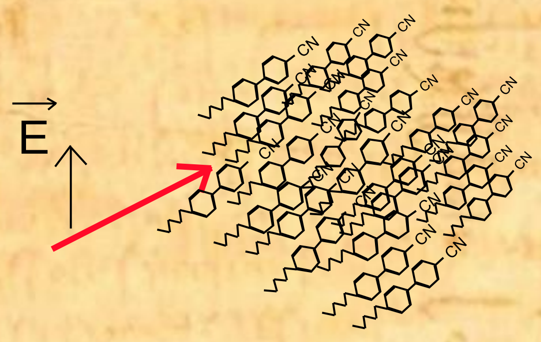

- Reorientation of molecules:
  - By electric or magnetic field
  - Switching time <50ms
  - µW range power

Large EO effect

- Versatility …. and complementarity

In cooperation with University of Roma “La Sapienza”,
Ministero degli Affari Esteri, Aristotle University of Thessaloniki (Grecia)

IMM-Roma

Liquid crystals photonics - Technology

Liquid crystal waveguides on silicon

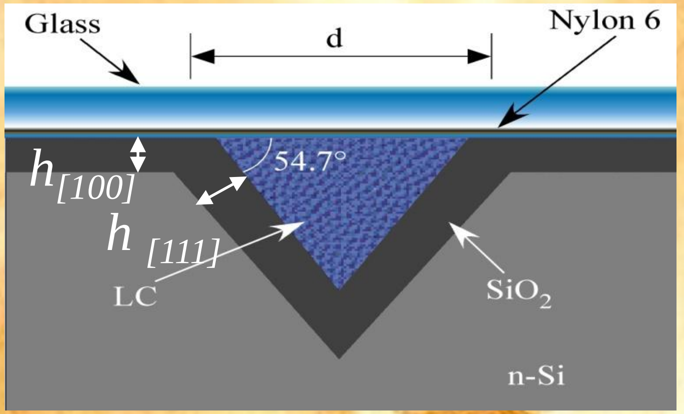

The pretilt angle induces a refractive index step between the waveguide core and the surrounding hybrid cladding for a quasi-TM mode

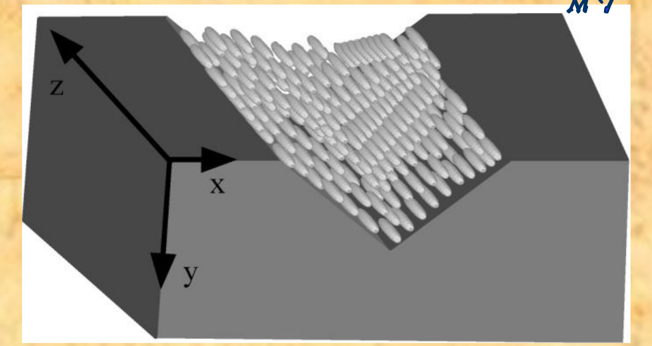

$$n_{LC}(\theta) = \frac{n_e n_o}{\sqrt{n_e^2 \sin^2\theta + n_o^2 \cos^2\theta}} \qquad n_e > n_o$$

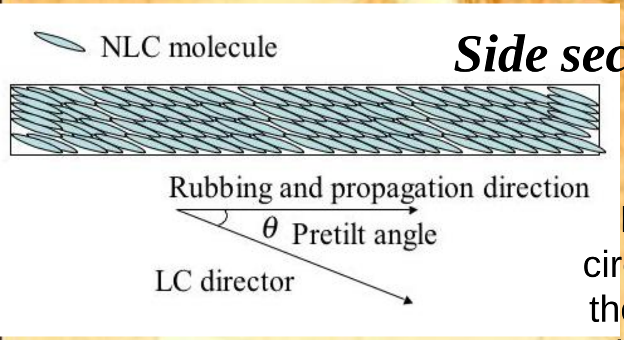

Side section

Coupling and packaging

Combining micromachining, microfluidics and photonics

Microfluidics circuit to infiltrate the liquid crystal in the groove waveguides

Sharp index-matched interface

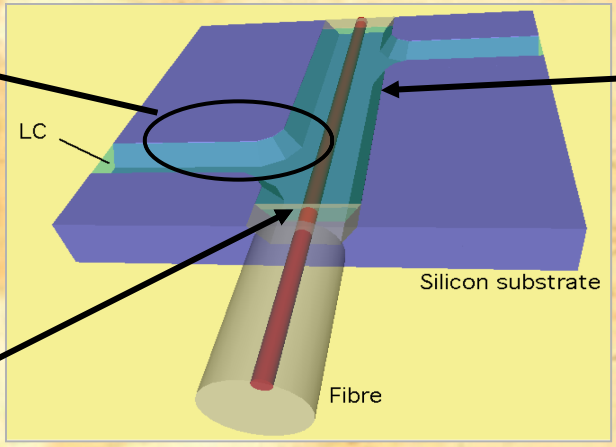

Light propagation in CL

IMM-Roma

Nematic Crystals for Microwave Applications

Utilization of Liquid Crystals (LC) for microwave applications. The nematic material is characterized by long polar molecules, which can be oriented by means of a magnetic or an electric external field.

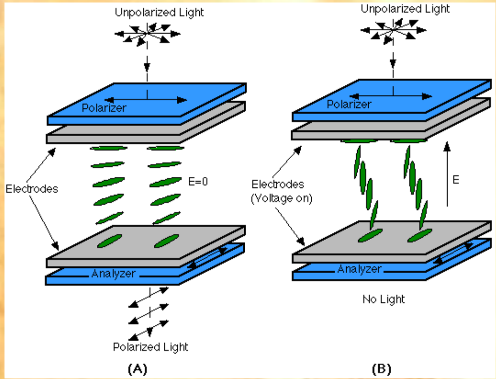

$$\Delta\varepsilon = \varepsilon_{\parallel} - \varepsilon_{\perp}$$

RF waveguide

$$\Delta\varphi \propto f, \Delta\varepsilon$$

Fine Tuning and Phase Shifter Applications are possible by using simple transmission line structures

State of Art

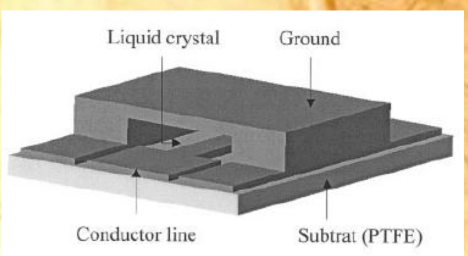

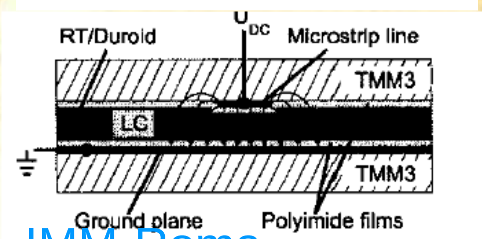

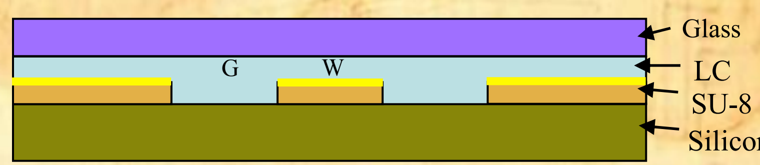

Elevated coplanar waveguide (CPW)

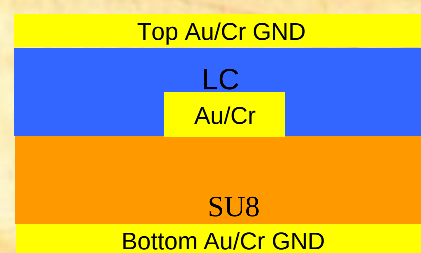

LC stripline

IMM-Roma

Phase Shifters based on LC and SU-8 Structures

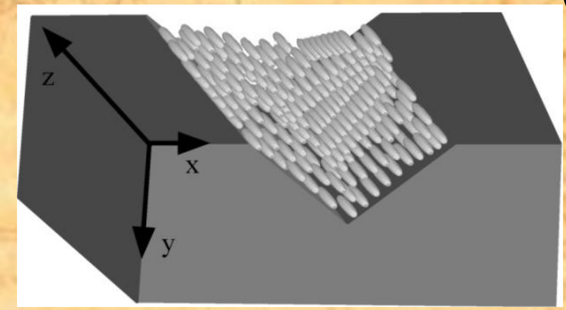

Re-orientation of molecules by E and H DC fields

- ❖Switching time < 50 ms
- ❖µW range power

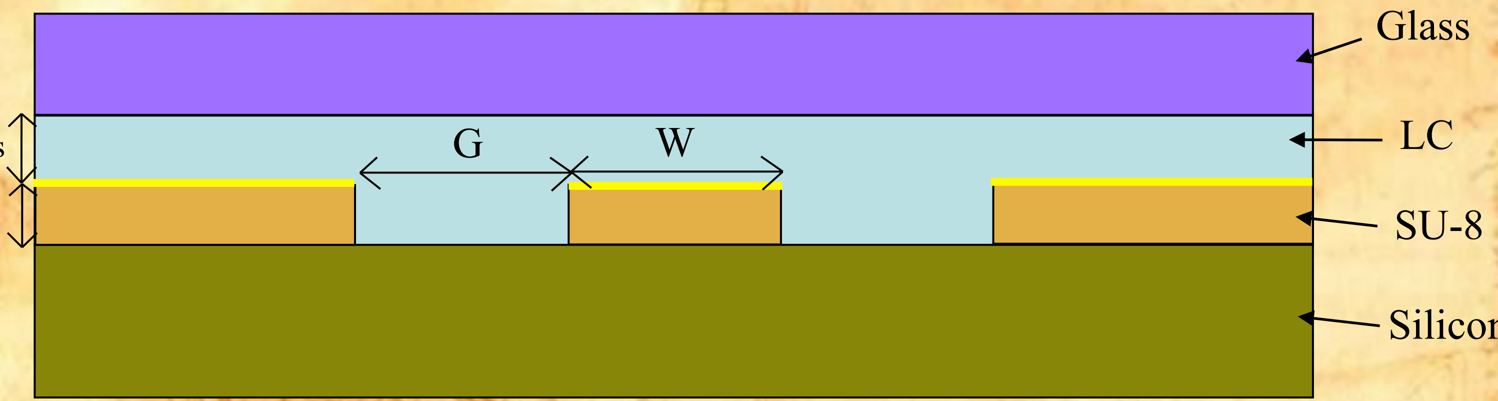

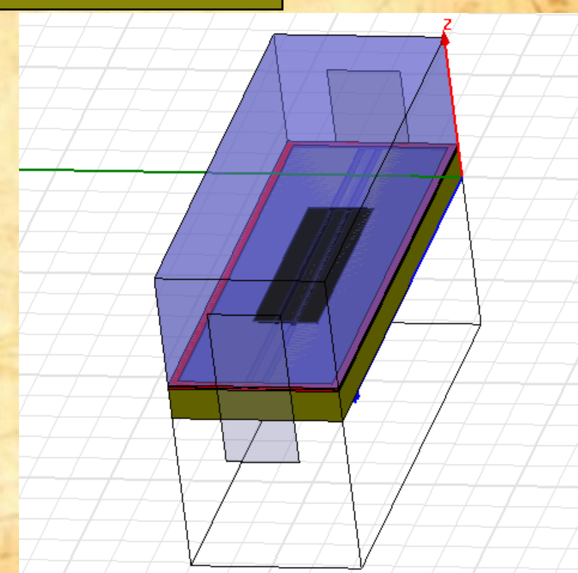

Dielectric Properties:

Silicon: ε_r=11.9, tanδ = 0,002 (low resistivity)
Silica: ε_r=3.8 – 4, range 1 GHz – 50 GHz
SU-8: ε_r=4,2
LC: ε_{par}=4.13, ε_{perp}=2.99, tan$\delta_{//}$= tan$\delta_{\perp}$ = 0.01

IMM-Roma

The Microwave WEB

Example: 25 µm LC

Length: 6 mm

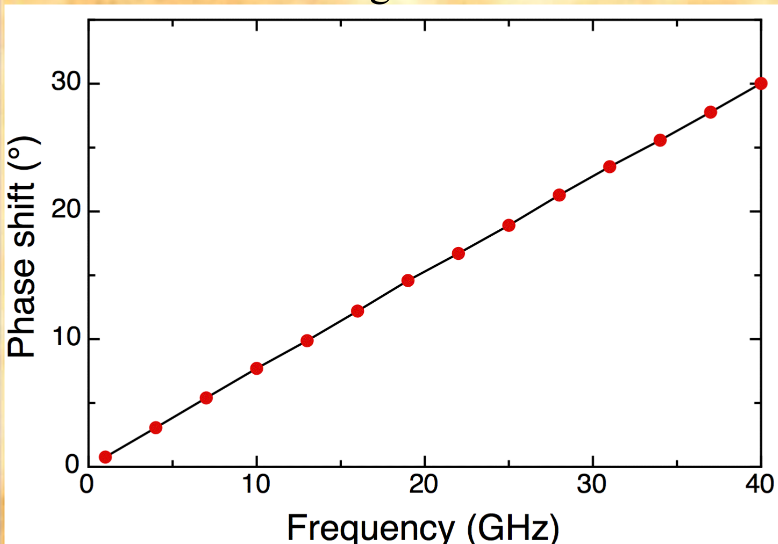

Length: 2 mm and 500 µm

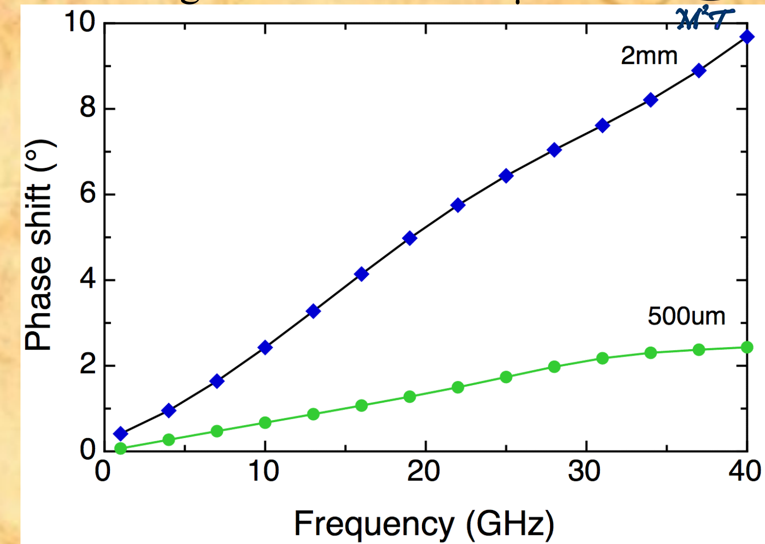

Phase shift is linear with the LC length.

Good electrical matching: S_{11} < -20dB, (L=6mm)

IMM-Roma

LC Thickness Influence

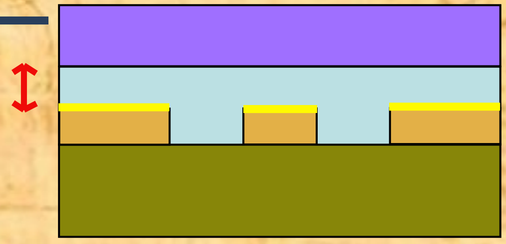

Phase Shift Vs. LC Thickness, CPW 2mm long:

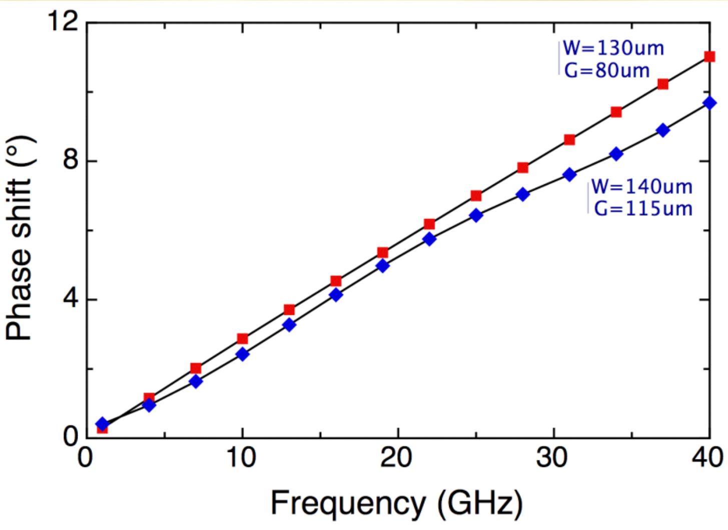

LC: 25μm

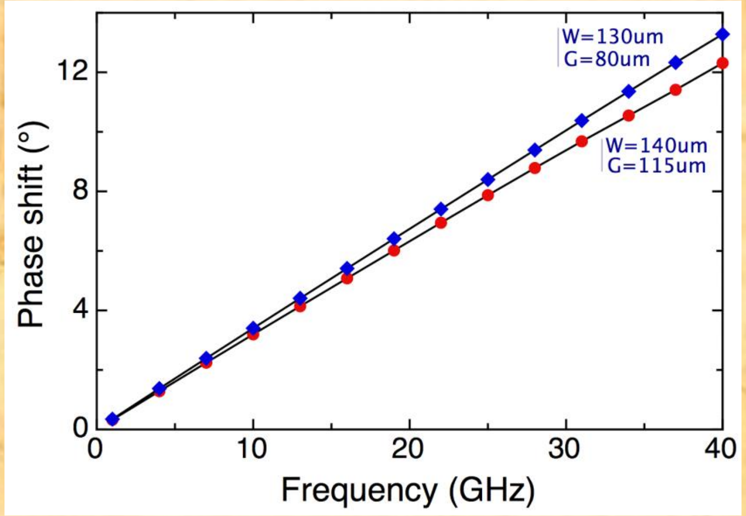

LC: 50μm

Phase shift is calculated as the phase difference between the biased and the un-biased LC.

IMM-Roma

The designed structures allow for an almost doubled phase shifting per unitary pathlength with respect to literature results based on the same LC.

$$\Delta\Phi' = 0.821\,°/GHz\ /cm$$

Classic CPW covered by LC

$$\Delta\Phi' = 1.312\,°/GHz\ /cm$$

SU-8 elevated CPW filled by LC

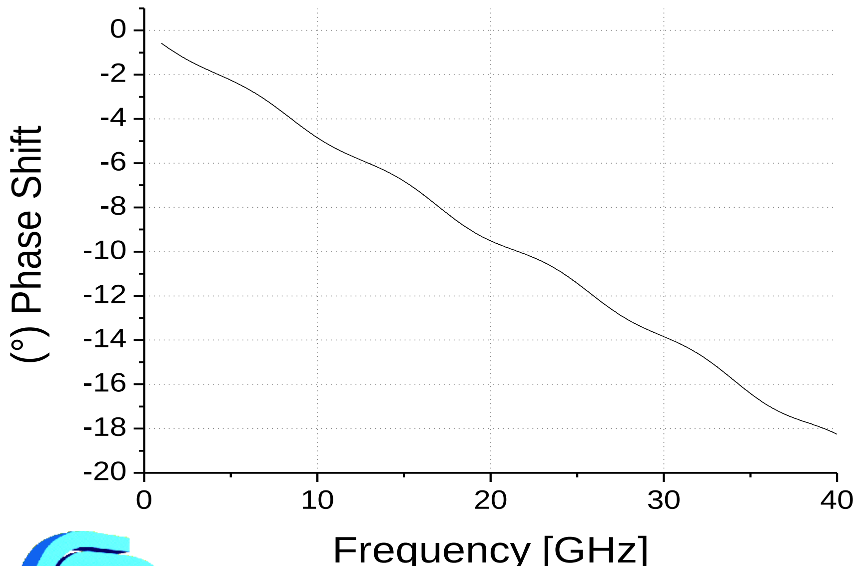

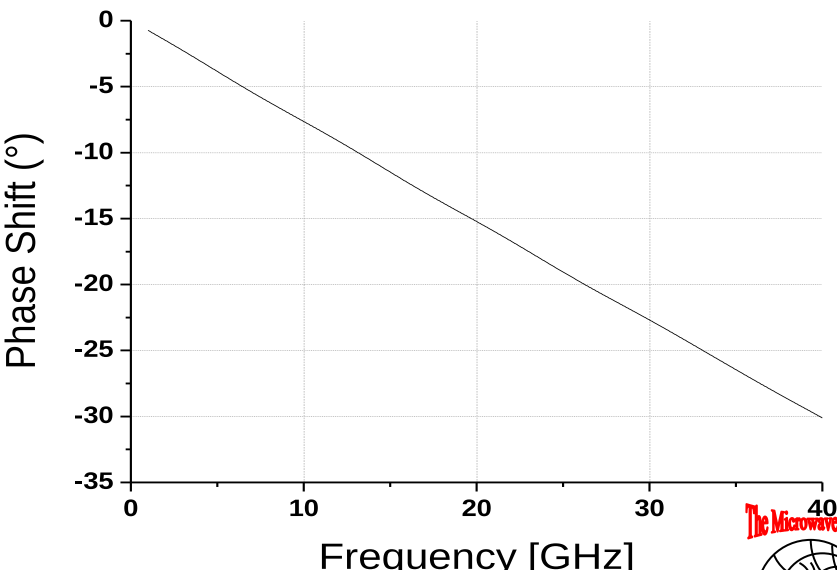

IMM-Roma

The Microwave WEB

RF MEMS Technology	Purpose	Cost	Advantages	Drawbacks	Sacrificial Layer Release/Micromachining
Silicon	Devices, 2D/3D Microsystems	Low-Medium	reliable, low loss	low-medium power, charging (?)	Photoresist: high pressure O2 plasma process performed in asher
GaAs	Devices, 2D/3D Microsystems	Medium-High	reliable, low loss	non-CMOS compatible, charging (?)	Photoresist: high pressure O2 plasma process performed in a barrel etcher
Alumina	Devices, 2D Structures, low-level packaging	Low-Medium	medium-high power, well established	surface roughness, lossy	SiO2: Wet etching with subsequent rinse in water/IPA/cyclohexane and freeze and sublimation
LTCC	Devices, 2D/3D Microsystems, Packaging	Low	3D integrability	surface roughness, shrinking effect after LTCC cofiring, lossy	SiO2: Wet etching with subsequent rinse in water/IPA/cyclohexane and freeze and sublimation
SU-8	Devices, 2D/3D Microsystems, Packaging	Low	Photolithographic processing	low breakdown voltage, leakage, sacrificial layer removal (viscosity)	Resist or SU-8: wet or O2 assisted RIE
LC	Devices, 3D Microsystems, Packaging	Low-Medium	analog signal processing, tuning	slow re-configuration time	Micromachining

Electro-Magnetic Band-Gap (EMBG) Resonators

Periodic change of the impedance to create forbidden gaps in the propagation

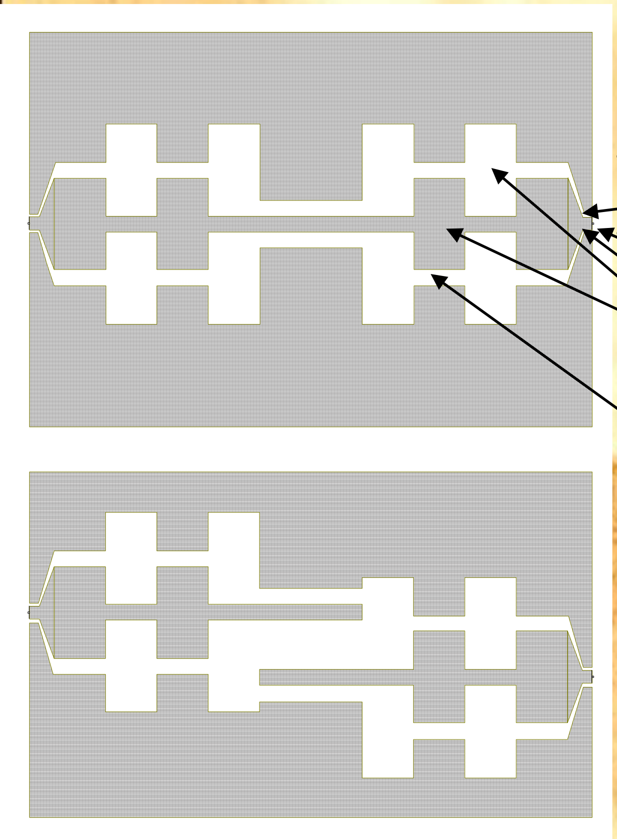

f = 50 GHz <=> L0= 600 µm (λ/4 length)

L = 18600 µm (the length of the entire structure)

L_{taper} = 500 µm (the length of the taper)

W_{taper} = 260 µm,

S_{taper} = 60 µm

w = 1860 µm (CPW line width alternating with the dimension of the slot)

s = 360 µm (CPW line slot)

H = 400 µm,

T = 0.5 µm,

ε_r = 11.9 µm,

Rho = 1

where

ε_r =silicon dielectric constant,

H= thickness of silicon bulk substrate,

T= thickness of the aluminium layer,

Rho= metal bulk resistivity normalized to gold

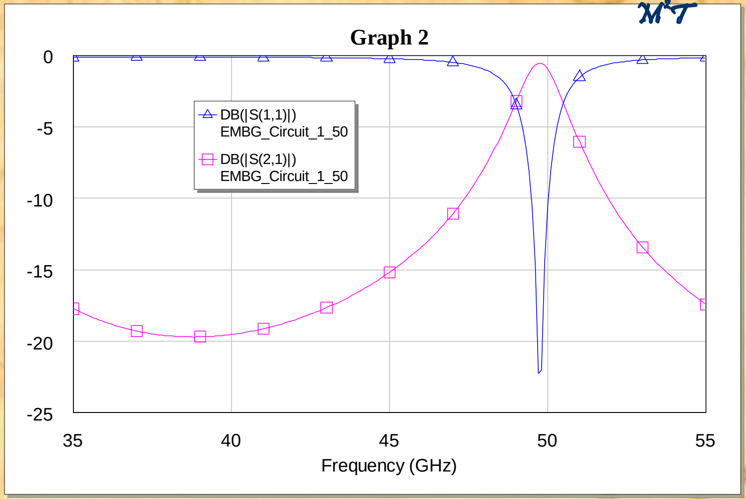

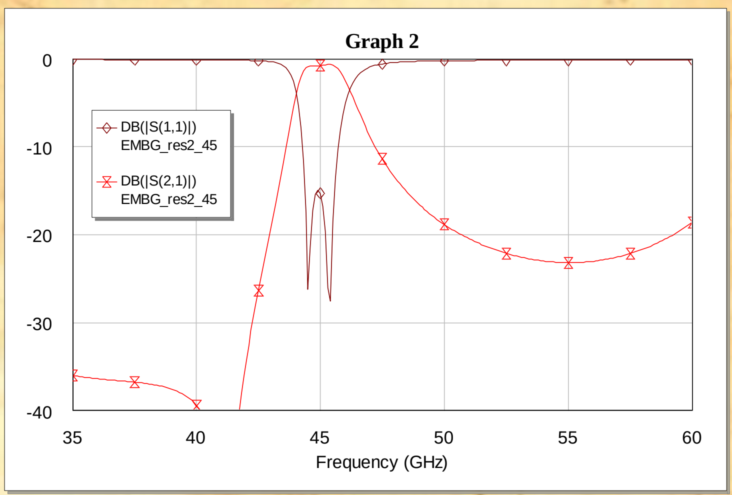

With UNI RM1, RM2 and RM3. IMT Bucuresti

IMM-Roma

Possible implementation by using “trenched lines” with SU-8 and tunability by magnetic materials

Metamaterials and Metacircuits

- Artificial meta-materials (MMs) by using artificial LH (Left-Hand) transmission lines implemented by chip capacitors and inductors, series and parallel connected, respectively
- For higher frequencies, series connected interdigital capacitors and parallel connected short-ended microstrip lines inductors, for CRLH (Composite Right/Left-Handed) artificial transmission lines. CRLH cells were the key concept for a new class of devices and applications such as backward-wave directional coupler, leaky-wave (LW) tunable radiation angle antennas, zeroth-order resonator antennas.
- CRLH based LW antennas have an important advantage over the classical LW antennas, because of the frequency scanning of the radiation pattern. Also, CRLH based zeroth-order resonator antennas could be made arbitrarily small depending on the technological resolution.
- CRLH based circuits up to now involved microstrip lines and hybrid technology. As an alternative, silicon substrate and CPW (CoPlanar Waveguide) transmission lines can be used to design them. CRLH structures can be designed with CPWs and antenna integrated on Si substrate.
- A coupler is composed by two-coupled artificial transmission lines, each one consisting of a number of cascaded CPW CRLH cells. The cell must have a balanced structure for the coupler central frequency. This means that the series resonance frequency must be equal to the parallel resonance frequency and also equal to the central frequency of the coupler, f_0.

Metamaterials for High-Frequency Electronics

CHRISTOPHE CALOZ AND TATSUO ITOH,
PROCEEDINGS OF THE IEEE, VOL. 93, NO. 10, OCTOBER 2

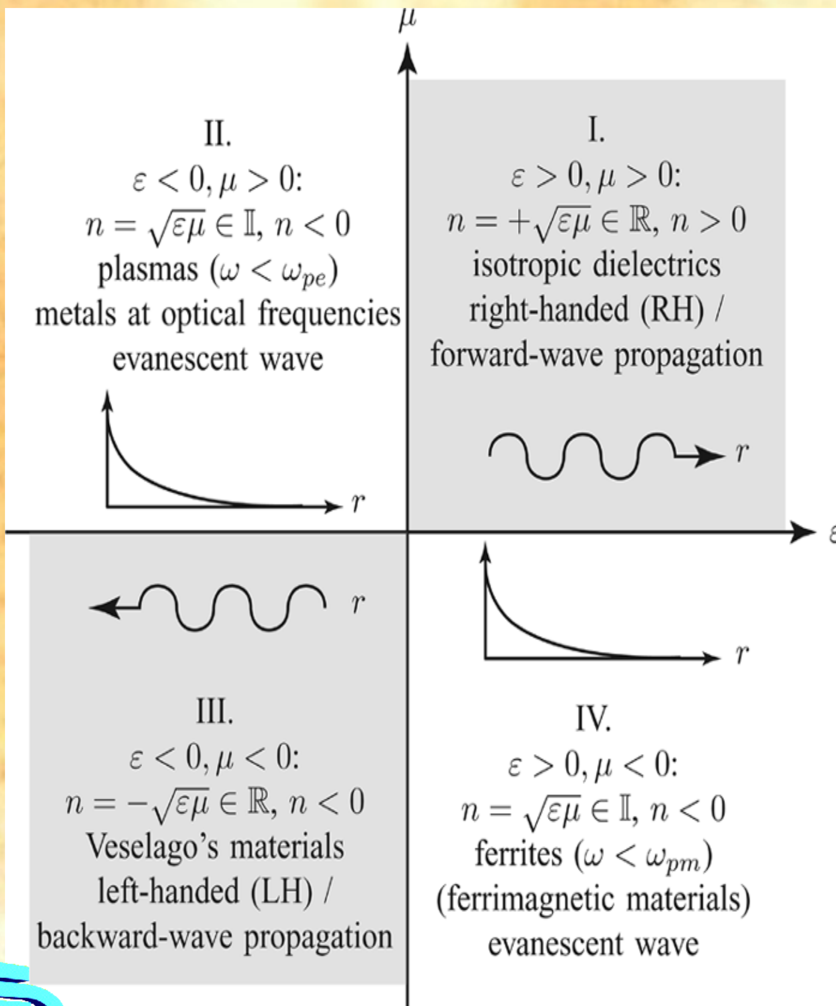

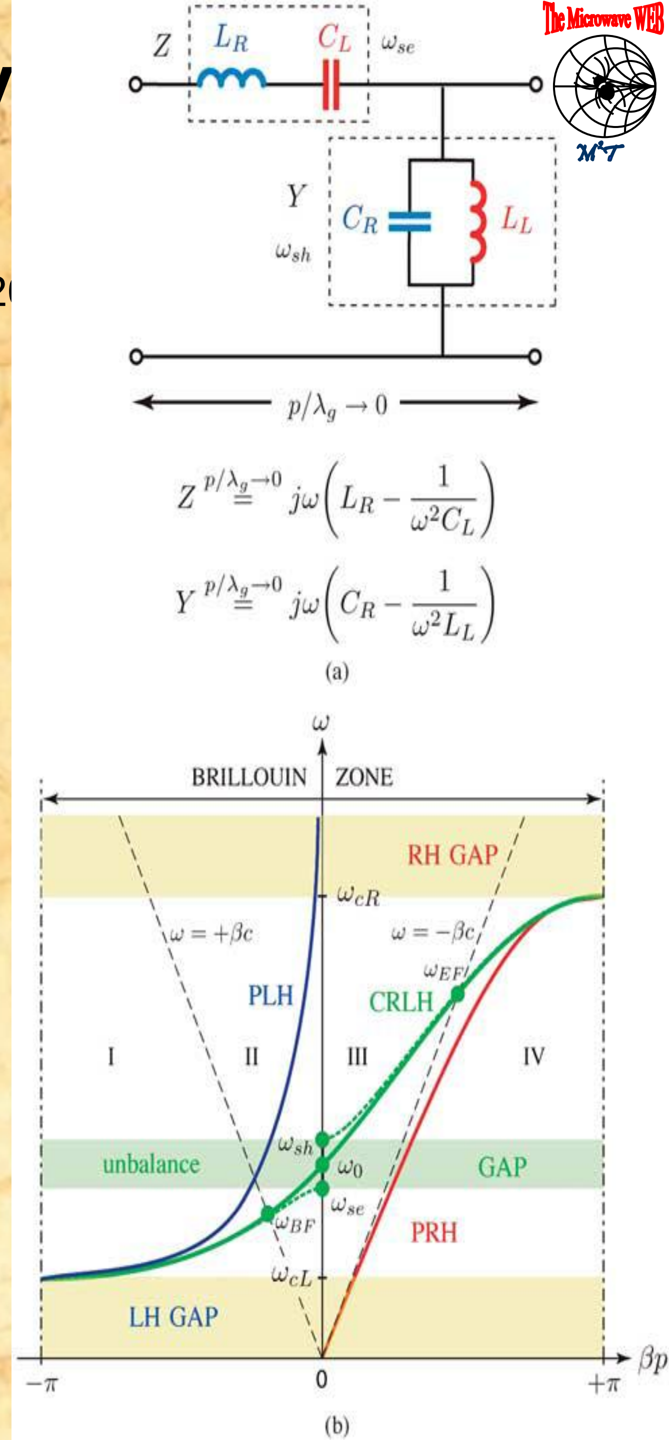

IMM-Roma

IMM-Roma

Meta-advantages

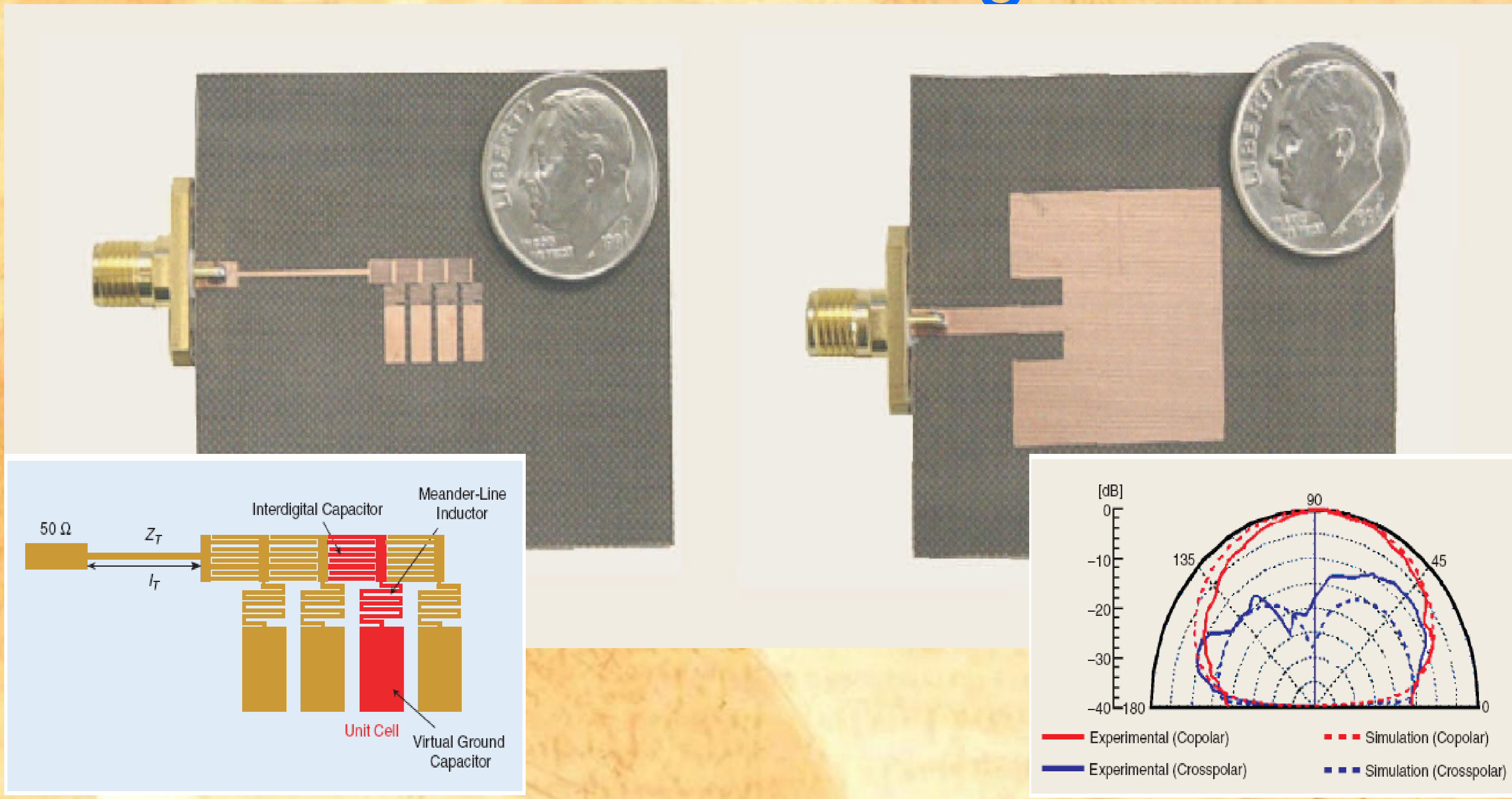

Antenna comparison. (a) Four-cell ZOR antenna (f_0 = 4.88 GHz). (b) Microstrip patch antenna on the same substrate (f_0 = 4.90 GHz). The same performances, but decreased size of the device !

Metacircuit Antenna

In cooperation with IMT Bucuresti

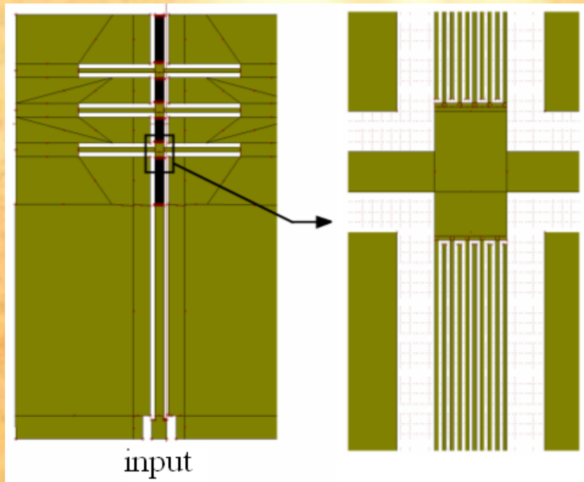

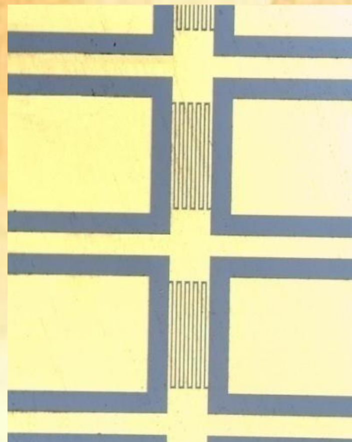

Layout of the CPW zeroth-order resonance antenna (a) and detail + photo of this layout (b), used in IE3D – Zeland software to obtain the simulation results

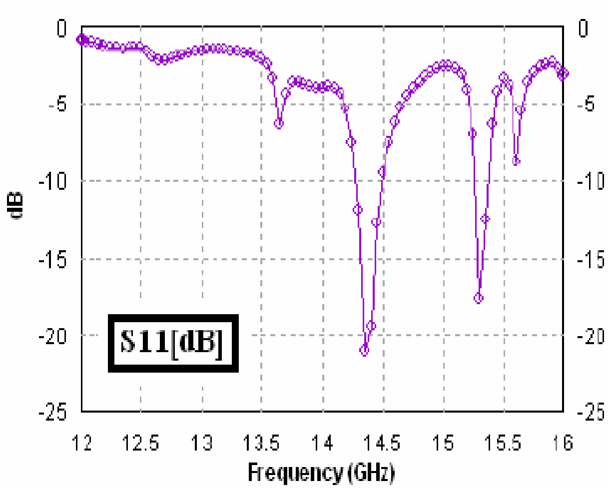

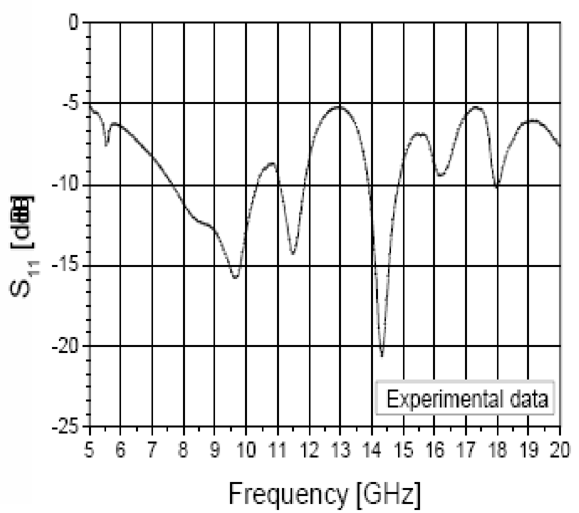

Metacircuit Directional Coupler

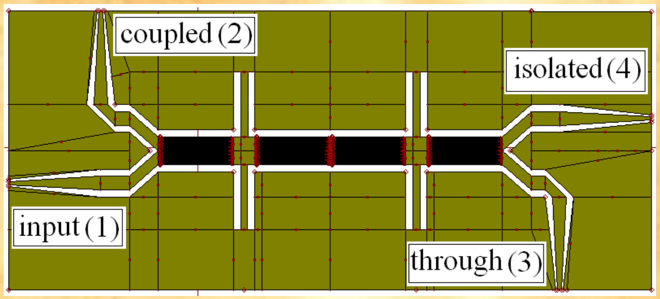

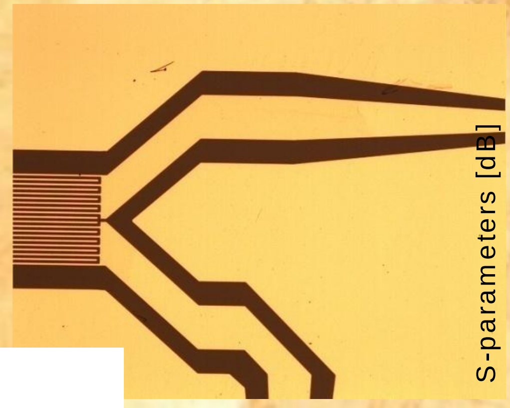

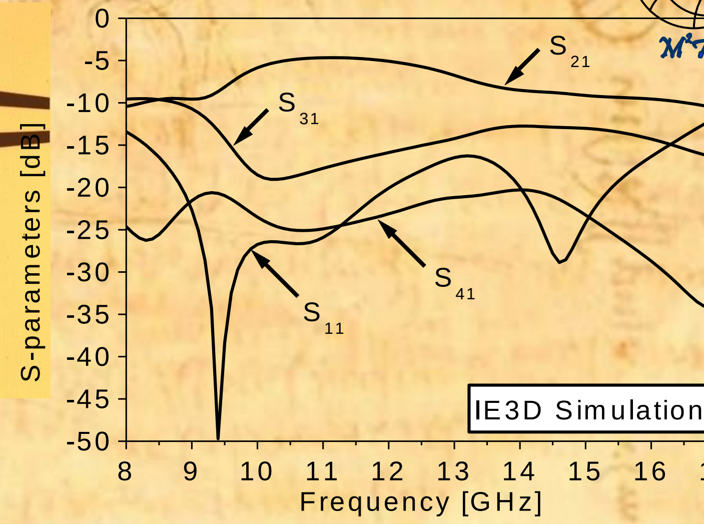

IE3D-Zeland Structure, Realization, and Test

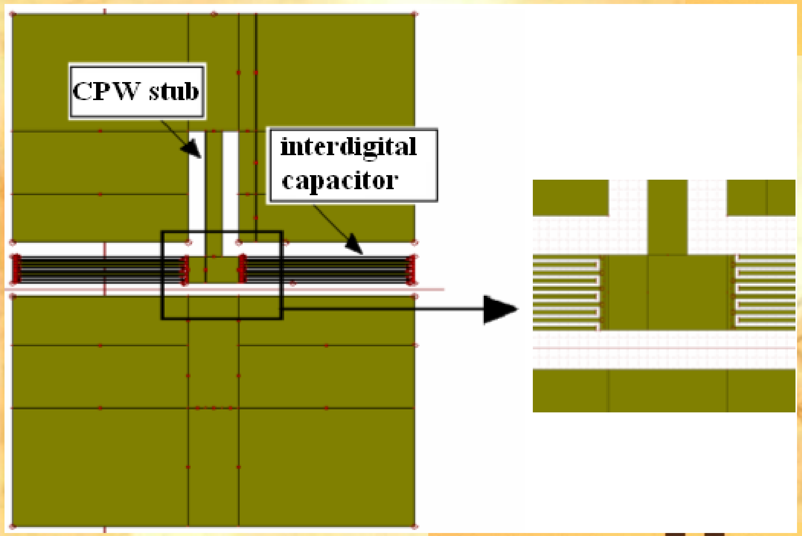

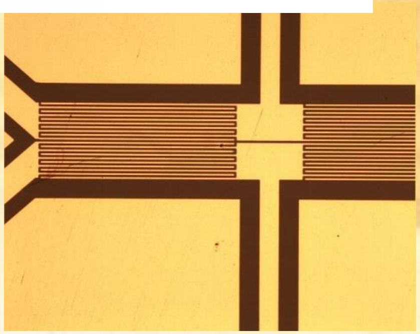

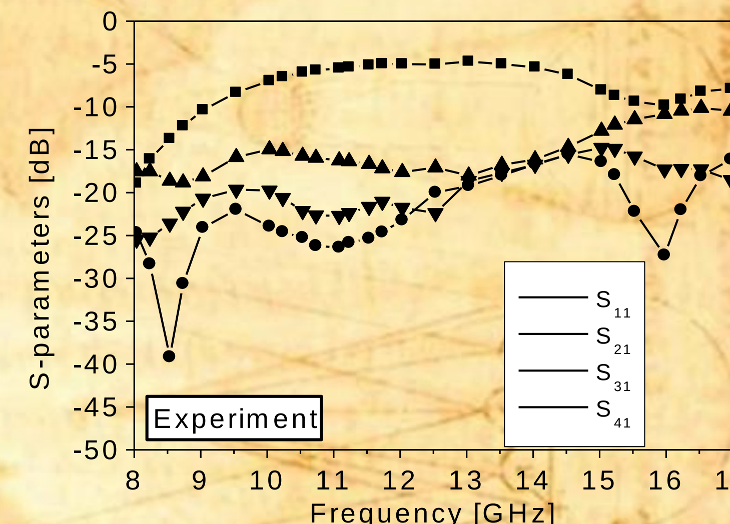

IMM-Roma

In cooperation with IMT Bucuresti

Further Developments (Filters and NLTL)

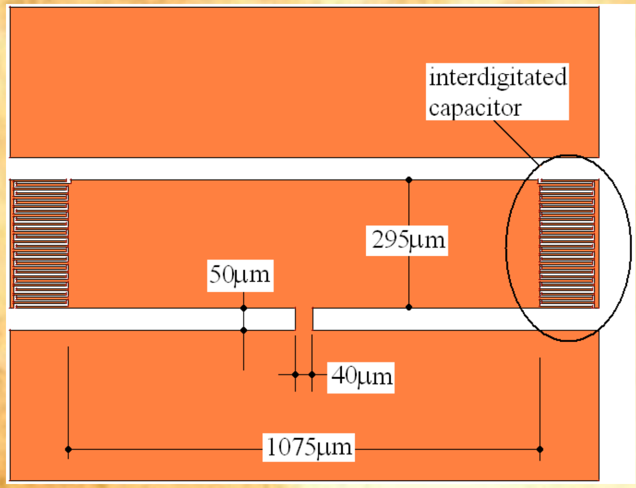

layout in CPW technology for the circuit

Simulation for the filter consisting of four cascaded structures

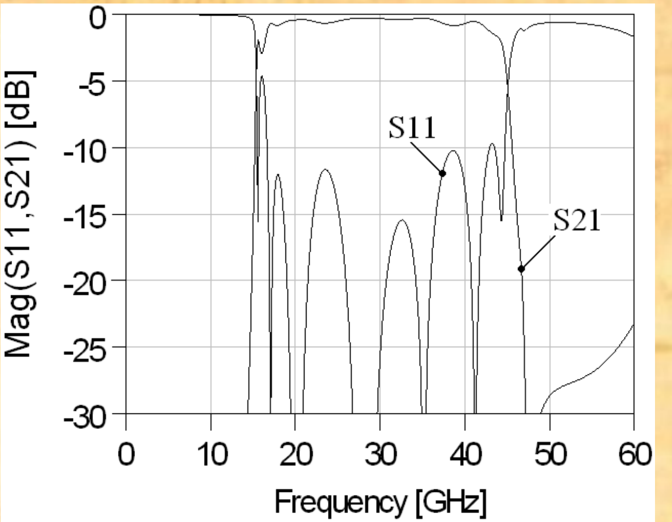

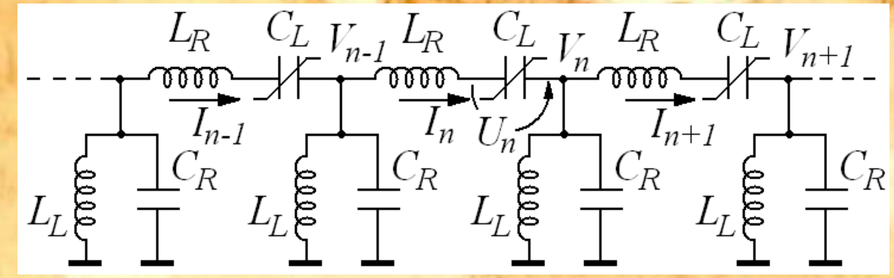

NLTL and Output voltage on the second harmonic normalized to the input voltage on the fundamental frequency versus the input frequency, for *n* = 3

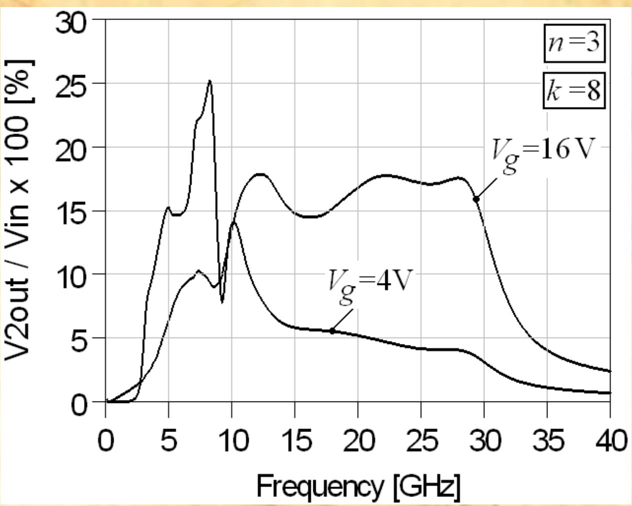

MEMS and nano-technology: CNT and nano-wires

- Potential applications and understanding of carbon nano-tubes (CNTs) and nano-wires in fields where AC properties can be useful for their integration in high frequency (HF) sub-systems.
- Development of methods based on microstrip and coplanar approaches for measurements at GHz frequencies.
- Definition of standards for how-to-characterise nano-tubes and nano-wires and their reliability and/or figure of merit for HF applications.
- *Stability of the electrical response for CNT and nano-wires in HF devices by using different solicitations (wave-forms, power, temperature, pressure …)*
- NEMS, based also on mechanical properties

IMM-Roma

Potential Aims

- Low loss planar and vertical interconnections at the nano-scale (high density of interconnections in hybrid configurations, different substrates, …)
- Miniaturized filters for millimeter wave sub-systems (patterning and coupling between CNTs, …)
- Band-gap engineering and modelling of nano-systems by using external sources (magnetic field, electric field, pressure) to modify the electrical response for both signal processing and sensing applications.
- Higher frequencies propagation (THz) by means of surface propagation and/or photonics
- Graphene properties …. *Nobel Prize just arrived*
- Nano-antennas

CNT for switching and THz

Microwave applications of the CNTs encompass many concepts such as microelectromechanical systems (MEMS), nanoelectromechanical systems (NEMS), field emission, quantum confined electron devices as well as electromagnetic field propagation phenomena in the range 1 GHz-3 THz. A microwave device based CNT is a combination of some of the above concepts.

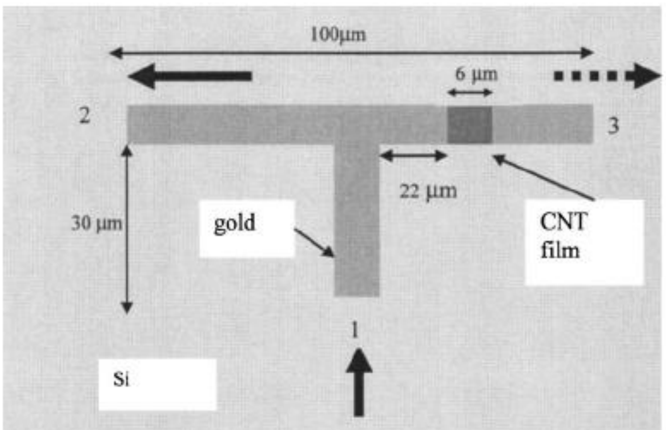

FIG. 3. Microwave T circuit with a CNT film in one arm.

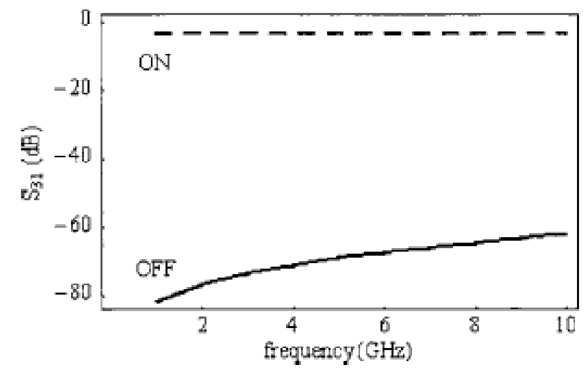

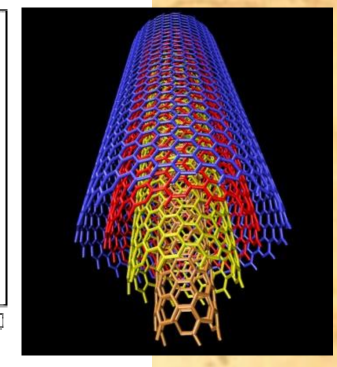

FIG. 4. The simulation of the CNT switch. The transmission $S_{21}(f)$ in the OFF state (solid line), (bias voltage −4 V) and ON state (dashed line), (bias voltage +4 V).

…..A Mott-like transition from semiconductor state to a metallic state is encountered in vertically or horizontally aligned semiconducting single-walled carbon nanotube SWCNT arrays sandwiched between two conducting electrodes, when a dc electric field is applied transverse to nanotube axes. Applying a dc voltage in the range −4 to +4 V, the conductance of the array ranges from 5 μS to 0, thus obtaining a decrease of six orders of magnitude……

M. Dragoman et al., Appl. Phys. Lett. **88**, 073503 2006

In cooperation with IMT Bucuresti, UNI RM “Tor Vergata”

Transmission Line and Contacts Modelling

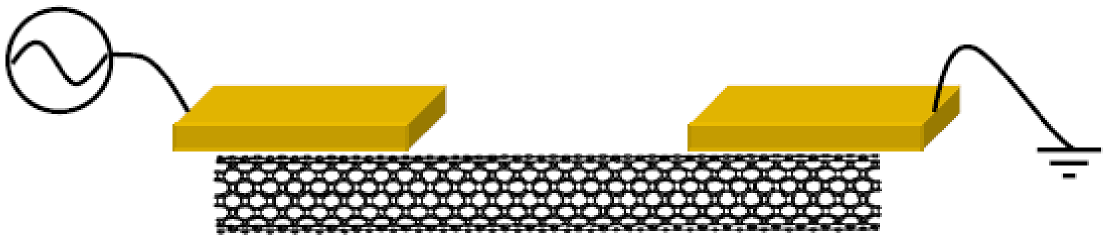

P. J. Burke, I. B. Spielman, J. P. Eisenstein, L. N. Pfeiffer, and K. W. West, "High frequency conductivity of the high-mobility two-dimensional electron gas,“ *Applied Physics Letters*, vol. 76, pp. 745-747, 2000.

The distributed circuit elements are:

Kinetic inductance per unit length: $L_k = \dfrac{h}{2e^2 v_F}$ (1.2)

Electrostatic capacitance per unit length: $C_E = \dfrac{2\pi\varepsilon}{\cosh^{-1}(2h/d)} \approx \dfrac{2\pi\varepsilon}{\ln(h/d)}$ (1.3)

Quantum capacitance per unit length: $C_Q = \dfrac{2e^2}{h v_F}$ (1.4)

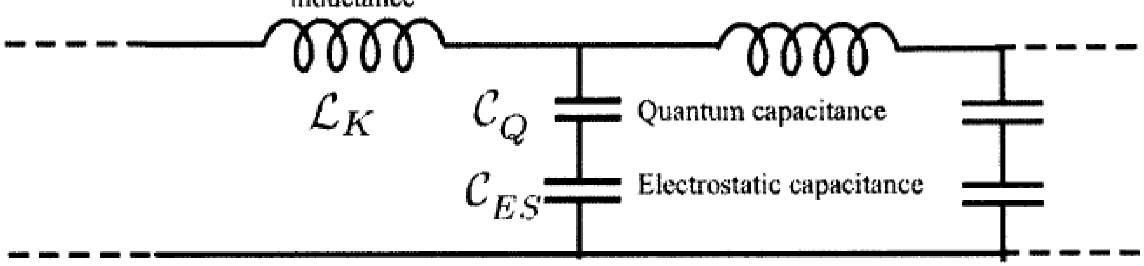

Vertical Interconnections

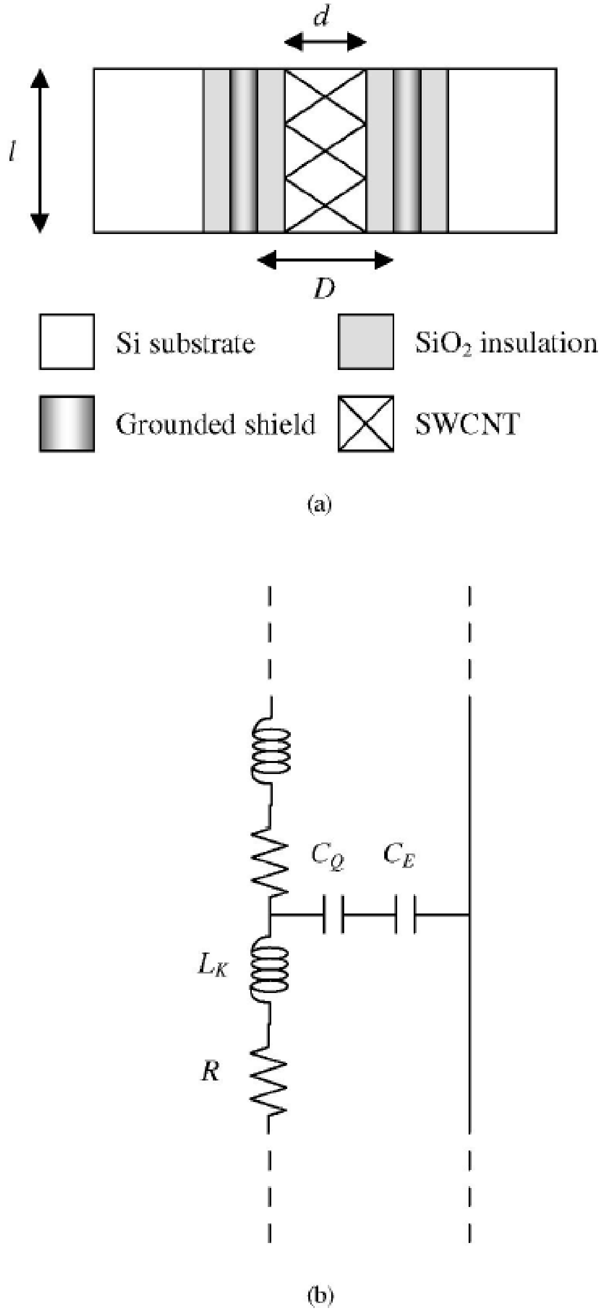

Fig. 1. (a) Cross-sectional view of a SWCNT via and (b) RLC model of a SWCNT via.

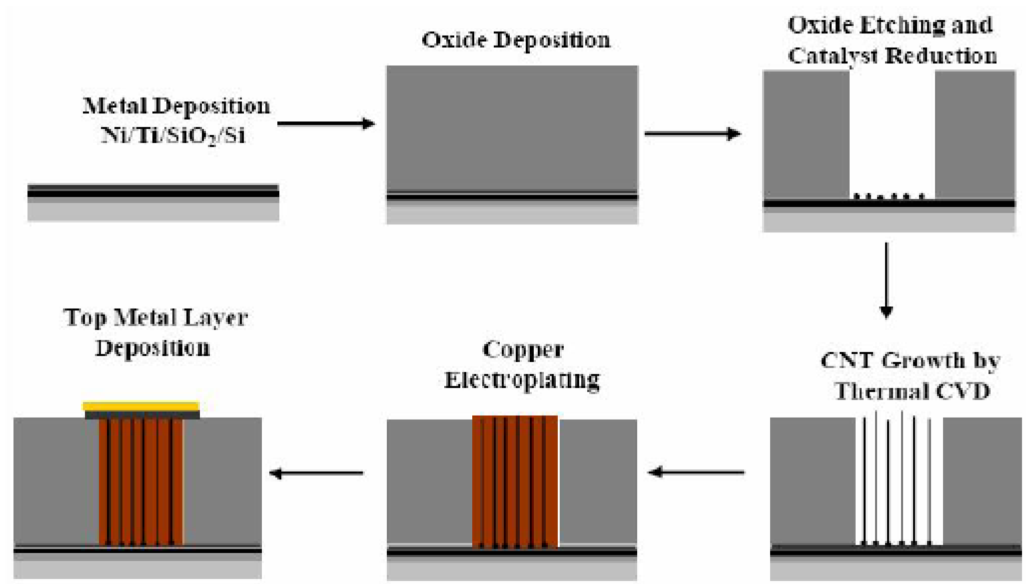

Figure 1. Schematics of the process flow to fabricate CNT via and CNT/copper composite via.

Reliability Evaluation of Carbon Nanotube Interconnect in a Silicon CMOS Environment
Yang Chai, Min Zhang, Jingfeng Gong and Philip C. H. Chan (2006)

IMM-Roma

RF Measurements of CNT and Nano-Wires

(open to collaboration with other IMM Units)

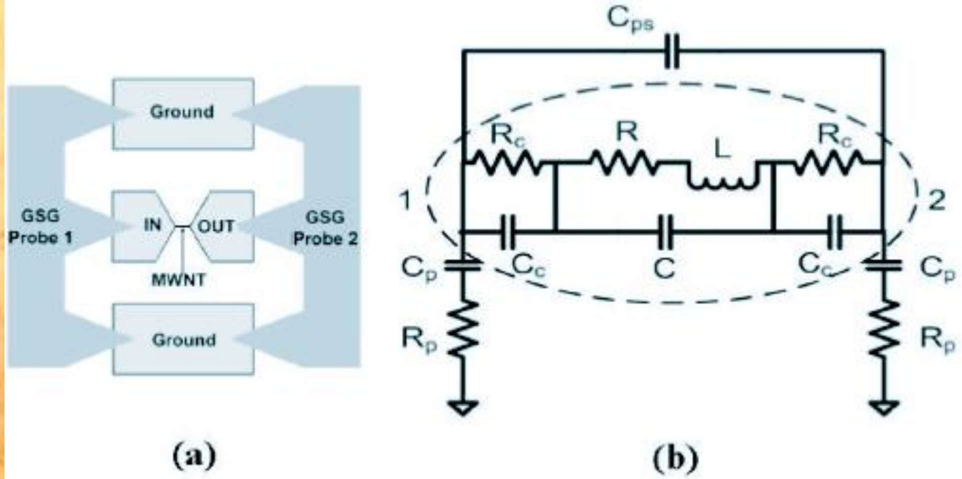

Measurements and modelling (a) schematic diagram of the Cr/Au bilayer electrodes fabricated for ground–signal–ground probing, (b) equivalent circuit model for a sample with an MWNT. The dotted circle represents the MWNT part. C_p and R_p denote the capacitance and resistance of the probing pads, C_{ps} denote the parasitic capacitance of the gap, R_c and C_c denote the contact resistance and capacitance between the MWNT and the electrodes, and R, L, C are the resistance, inductance, capacitance of the MWNT.

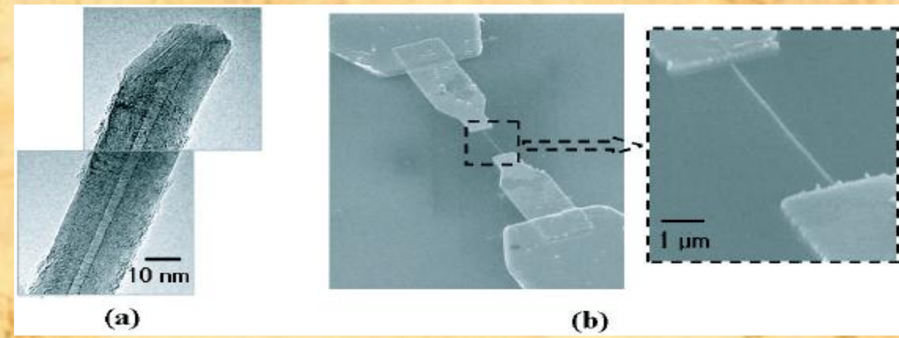

Photos from Fig. 1 of (*). A sample prepared for two-port S-parameter measurements (a) TEM image of a selected CNT, (b) SEM image of the CNT part of the sample, which shows an MWNT connecting the IN/OUT electrodes.

(*) Seong Chan Jun, X M H Huang, Sungwon Moon, H Jin Kim, James Hone, Y W Jin and J M Kim, “Passive electrical properties of multi-walled carbon nanotubes up to 0.1 THz”, *New Journal of Physics* **9** (2007) 265 (2007).

Preliminary Results

- Simulations of CNT coplanar and microstrip configurations, looking for switching properties based on the band-gap engineering
- For all of the following simulations the values used for the conductivity of the CNT in the two states are $\sigma(ON)=2.6x10^7$ S/m and $\sigma(OFF)=26$ S/m

CNT band-gap engineering the effect of an external pressure

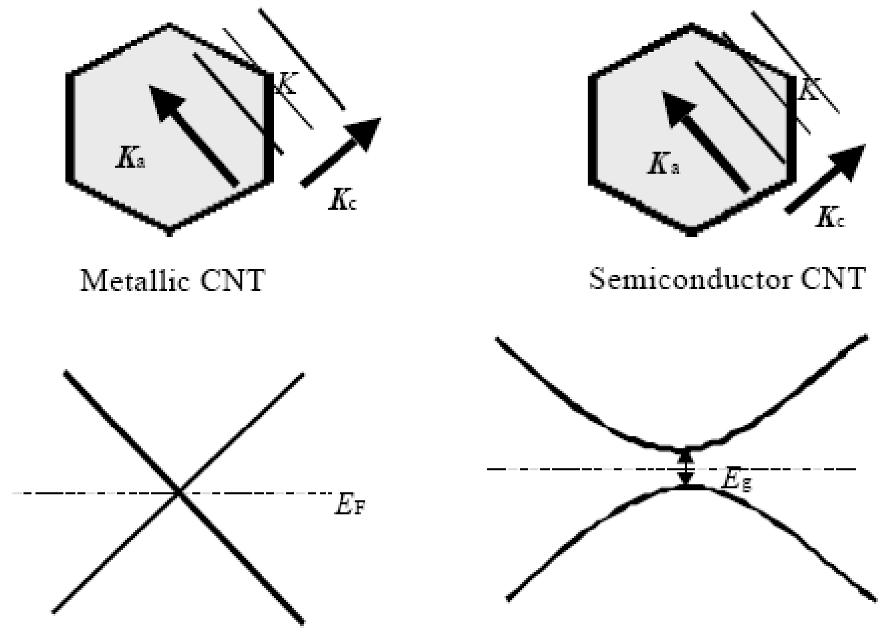

CNT band structure (*After*: [4]).

From D. Dragoman and M. Dragoman, Nanoelectronics, Artech House (2006)

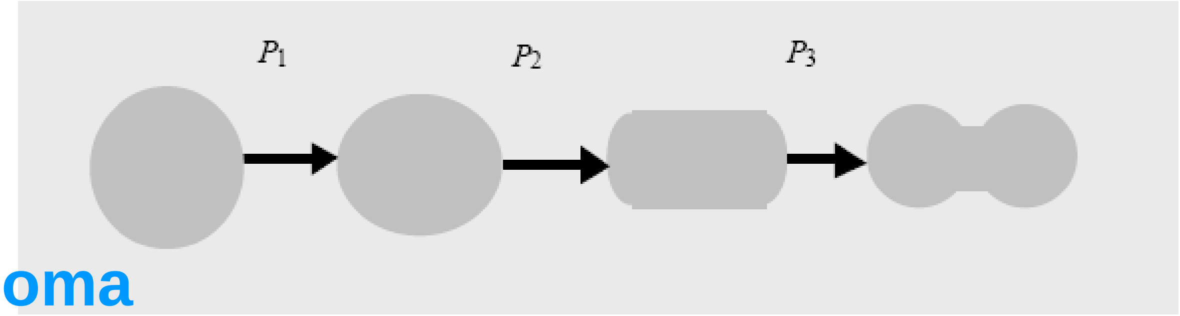

IMM-Roma

SPST Microstrip – capacitive gap

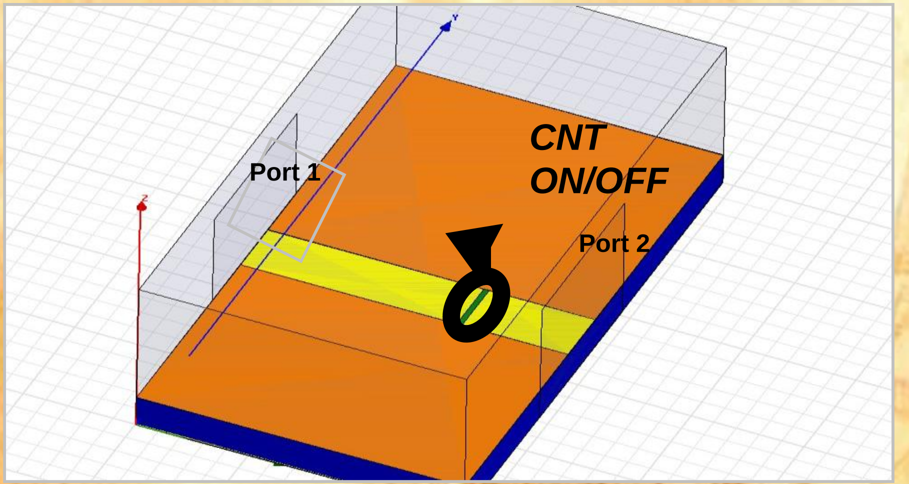

Fig. 1. Simulation of a 50 Ohm switch in micro-strip configuration, with a bundle of CNTs filling a gap. The ON and OFF states depend on the metal-semiconductor transition.

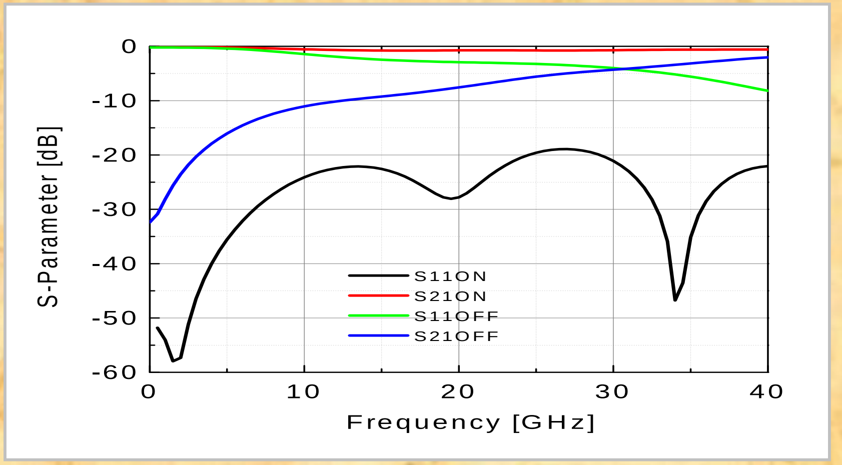

Fig. 2. Simulation results for the scattering parameters for the ON and OFF states of the CNT-based switch. The matching is very good for the ON state until 40 GHz

IMM-Roma

The Microwave WEB

IMM-Roma

SPDT Microstrip – capacitive gap

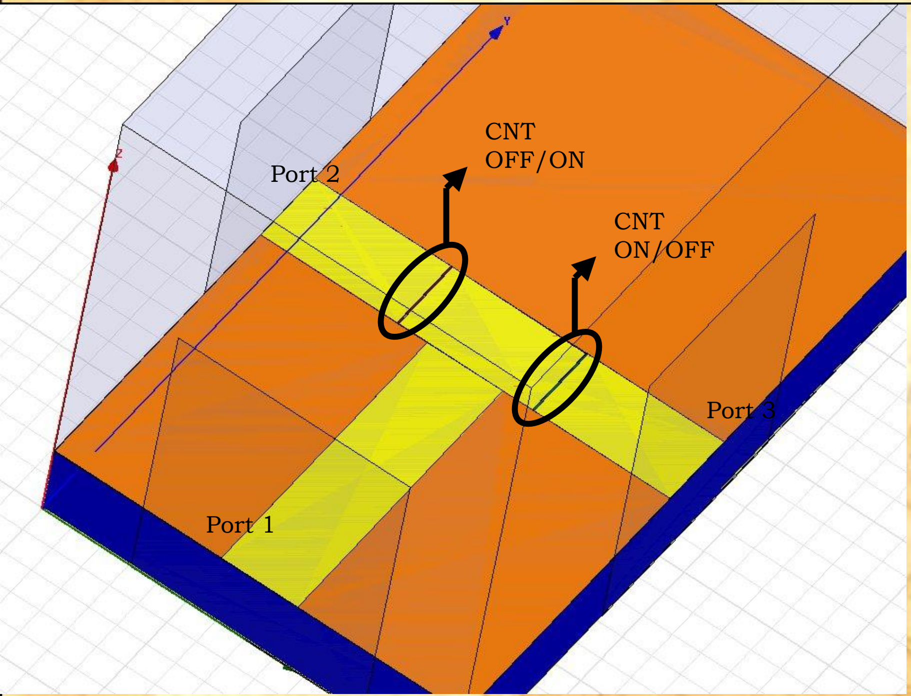

Fig. 3. Simulated structure. A 50 ohm matched SPDT device has been obtained by using Au metallization on a high resistivity, oxidized, Silicon wafer. The Au lines are 523 μm wide and 2 μm thick, while 50 μm gaps have been filled with CNT in ON/OFF states.

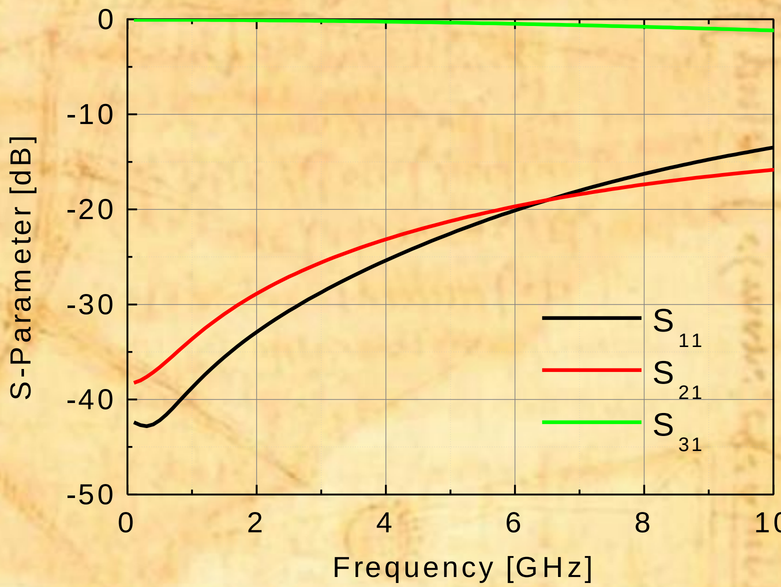

Fig. 4. Simulation results for the scattering parameters. In this case, on port 3 has been imposed the condition for the CNT ON state, thus allowing the transmission of the signal with port 2 isolated (CNT in OFF state).

IMM-Roma

SPST Microstrip – dual layer

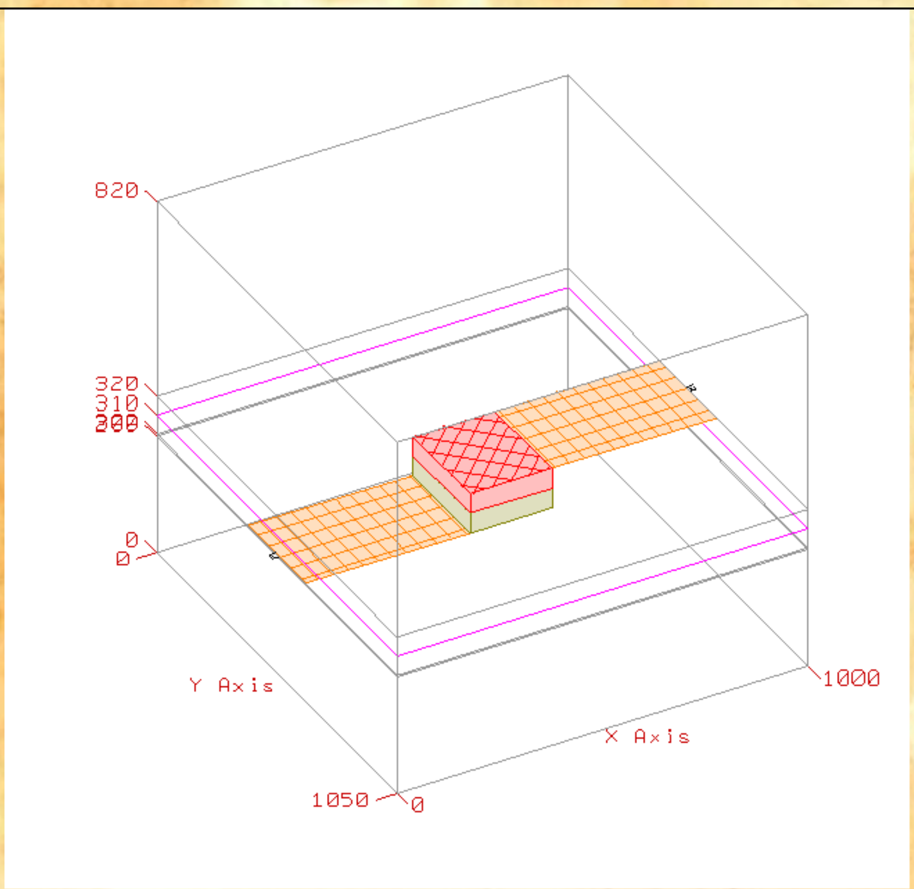

Fig. 5. Simulation of a 50 Ohm switch in a micro-strip dual-layer configuration with a via hole filled by a bundle of CNTs.

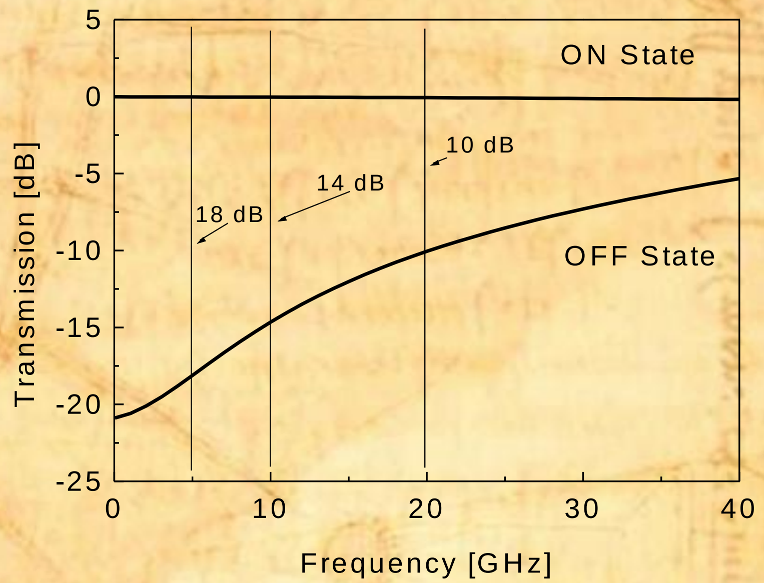

Fig. 6. Simulation results for the scattering parameters for the microstrip dual-layer configuration using a bundle of CNTs. The transmission signal decreases rapidly with the frequency.

IMM-Roma

SPST CPW – horizontal CNTs

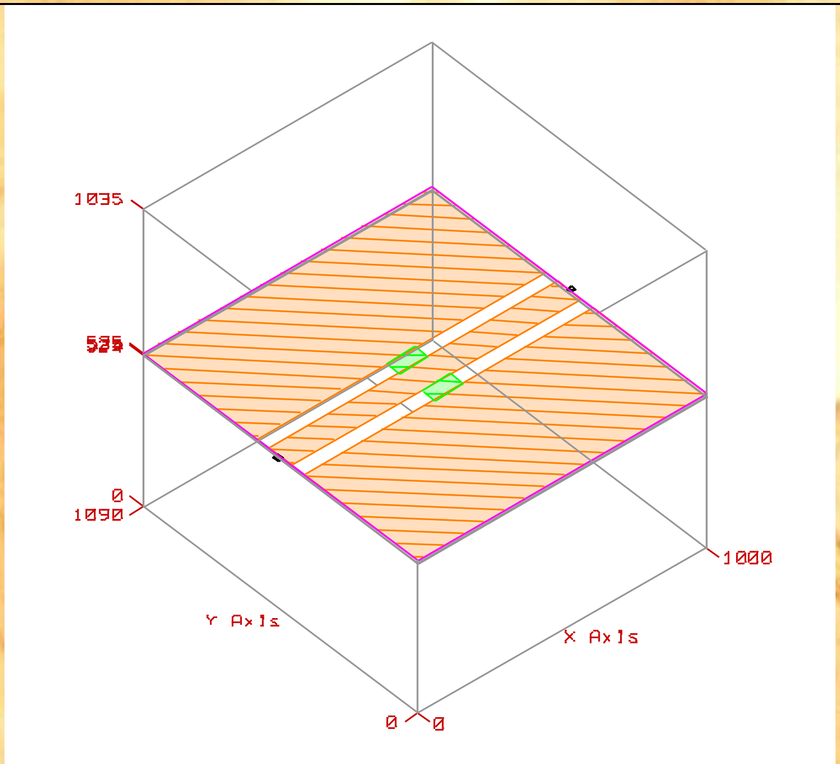

Fig. 7. CPW switch with CNT aligned orthogonally with respect to the central conductor, in the plane of the substrate.

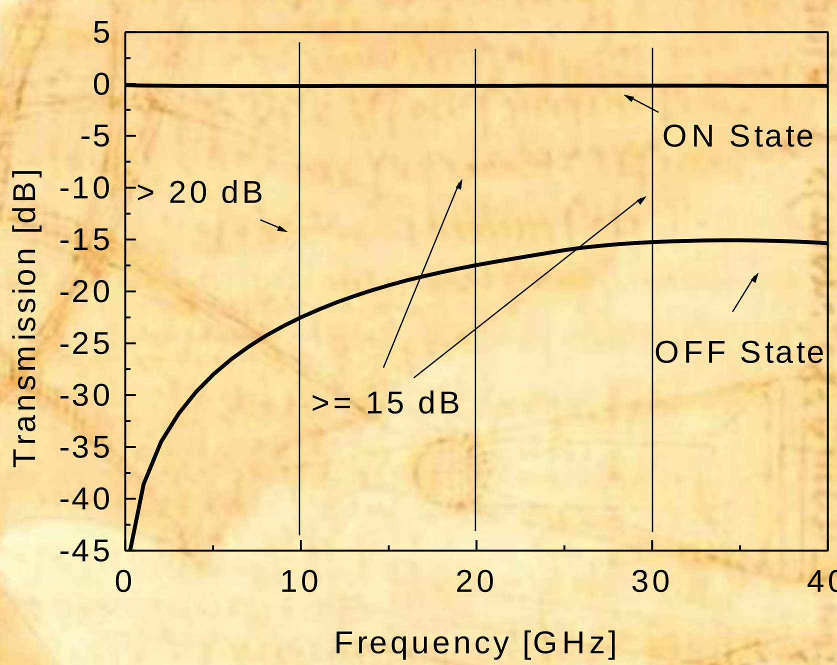

Fig. 8. Simulated response of the CPW switch with horizontally placed CNTs.

SPST CPW – CNT in via hole

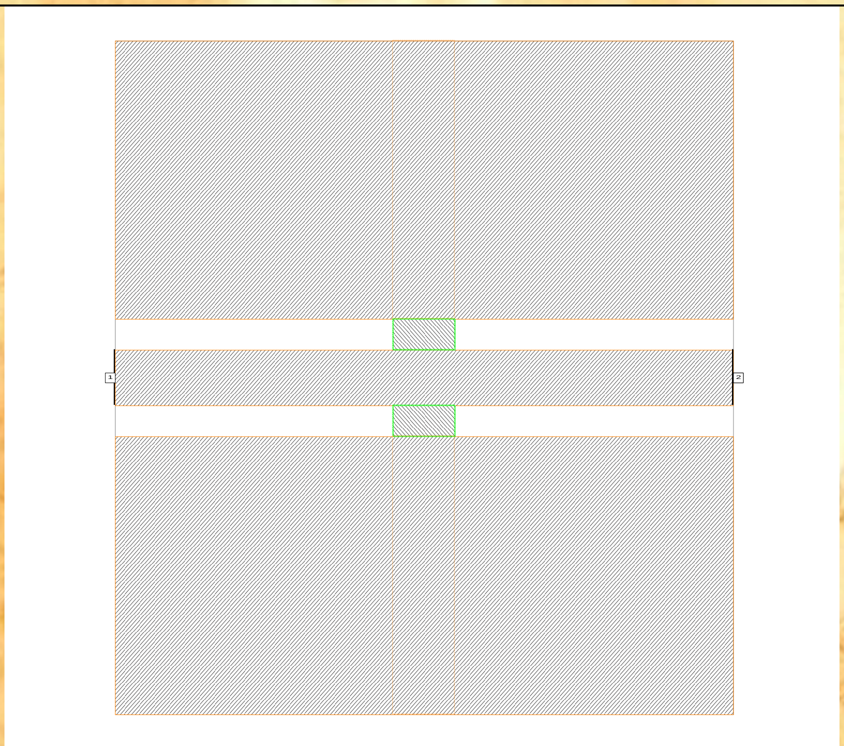

Fig. 9. Top view of the simulated structure. The green boxes are via-holes filled by vertically grown CNTs. The shaded narrow area under the plane of the CPW, orthogonal with respect to the central conductor, is a Au strip providing a ground reference in common for the RF and for the DC signals.

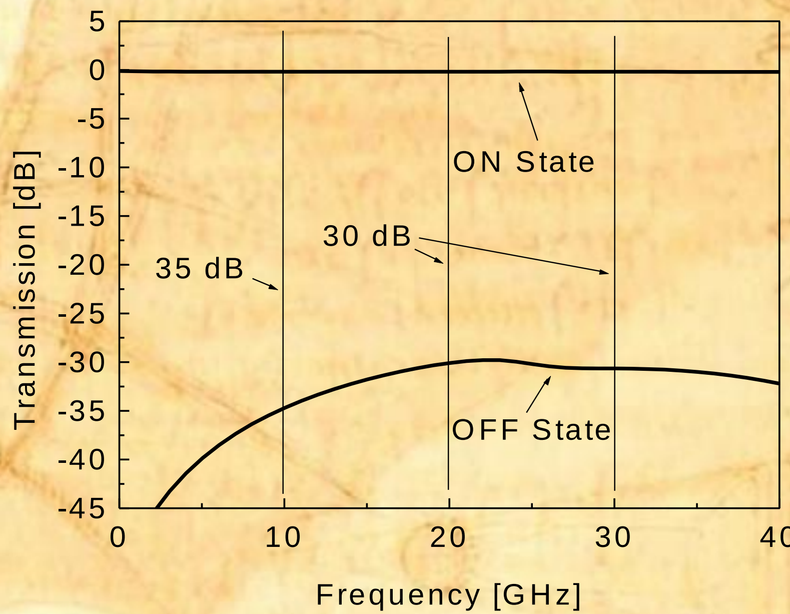

Fig. 10. Electrical response in transmission of the CNT based CPW switch.

AFM-HF Measurements – 1

Scanning Microwave Microscopy *(SMM)*

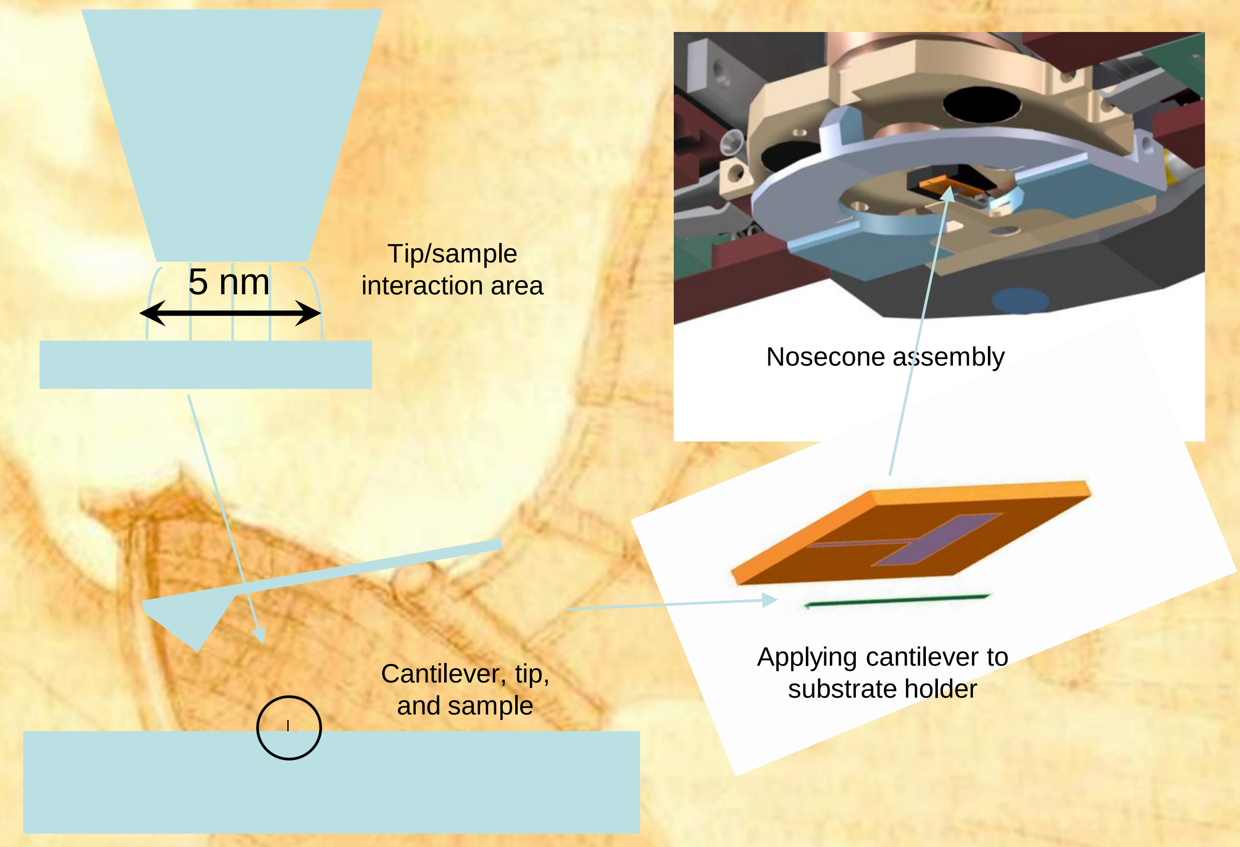

SMM is a near field system, and the resolution is determined by the electric field interaction area with the sample, which is usually is on the order of 5-10 nm. SMM uses a network analyzer to measure the vector reflection coefficient caused by the tip-sample interaction; this gives information about the material properties (dielectric properties). In particular, while an AFM needs “contact” to make a measurement the SMM can measure without contact. You can be 1-10 nm away from the sample and still have good sensitivity. Schematic of the principle of operation for the SMM instrument currently developed by Agilent.

IMM-Roma AFM-HF Measurements - 2

Standard Network Analyzer

Reflection Only

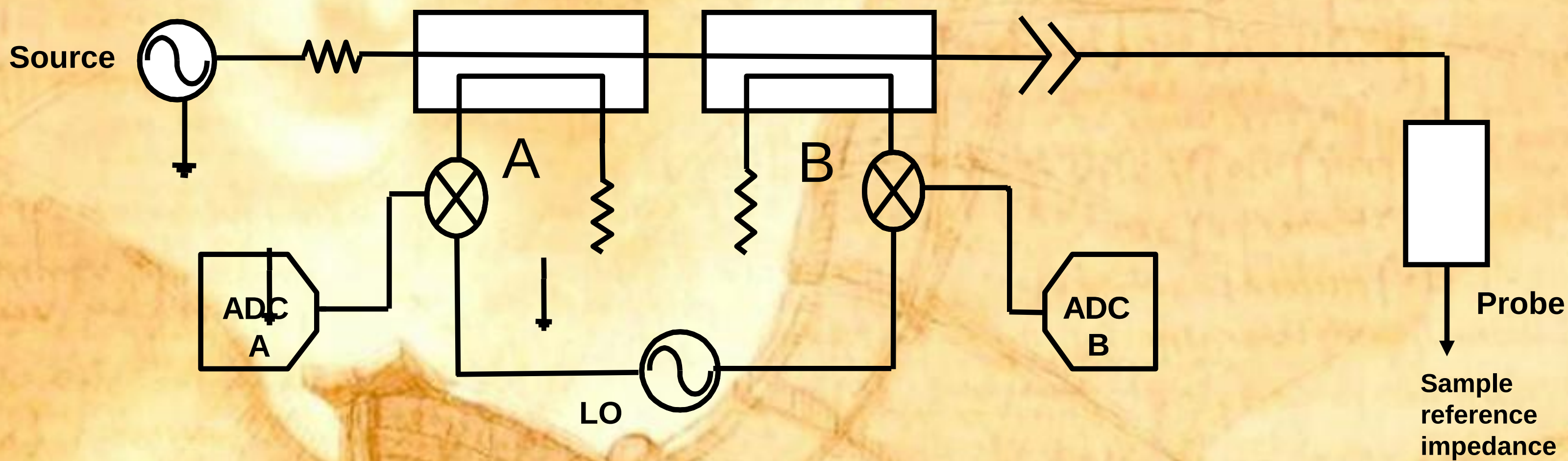

$$S_{11} = \frac{Z_L - Z_0}{Z_L + Z_0} = B/A$$

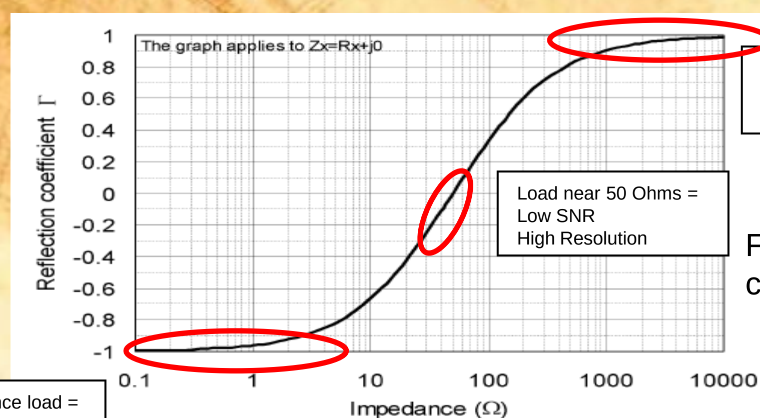

Figure 1: reflection coefficient vs impedance

AFM-HF Measurements - 3

Arbitrary Impedance Network Analyzer

Reflection Only

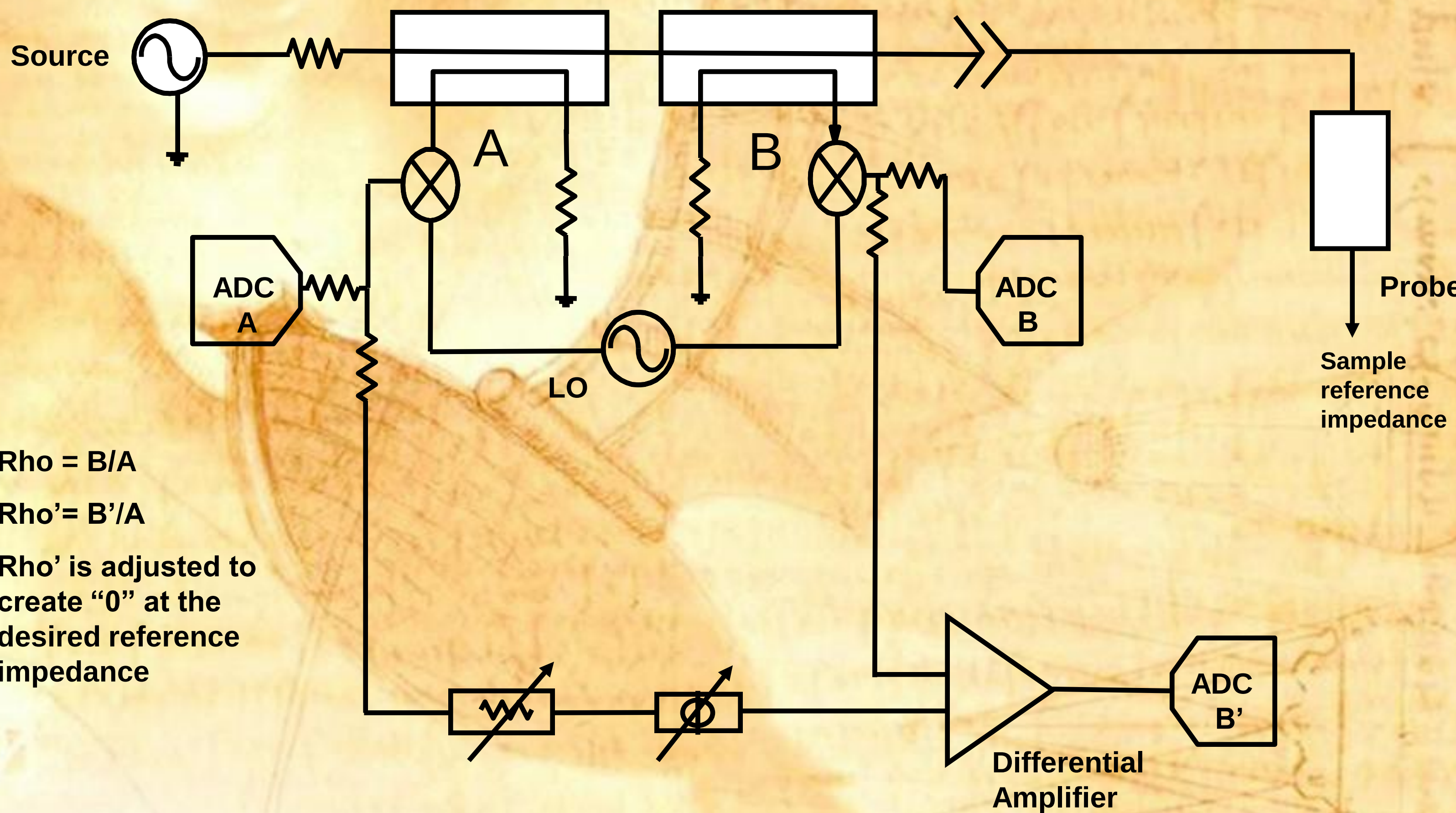

Rho = B/A

Rho’= B’/A

Rho’ is adjusted to create “0” at the desired reference impedance

The Microwave WEB

Setups to be investigated

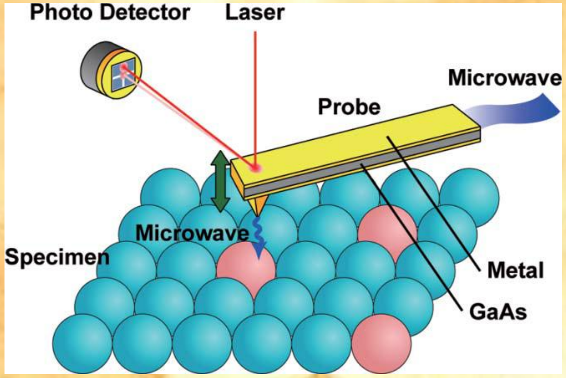

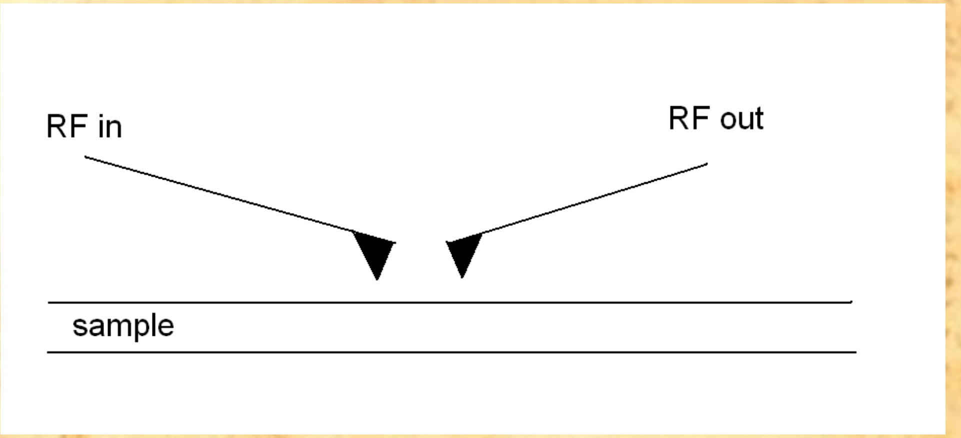

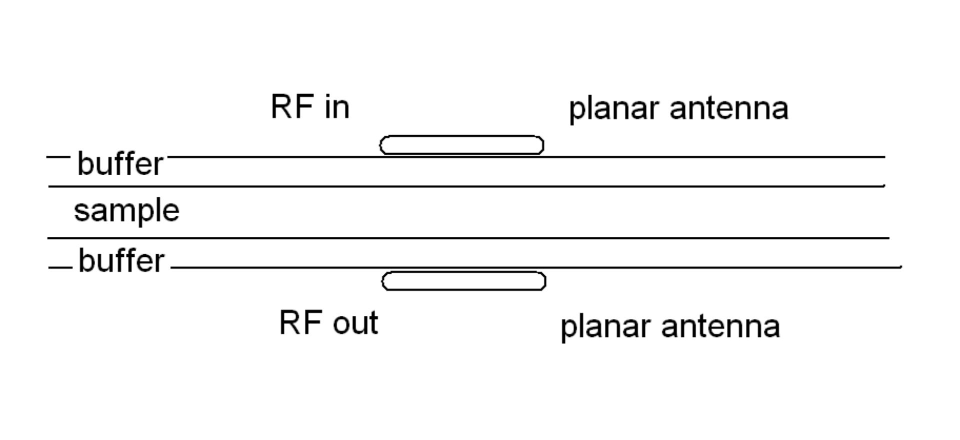

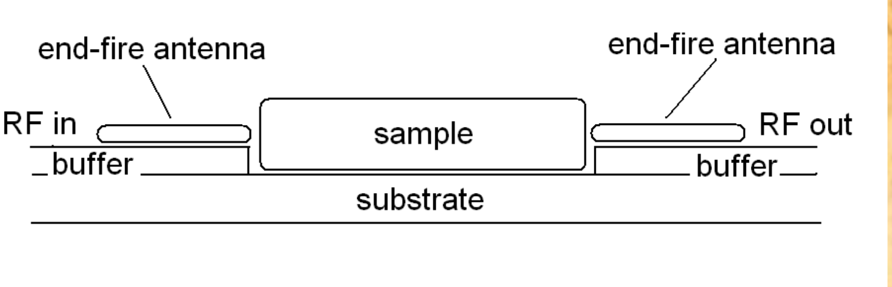

GOAL

Antenna lobes to be used instead of tips for non-contact, transmission measurements

SMM Applications

(open to other units of IMM, current contacts with AGILENT)

- Nano-interconnections and multiple-port devices for High Impedance High Frequencies (CNT, nano-wires, …)
- Characterization of nano-structured materials (graphene, …) from 2D to 3D environment, including transmission
- Imaging and Diagnostics for Microelectronic Components, Biological and Cultural Heritage Samples

Conclusions

- Micro-Systems implemented by using different technologies are low-cost, highly-reliable solutions for high frequency signal processing, suitable of Nano-implementations
- Substrate materials allow for microwave to THz applications by properly scaling the geometries and selecting the interesting frequency range
- Antennas, filters, resonators, guided wave devices and signal routing structures can be manufactured, provided the optimization of surface or bulk micromachining and compatibility between different technologies and materials, also for hybrid sub-systems
- Device Modelling and Design based on new concepts are necessary, as they involve meta-concepts, plasmonics and quantum physics
- SMART Systems could implement the integration of components and functionalities for sub-modules in internet based embedded networks (Internet of Things) for Safety, Security, and ITC applications

➔ New Software Tools + Update of Measurement Techniques

➔ Inter-disciplinary skill required